

DEVELOPMENT, VERIFICATION, AND IMPLEMENTATION  
OF A HORIZONTAL BURIED PIPE GROUND HEAT  
TRANSFER MODEL IN ENERGYPLUS

By

EDWIN LEE

Bachelor of Science  
Oklahoma State University  
Stillwater, Oklahoma  
2006

Submitted to the Faculty of the  
Graduate College of  
Oklahoma State University  
in partial fulfillment of  
the requirements for  
the Degree of  
MASTER OF SCIENCE  
May, 2008

COPYRIGHT ©

By

EDWIN LEE

May, 2008

DEVELOPMENT, VERIFICATION, AND IMPLEMENTATION  
OF A HORIZONTAL BURIED PIPE GROUND HEAT  
TRANSFER MODEL IN ENERGYPLUS

Thesis Approved:

Dr. Daniel Fisher

---

Thesis Advisor

Dr. Jeffrey Spitler

---

Dr. David Lilley

---

Dr. A. Gordon Emslie

Dean of the Graduate College

## ACKNOWLEDGMENTS

There are many people who have helped me along the way. Some have directly helped me with my studies or by providing a bit of humor to ease stressful times. Some have provided inspiration to keep moving in the right direction. It is not conceivable that I could write such a brief summary that would express all the gratitude that I hold for all the ways I have been helped, but I'll give it the old college try.

My utmost praise and worship go to our Lord God Almighty. Without him, there would be nothing, and through him my life has been realized.

My mother and father raised me to always be grateful for what I have, and always remember that I have brothers in this world, and guardian angels in the next world watching over me. They have always supported my ventures, even when they seemed sudden and unclear.

My brother and sister have always shown me dedication which is unmovable. Throughout tough times, they persevered and created a wonderful family that I am very proud of. They show me understanding when my life seems so busy, and they remind me that there is always time for family.

My nieces are seemingly proof that energy is not conserved. They are full of jokes, laughter, smiles, and excitement twenty-four hours a day. Every time I see them, I remember that there is so much in this world to be thankful for, and to never take time for granted.

My grandparents have been great rocks which I have clung to. They have always shown courage, and they have always made an effort to make sure I made the right decisions in life. Of my four grandparents, two have passed on, and I miss them very

much, but I always keep their memories in my heart, and I know they watch over me.

My advisors throughout my collegiate career have had drastic influences in my life. Dr. Cremaschi gave me my first work opportunity during my master's degree, and I learned a great deal from him and my experiences. Dr. Spitler has always been a tough professor, but his lessons are all worth learning, and I have gained invaluable tools throughout my work with him. My graduate advisor, Dr. Fisher, was also my undergraduate advisor. He was the person who opened my eyes to the thermal sciences and created an excitement within me to pursue my master's degree in this field. His enthusiasm for this field spreads everywhere he goes, and I thank him for motivating me at many times to keep going forward.

My master's degree was not all about hard work, I enjoyed making some great friends throughout this time as well. Sankar, Xiaowei, Steve, Jason, Sam, Michael, Chris and Yang have been there to either play frisbee, soccer, printer tossing, or just to enjoy some dinner with friends. I have always looked forward to their camaraderie.

The most influential person in my life is also the love of my life. My wife has been with me for over four years at the time of this writing, and motivated me to continue working no matter how tough it seemed. I have needed her kind words and unwavering love throughout these past years. I have experienced a deep re-commitment to Christ since meeting her, and I couldn't be more proud to call her my wife.

## TABLE OF CONTENTS

Chapter	Page
<b>1 Introduction</b>	<b>1</b>
<b>2 Literature Review</b>	<b>4</b>
2.1 Semi-Analytic Solutions . . . . .	4
2.2 Numerical Analysis . . . . .	8
2.3 Response Factor Models . . . . .	11
2.4 Experimental Work . . . . .	13
2.5 Earth Air Heat Exchanger Analysis . . . . .	14
2.6 District Heating . . . . .	17
2.7 Soil Property Prediction . . . . .	18
2.8 Transport Delay . . . . .	19
2.9 Literature Summary . . . . .	21
<b>3 Fluent Reference Model</b>	<b>23</b>
3.1 Fluent Model Description . . . . .	23
3.2 Fluent Model Grid Refinement . . . . .	24
<b>4 Earth Tube Model</b>	<b>28</b>
4.1 Earth Tube Model Description . . . . .	28
4.2 Model Comparisons: VBA Earth Tube vs. Fluent . . . . .	33
4.3 Model Comparison Results: VBA Earth Tube and New Fluent Earth Tube . . . . .	35
4.4 Earth Tube Conversion to Pipe Model . . . . .	40

4.5	Earth Tube Model Guidance . . . . .	45
4.6	Earth Tube Model Conclusions . . . . .	48
<b>5</b>	<b>Mei Model</b>	<b>49</b>
5.1	Model Description . . . . .	49
5.2	Modifications to Mei Model . . . . .	62
5.3	Model Testing . . . . .	63
5.3.1	Fully Constant Model Testing . . . . .	63
5.3.2	Constant Wall Temperature Testing . . . . .	63
5.3.3	Initial Condition Independence Testing . . . . .	66
5.3.4	High Flow Rate Testing (2D Model Simulation) . . . . .	68
5.4	Mei Model Conclusions . . . . .	70
<b>6</b>	<b>Piechowski Model</b>	<b>73</b>
6.1	Model Description . . . . .	73
6.2	Simplified Piechowski Model . . . . .	83
6.3	Analysis of Piechowski Model Grid Dependence Parameters . . . . .	85
6.4	Initial Model Testing . . . . .	89
6.4.1	Code Integrity Test . . . . .	90
6.4.2	Steady State Test . . . . .	90
6.4.3	Initial Condition Independence Testing . . . . .	94
6.4.4	High Flow Rate Test . . . . .	94
6.5	Comparison to Verification Model . . . . .	95
6.6	Piechowski Model Conclusions . . . . .	102
<b>7</b>	<b>Model Selection</b>	<b>103</b>
7.1	Individual Model Results Summary . . . . .	103
7.1.1	Transfer Function Methods . . . . .	103
7.1.2	Earth Tube Pipe Model . . . . .	104

7.1.3	Mei Model . . . . .	104
7.1.4	Piechowski Model . . . . .	105
7.2	Selection and Summary of Final Model . . . . .	106
<b>8</b>	<b>Model Implementation in EnergyPlus</b>	<b>107</b>
8.1	Buried Pipe Module Description . . . . .	107
8.2	EnergyPlus Code Changes . . . . .	109
8.2.1	Weather Manager . . . . .	109
8.2.2	Plant Managers . . . . .	115
8.2.3	Plant Loop Equipment . . . . .	115
8.3	Error Handling . . . . .	115
8.4	Preliminary Evaluation of the Model . . . . .	116
8.4.1	Input File Description . . . . .	116
8.4.2	Discussion of Results . . . . .	117
8.4.3	Direct Implementation Comparison: EnergyPlus vs. VBA . .	121
8.5	EnergyPlus Documentation . . . . .	123
8.6	Computation Time . . . . .	123
<b>9</b>	<b>Conclusions</b>	<b>125</b>
9.1	Model Development . . . . .	125
9.2	Final Model Implementation . . . . .	126
9.3	Future Work . . . . .	127
<b>A</b>	<b>Earth Tube Model Code</b>	<b>138</b>
<b>B</b>	<b>Gambit Journal File</b>	<b>143</b>
<b>C</b>	<b>Entering Water Temperature Summary</b>	<b>145</b>
<b>D</b>	<b>Modified Piechowski Model Code</b>	<b>150</b>



<b>E</b>	<b>Modified Mei Model Code</b>	<b>168</b>
<b>F</b>	<b>Analytic Constant Wall Temperature Code</b>	<b>185</b>
<b>G</b>	<b>EnergyPlus IDD Object</b>	<b>187</b>
<b>H</b>	<b>EnergyPlus IDF Object</b>	<b>189</b>
<b>I</b>	<b>EnergyPlus Input Output Reference Contribution</b>	<b>191</b>
<b>J</b>	<b>EnergyPlus Engineering Reference Contribution</b>	<b>195</b>

## LIST OF TABLES

Table	Page
2.1 Variable Definitions for equation 2.1 . . . . .	6
3.1 Results of Grid Independence Study . . . . .	26
4.1 Earth Tube Model Inputs . . . . .	30
4.2 Variable Descriptions for Eq. 4.1 . . . . .	31
4.3 Variable Descriptions for Eq. 4.7 . . . . .	32
4.4 Calculation of Earth Tube Outlet Temperature . . . . .	33
4.5 Common Input Data For Earth Tube Models . . . . .	36
4.6 Convection Correlation Information for Circular Pipe Flow . . . . .	42
4.7 Earth Tube Model Sensitivity Study Results . . . . .	47
4.8 Earth Tube Model Influence Coefficients and Percent Error . . . . .	48
5.1 Mei Model Update Equation Organization . . . . .	54
5.2 Mei Model Nomenclature . . . . .	55
6.1 Symbols and Variables used in Piechowski Model . . . . .	80
6.2 Piechowski Model Symbol Definitions . . . . .	83
6.3 Piechowski Input Variable Tabulated Results . . . . .	87
6.4 Simulation Parameters for Piechowski Verification . . . . .	98
6.5 Piechowski Verification: Exiting Temperature RMS Error . . . . .	99
6.6 Piechowski Verification: Heat Transfer Rate RMS Error . . . . .	101
8.1 Computation Time Results . . . . .	124

## LIST OF FIGURES

Figure	Page
1.1 Three Possible Horizontal Pipe Configurations . . . . .	2
2.1 Kusuda and Achenbach Ground Temperature Prediction . . . . .	20
3.1 Generic Fluent Buried Pipe Model . . . . .	25
3.2 Fluent Model Mesh . . . . .	27
4.1 Earth Tube Models: Exit Air Temperatures . . . . .	38
4.2 Earth Tube Models: Exit Air Temperature Deviations . . . . .	39
4.3 Earth Tube and Fluent Heat Transfer Rates . . . . .	40
4.4 Earth Tube Pipe Model Results . . . . .	43
4.5 Fluent and Earth Tube Pipe Model Exit Temperatures . . . . .	44
4.6 Fluent and Earth Tube Pipe Model Delta Exit Temperatures . . . . .	44
5.1 Mei Model Domain Description . . . . .	51
5.2 Mei Model Finite Difference Grid . . . . .	51
5.3 Mei Model Update Equation Locations . . . . .	53
5.4 Mei Model Description: Angular Grid Locations . . . . .	59
5.5 Mei Model Test Results: Constant Wall Temperature . . . . .	65
5.6 Mei Model Test Results: Initial Condition Independence . . . . .	67
5.7 Mei and Fluent Model Boundary Differences . . . . .	69
5.8 High Flow Test: Mei and Fluent Cross Section Temperature Profiles .	70
6.1 Large Scale View of Piechowski Domain Cutaway . . . . .	74
6.2 Small Scale View of Piechowski Domain Cutaway . . . . .	74

6.3	Case Layout and Node Descriptions for Piechowski Model . . . . .	77
6.4	Piechowski Radial Grid Distribution . . . . .	81
6.5	Piechowski Input Variable Study Results . . . . .	88
6.6	Constant Wall Temperature Model Results . . . . .	93
6.7	Piechowski Initial Condition Independence Results . . . . .	94
6.8	High Flow Rate Test Results: Piechowski Model Cross Section Tem- perature Distribution . . . . .	96
6.9	High Flow Rate Test Results: Fluent Model Cross Section Temperature Distribution . . . . .	96
6.10	Piechowski Verification: Exiting Water Temperature Results . . . . .	100
8.1	Main Pipe Simulation Manager Routine Flow . . . . .	108
8.2	Pipe Initialization Routine Flow . . . . .	110
8.3	Main Pipe Calculation Routine Flow . . . . .	111
8.4	Buried Pipe Calculation Routine Flow . . . . .	112
8.5	Buried Pipe Radial Region Routine Flow . . . . .	113
8.6	Buried Pipe Water Boundary Routine Flow . . . . .	114
8.7	Results Section 1: 12-Feb to 28-Apr . . . . .	118
8.8	Results Section 2: 31-Mar to 8-Apr . . . . .	119
8.9	Results Section 3: 31-Mar to 28-Apr . . . . .	120
8.10	Results Section 4: 2-Jun to 17-Jun . . . . .	120
8.11	Implementation Comparison, EnergyPlus to VBA: Exiting Temperature	121
8.12	Implementation Comparison, EnergyPlus to VBA: Total Heat Transfer Rate . . . . .	122

## CHAPTER 1

### Introduction

Heat transfer from buried horizontal pipes has been studied for a majority of the twentieth century, encompassing such fields as residential and commercial ground source heat pump system design, industrial pipelines, district heating and cooling, buried power cables, and the use of earth tube heat exchangers. These applications have led to studies of soil properties, effects of moisture on underground heat transfer, effects of multiple buried pipes along with different insulation methods. The results of all these studies have shown that the problem is not trivial. There are many factors which increase the difficulty of finding an accurate solution to the problem of the horizontal pipe. The ground is heterogeneous; soil conductivity varies with temperature, soil type, and moisture content. The ground surface changes constantly based on the annual and daily temperature cycles, ground cover materials (grass, concrete slab, etc.), rain, and snow cover conditions. The fluid in the pipe will not maintain constant behavior along the entire length of the pipe, with properties such as viscosity and density changing with temperature. The geometric complexity is increased when multiple pipes are laid in the same trench. Even within this multiple pipe layout there are different configurations, as shown in figure 1.1. These complexities make finding a quick solution nearly impossible. As with any engineering analysis, the solution begins with a set of valid assumptions.

The inclusion of a buried pipe model in an annual simulation program is a necessity for properly modeling horizontal ground loop heat exchangers. It is also important for district heating and cooling systems. With low-energy houses and buildings using

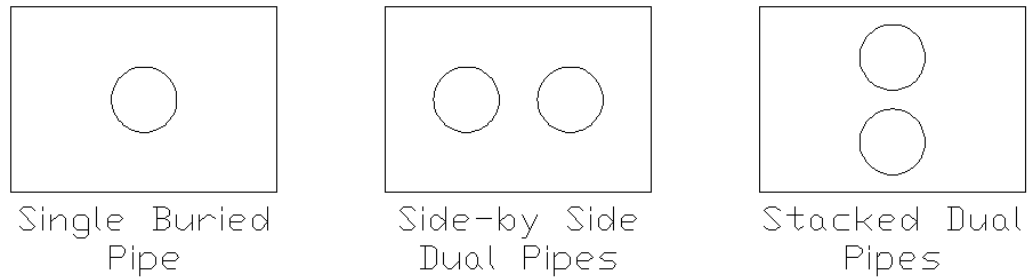


Figure 1.1: Three Possible Horizontal Pipe Configurations

ground heat transfer, the model becomes even more important, as every degree of pre-cooling required of a water source and every degree of heat lost from a heating pipe can be costly.

The main purpose of this current study is to identify a buried pipe heat transfer model which balances accuracy and computation time, and implement that model in the EnergyPlus (2007a) program. The study accomplishes this by the following procedure:

1. Examine previous work in the field. This includes experimental work, which would help define the important aspects of a buried pipe system, and modeling work, which would help define the assumptions that other studies have made in order to form a tractable solution.
2. Develop a reference model. Without experimental data, a robust model must be utilized to provide a comparison tool.
3. Evaluate currently implemented models in EnergyPlus. This step includes looking into models which may not initially be included as buried pipe models, but may be modified to fit such a problem.
4. Develop models for analysis. Each model that seems like a useful option is developed in some form and tested to determine the quality of the results.

5. Select a single buried pipe model to implement. The best choice for the model will balance accuracy and computation time, while providing a general purpose solution to fit all applications of buried pipes.
6. Implement the model in EnergyPlus. The model will act as its own module in the EnergyPlus environment, and it will be tested thoroughly to ensure proper operation.
7. Provide user documentation for the model. This documentation will be included as part of the EnergyPlus documentation state what inputs and outputs are available for the model, as well as a reference showing how the model works.

During many of the tests and simulations included in this work, hourly weather and entering water temperature data are used as boundary conditions. The weather data are annual hourly data from Atlanta, GA. The entering water temperature data are also hourly data, but it is from an experimental source, the ground source heat pump plant at Oklahoma State. Even though this data is not applicable as model validation, it does provide realistic inputs to the models.

This report includes a total of 9 chapters, including this introduction as chapter one. Chapter two is a literature review of different modeling techniques and other aspects of buried pipe design. Chapter three is an introduction to the Fluent reference model used to evaluate the current modeling work. Chapter four evaluates an existing EnergyPlus model, the earth tube model, for modification and use as a buried pipe model. Chapter five evaluates a fully radial model with variable boundary conditions. Chapter six evaluates a model which mixes both cartesian and radial coordinates within the same domain. Chapter seven summarizes results from each model, and selects a model for EnergyPlus implementation. Chapter eight discusses implementation of this model in the EnergyPlus program. Chapter nine summarizes the conclusions of the study and proposes future work.

## CHAPTER 2

### Literature Review

In order to find a proper model to implement, it is necessary to look into literature to see what attempts have previously been made. When looking for a buried pipe model, the search may be broadened slightly as well, to include buried 'earth tubes', since a detailed analysis of a buried air tube shares many aspects with a buried water pipe. The key when looking at these models is to understand the underlying assumptions and ensure that they remain valid for the system at hand. There are several approaches for solving the buried pipe problem, including semi-analytic solutions, finite difference solutions, and finite volume solutions. All of these calculation methods are important, but an understanding of experimental work is required in order to validate the applicability of any model. The current search is broad enough to include the experimental studies and understand the important aspects of a buried pipe system design. Some of the other related material comes from district heating literature, which typically includes substantially long piping systems; soil property prediction, which is an important boundary condition for any simulation dealing with the soil; and transport delay, which can be a significant factor, especially with longer piping systems.

### 2.1 Semi-Analytic Solutions

The semi-analytic solutions typically consist of a line source or cylinder source solution. In this solution, the soil is assumed infinite in all directions, and an infinitesimally small heat source is applied which represents the pipe. In some cases, this



heat source is the input to the model, resulting in pipe outlet temperatures or ground temperatures. The model can be re-formulated to instead determine the heat rate when temperatures are given as inputs. Even with this formulation, there are other limitations of the model. The model does not account for ground surface interaction, does not readily account for initial ground temperature gradients, and the line source is also variable along the length of the pipe due to the fluid temperature changing, so this method cannot suitably predict the behavior along the pipe. In many cases these models also use annual average data which can produce a typical annual result.

One of the earliest line source models was introduced in a 1948 paper in ASHVE by Ingersoll & Plass (1948). The key in this paper is describing the temperature distribution around a buried pipe. An equation is offered, (2.1), based on the assumptions mentioned above, that can give the temperature of any radial distance away from the line source, valid from the pipe wall to a large distance away. This model assumes that the pipe is the only cause of temperature change in the soil.

$$T - T_O = \frac{Q'}{2\pi k} \int_x^\infty \frac{e^{-\beta^2}}{\beta} d\beta = \frac{Q'}{2\pi k} I(x) \quad (2.1)$$

where the variables are defined in table 2.1.

The paper offers values of  $I(x)$  for numerous values of  $x$ , and an equation approximating  $I(x)$ , which would be more suitable to a simulation program than a lookup table. The original equation was only valid for a small range of  $x$ . For the purpose of this current thesis work, the equations were adjusted, and equation (2.2) results, and is valid for a wider range of  $x$ .

$$I(x) = 2.303 \cdot \log\left(\frac{1}{x}\right) + \frac{x^2}{2} - \frac{x^4}{8} + 0.1128 \cdot x^3 - 0.2886 \quad (2.2)$$

The rest of the paper deals with different pipe situations, and solving examples. The examples range from simple single buried pipes to double buried pipes, and then to simulations where the heat rate changes from month to month. Although these

Table 2.1: Variable Definitions for equation 2.1

Variable	Definition
$x$	$\frac{r}{\sqrt{2\alpha t}}$
$T$	Temperature in soil at any selected distance from the pipe [deg F]
$T_o$	Initial temperature of soil [deg F]
$Q'$	Heat emission of pipe (negative for absorption) [Btu/linear ft/hr]
$r$	Distance from centerline of pipe [ft]
$k$	Thermal conductivity of soil [Btu/hr/ft <sup>2</sup> /F]
$\alpha$	Thermal diffusivity of soil = $\frac{k}{\rho C_p}$
$\rho$	Density of soil [lb/ft <sup>3</sup> ]
$C_p$	Specific heat of soil [Btu/lb/F]
$t$	Time since start of operation [hr]
$\beta$	Variable of integration

examples do show that the line source approach is a widely applicable method, it still fails in the limitations discussed previously (uniform boundaries, no ground surface interaction). The method still offers incredible simplicity, and has been used for a significant time frame, but with simulations requiring more accuracy, especially in green design, this method does not seem to be the ideal solution.

The simplifications for line source applications can be modified and built upon to account for different pipe configurations. In Persson & Claesson (2005), the multi-pole method is combined with the line source approach in order to account for multiple pipes using a steady state analysis. In this situation, each pipe is considered as a line source, and the resulting temperature distribution around the pipe can be described by an infinite series solution. When this is performed for each pipe, the temperatures and heat flows can be constrained to 'line up' in between the pipes, thus creating an infinite series of equations describing the system. This infinite series can be truncated

to a desired level of accuracy, resulting in a solution accounting for both pipes. In this paper, multiple pipes are simulated in a vertical configuration (one pipe above the other), as well as a horizontal configuration (each pipe next to the other). In the vertical configuration, the supply pipe is simulated both on top and on the bottom. The pipe system is modeled using district heating data (geometry, temperatures) as inputs. It is found that using these simplifications, a fourth order approximation to the infinite solution can provide results of significant accuracy with a computation time of a few seconds.

A different analysis using line sources is found in Saastamoinen (2007). In this analysis, a rigorous development of unsteady state equations is performed. The application is a floor heating system, in which there is a conducting layer within the floor where heating pipes are contained. Above this, a layer of carpet is modeled, and underneath the conducting layer is insulation. The development includes a convective boundary condition on the top, and constant temperature boundary condition on the bottom. The unsteady behavior is modeled as a fourier series of periodic on-off cycles. The model assumes the shapes of the isotherms around the line sources are nearly circular near the pipe in order to simplify the model to a tractable solution. The effects of ranging placement of the coils and surface Biot numbers are studied in steady state mode and discussed.

Another approach which uses semi-analytic methods is performed by Arimilli & Parang (1983) on dual horizontal buried pipes. The method used is a boundary integral method. In this method, a steady state version of Laplace's equation, represented in Eq (2.3), is written for a two-dimensional domain according to boundary integral methods, with the modified version given in Eq (2.4).

$$\nabla^2 T = 0 \tag{2.3}$$

$$\frac{1}{2}T(Y) + \int_B \left( T \frac{\partial g}{\partial n} - g \frac{\partial T}{\partial n} \right) ds = 0 \quad (2.4)$$

In Eq (2.4), the B subscript refers to integration over the entire boundary,  $T(Y)$  represents the temperature at any point Y on the boundary, and  $g(X,Y)$  is a harmonic function over the solution domain.

The boundary integral involves the temperature along the boundary as well as the derivative at the surface (heat flux for the thermal analysis case). By using this method, the integral can be discretized over a set of segments in the domain. This is similar to a finite difference method, however the boundary integral approach only involves values at the boundaries, and not intermediate values in the center of the domain, which are not of interest in most studies. The resulting equations can be solved with iterative means until convergence. This paper provides the equations required to solve for the general case and describes their simplicity of use, although no validation or verification is given so the accuracy is uncertain.

## 2.2 Numerical Analysis

In many cases, the geometry may be too complex to model properly with a line source approach. For these cases a numerical analysis lends itself well. The numerical approach could be a simple 1D finite difference model, or a 2D finite difference model with variable boundary conditions, or a full 3D finite volume model with unstructured boundary conditions. The approach taken would depend on the pipe configuration, accuracy required, and computation time allowed. The following works span a broad spectrum of numerical solutions and each can provide their own insight into a satisfactory model for implementation in an annual simulation program such as EnergyPlus.

There are many variations in ground heat exchangers including concentric tubes, horizontal trenches, and vertical boreholes. In order to develop a model of a vertical heat exchanger, some of the same assumptions can be made, and some different

assumptions also. For instance, in a vertical heat exchanger, there will almost always be two tubes in very close proximity. In this configuration, it would be a very bad approach to neglect interaction between the pipes. In many cases, a single horizontal heat exchanger will be placed in a trench, in which case this assumption would be valid. For a vertical heat exchanger, the effects of ground surface will be minimal, as the majority of the pipe will be buried deep underground, while in a horizontal heat exchanger, the entire length of the pipe is affected by the behavior above the ground surface. Chiasson & Spitler (2000) describes the model development of a heated bridge deck using a ground source heat pump system. Lei (1993) presents a validated, computationally efficient model for vertical ground heat exchangers. The model is simplified by neglecting the interface resistance between the pipes and the surrounding material. The effects of the U-tube at the end of the pipe are also neglected. The model's computational efficiency is improved by using a dual domain configuration. A fine region is used in the high gradient regions near the pipe, along with a fully implicit solution scheme. The coarse region farther away is solved using an explicit scheme. The time step used is efficiently selected based on the geometry. In both regions, adaptive grid spacing is employed to avoid wasting computation power where it is not needed. With these assumptions and improvements in place, the cylindrical transient equations are discretized and applied to each node in the domain, and the simulation is solved. The results are compared to experimental results, with high accuracy while the piping system is active. When the flow is stopped, as in the pumping off cycle, the results deviate somewhat. The exiting water temperature during these time steps is not drastically important in most engineering analysis, as long as the model simulates correctly once the flow comes back on.

A set of studies is performed by Mei (1988, 1986*a*) in which both single and double horizontal pipes are simulated. In Mei (1988), a dual pipe is studied, with particular interest in the effects that the second pipe has in the temperature distribution around

the first pipe. A quasi-3D finite difference code is developed, based on energy balance equations, which simulates both a single pipe and a dual pipe in a tube-over-tube configuration. The model assumes that the temperature from inside the pipe up to the pipe wall is radially symmetric, and a circular far field boundary condition is applied which is centered in the bottom tube, and with the top at the ground surface. In order to simplify the model, axial heat transfer is neglected in the pipe and soil, and therefore axial heat is only allowed to flow through the fluid. The model results are compared to experimental data in terms of daily energy absorption in the ground, with the model producing an average error of less than 12%. Mei (1986*a*) describes three models, each with their own distinct purpose: soil freezing, seasonal ground temperature variations, and thermal interference. Each model is described in detail including mathematical development, computer implementation, validation, and parametric studies. It is found that for soil freezing around the pipe, the effect is minimal as long as the entering temperature is not less than  $-4^{\circ}\text{C}$ , which is typically used as a design constraint anyway to maintain sufficient heat pump capacities. The seasonal ground temperature variation model provides a very high quality simulation of the temperature distribution around a pipe, and also allows for studies of different backfilling materials. This model seems promising for simulation applications and is evaluated further in chapter 5. The thermal interference model is used for any case with multiple buried pipes in the same trench, and is not investigated in the current work, although analysis of multiple buried pipes is recommended as future work.

A study which involves both heat and mass transfer was performed by Piechowski (1996, 1998, 1999). In the thesis, Piechowski (1996) described every aspect of the model development in great detail, while the other two papers, Piechowski (1998, 1999), give insight into the model validation and theoretical development, respectively. The model contains aspects that most buried pipe models do not, such as moisture diffusion through the soil, and the addition of thermal storage into the system. The

model assumes that the soil temperature a certain distance away from the pipe is not affected by the pipe presence. This becomes the far field boundary condition, and is based on a diurnal and seasonal temperature variation. In order to model moisture transfer in a tractable manner, the mass transfer is only modeled in the vicinity near the pipe, which is where the highest gradients will exist for both heat and mass transfer. The moisture equations therefore have a boundary condition which is in this vicinity. The heat transfer is simulated over a larger domain, with variable boundary conditions. The system is simulated in a 3D finite difference domain, and as with other models, heat and mass transfer are neglected in the axial direction in the pipe material and the soil. This allows for a set of 2D domains to be solved, connected only by the fluid transferred through the pipe. The model is validated against experimental data, and it is found that for a small temperature range, the inclusion of moisture effects (latent heat and moisture migration) does not significantly increase the accuracy, so for most models it would not be necessary. However, the soil thermal conductivity is a very significant input, and improper assumptions of soil properties will lead to inaccurate results. The Piechowski model is developed and tested in chapter 6.

Tarnawski & Leong (1993) presented a model of a ground coupled heat exchanger, but with more emphasis on the overall system simulation investigated. The model includes data for several heat pumps, soil properties, heat exchanger configuration (spiral HX included), and pipe materials. The model is verified against simulated results and previously published experimental work, and agrees with a fair amount of accuracy. The verification process was hindered by a lack of information from the verification source, including ground properties and initial conditions.

## 2.3 Response Factor Models

Another heat transfer model type involves the use of transfer functions or response factors. Transfer functions are typically confined to certain systems while response

factors can be developed for any system. These are already found in building simulation programs as a way to calculate transient heat transfer through walls using pseudo steady-state means. For each wall construction, transfer functions or response factors are developed which represent how the wall responds if there is a one degree change in temperature on one surface. Then superposition can be applied to determine the effects of general temperature changes. There are also response factors used in ground heat transfer, but there are limitations to this method. A short time step response factor model for vertical borehole heat exchangers was developed by Yavuzturk & Spitler (1999) and validated by Yavuzturk & Spitler (2001). In this model, a series of response factors are developed using a transient two dimensional finite difference system. With the response factors calculated, the model is able to produce the temperature response of the borehole field to a step heat input from the ground heat exchanger. This model type is appealing because once the response factors have been generated, the responses are computationally fast. The response factors developed in this work are also valid for short time steps, which is suitable for an energy simulation program such as EnergyPlus. This model proves to work quite well for vertical heat exchangers. Horizontal heat exchangers have a disadvantage for such an approach in that they are greatly affected by the ground surface. For a vertical heat exchanger, only the small section at the top will be affected, so the response factors are allowed to ignore this behavior. For a shallow horizontal heat exchanger, the response factors would need to include the response in the ground to not only a step heat input from the heat exchanger, but also to a step change in temperature or heat from the ground surface. The response factors must also be able to handle modeling a certain depth of soil. Currently, there is a horizontal surface heat exchanger model available in the EnergyPlus program that is based on a modified model from Strand (1995). This model uses transfer functions which are modified to include a heat source within the construction. This is also found when modeling radiant floor systems, in which



case a warm pipe is embedded within the construction. This method is quite useful and again, it is very fast compared to iterative finite difference techniques (the transfer functions in place are also iterative due to required surface heat balances). The major problem with using this model as a general purpose buried pipe model is the depth. Existing transfer functions do not work with very heavy constructions, and with approximately 1m of soil, the EnergyPlus transfer functions diverge. Response factors can be developed for any system such as a horizontal heat exchanger, however the work is beyond the scope of this thesis. The development of response factors is recommended as future work.

## **2.4 Experimental Work**

To ensure that any model is relevant and useful, there must be some experimental work in the field. This experimental work can provide a means of validating a model, provide ranges of useful input data, characterize important properties of the system that must be investigated and accounted for in the model, and also provide a proof of concept to ensure that model development is worth the time and effort.

Inalli & Esen (2004) provided details on a horizontal ground source heat exchanger system in heating season in Turkey. The study provides key data which could be used as input to a new model development. The study also provides experimental evidence that the soil properties play a significant role in the design of the heat exchanger, as it can easily lead to over-sizing of the components and therefore the whole system. In this study, the average coefficients of performance (COPs) of the system (2.66-2.81) were lower than in other experiments due to oversizing of the equipment. The data provided is presented more in terms of seasonal and daily averages. The data provided is not suitable as a source for model validation.

An article that discusses not only experimental apparatus, but also useful design techniques, was presented by Klimkowski et al. (1985). The paper studies the long

term effects of average U-value for a given horizontal heat exchanger. Data is measured, and then resolved back into average conductance. After a period of continuous operation of the heat pump, the U-value approaches a steady constant, one value in winter, and another value in summer. It is recommended to use this value as a design criteria. The paper then offers a design process, which simply utilizes average earth temperature, fluid temperature, and a given U-value, along with a required capacity, to calculate a required HX length in both summer and winter. The longer of these two results is selected as the required pipe length. This type of analysis is a very simplified model which may provide a decent prediction of total annual energy usage, but gives no insight into the daily or hourly operation. These smaller time steps, along with accounting for energy storage in the ground, is where savings may be found using a more robust model, especially when looking at low energy applications.

## **2.5 Earth Air Heat Exchanger Analysis**

When developing a model for a buried pipe, it is desirable to look to different aspects of the heat transfer field in order to possibly find a suitable model that can be modified to fit the needs of a buried pipe. One example is an earth tube. In an earth tube, air is passed through a buried duct in order to pre-cool the air in summer, and pre-heat the air in winter. In this way, the demands of the conditioning equipment are reduced, while the ventilation requirements are easily met with fresh air. The earth tube models differ in the assumptions, as air is passing through the pipe instead of water or glycol. However, if a model shows good performance under earth tube conditions, it may be useful to modify it and analyze it further as a buried pipe.

Al-Ajmi et al. (2006) presented an earth tube model which employs a variable soil temperature variation, and applies steady state behavior and an effectiveness correlation in order to calculate exiting temperature conditions and overall heat transfer. The model is verified against previously published data and proves a high level of

accuracy. The model is then implemented into the TRNSYS environment and used in a full building simulation to show the benefits of using an earth tube, as the cooling load is decreased substantially.

Baxter (1992, 1994) provided a full description of experimental results of an earth tube system in both heating and cooling modes. The results show that one of the main factors that affects the earth tube performance is the temperature gradient that forms in the axial direction near the pipe. This indicates that assuming constant soil temperature near the pipe should be used cautiously, as it could be erroneous.

Bojic et al. (1999) simulated a pvc and a steel pipe together, and showed results of the model. The model was based on a 3D Finite Element Method, although no details were given about the meshing specifics. While the results are given, no validation or verification is offered. One conclusion is that the earth tube operates better in the summer months than the winter months. This may be due to the simulation climate and other temperatures used in the simulation.

Another approach to modeling an earth tube is given by De Paepe & Janssens (2003). In this paper, the authors developed a thermo hydraulic design of earth-air heat exchanger. In this model, both the heat transfer effects and the fluid mechanics effects are modeled, resulting in a very detailed study. The purpose of this model is to evaluate the balance between pressure drop and heat transfer when designing a heat exchanger. The paper develops an  $\epsilon$ -NTU correlation for the earth tube heat exchanger. A 'specific pressure drop' is developed to allow a designer to then calculate required lengths of parallel tubes in order to achieve the required capacities.

A very simplified model of an earth tube, which is implemented in the EnergyPlus simulation program, is developed by Lee & Strand (2006). This model is developed in a very simplified manner in order to achieve two main goals. The first goal is implementation in an annual simulation program. A full finite volume study of an earth tube would be too computationally intensive to re-calculate every time step

of an annual simulation. The second goal is available input data. A simulation engine such as EnergyPlus requires that the models have input to which designers have access. The model takes in simple average annual data, and at each time step, calculates a soil temperature in the near pipe region, and calculates soil, pipe, and convective resistances. A steady state approach then uses an energy balance between the soil and air to create an equation to calculate exiting air temperature as a function of pipe geometry, fluid characteristics, and soil data. The model can also account for fan power if mechanical ventilation is selected. This model is an almost instantaneous calculation model, and therefore lends itself well to being converted to a buried pipe model and re-analyzed. This model is evaluated in detail in chapter 4.

Mihalakakou et al. (1994) provides a model which discusses both heat and mass transfer around the pipe, and accurately predicts the exiting air temperature. The model uses a 3D finite element approach which uses concentric rings as the elements. The model offers the conservation equations which are applied to each node and include both heat transfer and moisture transfer. With boundary conditions specified, the model was used to simulate an earth tube over a period of 15 days. Over this time, experimental data was measured, and the results of the model were in very satisfactory agreement. This model was implemented within the TRNSYS environment, and provides a means of properly predicting earth tube exiting temperature as well as soil temperature variations.

In a study by Tzaferis et al. (1992), two sets of experimental data were measured, and eight different earth air heat exchanger models were simulated under these experimental conditions, and their results were compared, along with the model sensitivity. The models were split in two categories: those which analyzed ground heat transfer, and those which only analyzed heat transfer through the pipe. In the latter of these, temperatures at or near the pipe wall were required as inputs. The models range from assuming constant pipe wall temperature (analytic integral) to using finite difference

schemes. The root mean square (RMS) error for nearly all the models were below 3.5%, showing that even simplified models can provide decent results for an earth tube.

## 2.6 District Heating

One of the larger scale applications of a buried pipe model is in district heating systems. In these systems, a long pipe loop connects a large number of buildings, providing hot water, which can then be tapped and used as a primary heat source or as a source for heat pumps. In these systems, a good model for the pipe heat transfer effects should be used since even a small percentage of energy savings can be quite significant.

A simplified model by Bohm (2000) takes an approach quite different from other models. The model assumes that at each time step, there is a soil temperature that can be used in steady state equations to mimic transient behavior. This temperature would account for the storage effects in the ground by using a temperature from a previous time step. In this manner, the soil temperature near the pipe would be 'lagged' by a certain amount. The position of this undisturbed temperature in the ground is found by numerical simulations and experimentation. A function is developed for this temperature, although several restrictions were placed on the analysis. For the verification, a constant pipe temperature was used, and it is recommended to only maintain constant model inputs for very brief periods. In this study, as with most district heating systems, the pipe configuration is a dual pipe, with the pipes laid side by side. The results do compare well with experimental data taken, although, some of the model inputs come from predicted, or experimentally determined data.

A model of an indirect district heating system is offered by Chuanshan (1997). This model looks deeply at very detailed effects in a district heating system, and not so deeply at predicting the heat transfer of the buried piping. The study does offer

details on model parameters which are very useful if a buried pipe model is developed and tested in a district heating simulation.

Eriksson & Sunden (1998) detailed some new aspects of modeling, while still accounting for both heat and mass transfer in the soil. The model appears to be a 1D approach, with the solution using a tri-diagonal matrix algorithm (TDMA) approach. The key to this particular model is the investigation of pipe material breaking down through time. The thickness and conductivity of the pipe changing over time is studied over a long-term simulation, and the results show that the thermal conductivity of the pipe increases over time, but does not make a significant impact in the overall heat exchanger performance.

## **2.7 Soil Property Prediction**

In order to properly simulate a ground coupled heat exchanger, the soil effects must be modeled accurately as well. The effects of surface temperature variation is even more important when dealing with a horizontal heat exchanger than with a vertical heat exchanger because the pipe or duct is near the surface for the full length, not just a small initial section. This section discusses models and information found for predicting not only ground temperatures, but also ground properties.

A study by Abu-Hamdeh & Reeder (2000) shows that the thermal conductivity is highly dependent on other soil properties such as density, but the application of the study is not relevant for a buried pipe calculation. Fischer (1983) gives a brief summary of fourteen soil heat and moisture transfer models, describing each model's capabilities and limitations, but does not include any model development itself. A model in Kusuda & Achenbach (1965) is one of the more popular models for predicting ground temperatures. The model is based on an assumption that the earth is a semi-infinite solid, and that the surface boundary condition can be described by a sinusoidal temperature variation. In this manner, a simple correlation is given, based

on some simple input data, but the ground surface temperature and average annual amplitude of temperature variation must be known. The main equation (2.5) uses an exponential term to account for depth into the ground (delay), and a cosine term to account for annual variation.

$$T = A - BO \cdot e^{-x \cdot \sqrt{\frac{\pi}{DT}}} \cos \left( \frac{2\pi\theta}{T} - x \sqrt{\frac{\pi}{DT}} - PO \right) \quad (2.5)$$

In equation (2.5),  $T$  is the ground temperature at a given time  $\theta$  and depth  $x$ .  $D$  is the thermal diffusivity of the soil,  $T$  is the time period of the annual variation, and should be the same units as  $\theta$ .  $PO$  would be a phase angle to account for the date of minimum surface temperature.  $A$  is the annual average surface temperature, and  $BO$  is the annual average variation in surface temperature. As an example, to show the effects of ground heat diffusion, figure 2.1 shows the annual ground temperature for a series of depths. In this example,  $A$  was set to 18.333°C,  $BO$  was set to 11.667°C,  $D$  was set to 1.765E-3 m<sup>2</sup>/hr,  $PO$  was set to zero, and since the run was an annual simulation and diffusivity was in hours, the constant  $T$  was set to 8760 hours.

Kumar & Kaushik (1995) discusses a soil temperature model which is based on Kusuda & Achenbach (1965), but includes soil properties (conductivity, specific heat, density, and diffusivity) for ten different soil consistencies (dry light, damp heavy, average rock, etc.).

## 2.8 Transport Delay

One aspect that is typically not dealt with in detail is the transport delay problem. Most simulation programs have pipe models, but do not account for the time required for the fluid to pass through the pipe. In the past, this may have been neglected due to the additional computational strain that this would place on a simulation program. With computers becoming faster, this aspect should not be ignored when it is applicable to include it.

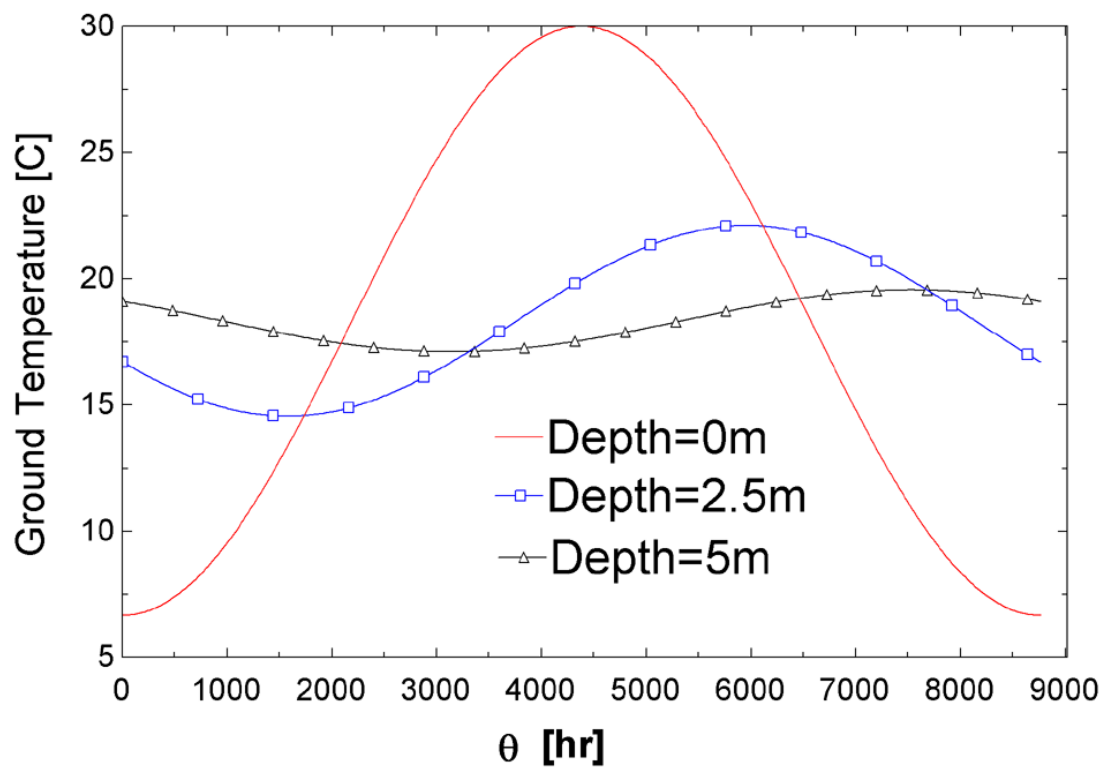


Figure 2.1: Kusuda and Achenbach Ground Temperature Prediction



Hanby et al. (2002) develops a model that is based on second order equations used at several nodes along the length of a pipe. The model accounts for the thermal capacitance of the fluid and the conduit wall. Each node is a well-mixed zone, and the node separation distance is based on capacity values and average fluid residence time. This residence time is a factor which can be assumed based on flow behavior or pre-calculated using CFD studies. The model shows very close agreement with experimental data.

Saman & Mahdi (1996) details some previous models that attempted to predict the transport delay problem, along with where these models fell short. The model in the paper is based on analytic energy balance equations discretized along the length of the pipe, and solved using finite difference methods. The results do follow the expected behavior, but no validation is offered in the paper, so the accuracy of the model cannot be determined.

## **2.9 Literature Summary**

This chapter has been a review of literature involving buried pipe heat transfer models, soil property prediction, and transport delay models.

The buried pipe models included semi-analytic methods, numerical simulation methods, and response factor methods. The response factor methods reviewed were generated for vertical heat exchangers, which allowed the ground surface to be ignored. The generation of response factors for a shallow horizontal heat exchanger is not in the scope of this thesis work, but is highly recommended as future work. The semi-analytic methods required a large number of assumptions and typically required input such as the line source strength; doing so requires a guess and therefore introduces high uncertainty into the results. The numerical methods varied in computational requirements and accuracy. The models selected for development in this work are the Earth Tube model, the V. C. Mei model, and the Piechowski model. These three

give varying degrees of assumptions and accuracy, and should give a nice comparison of what work has been performed, and which model is worthy of development within the EnergyPlus system.

The soil property prediction by Kusuda has been used for years covering different fields of study. For the models currently developed in this work, the Kusuda and Achenbach method will be used to predict boundary condition temperatures and surface temperatures when appropriate.

The transport delay models will currently not be developed, as the main goal of this thesis work is to get a buried pipe heat transfer model into EnergyPlus. The introduction of a transport delay model could be obtained by linking several smaller pipe models together once one is developed. This is left as another good recommendation for future work. However, with a transient buried pipe model, the effects of a transport delay are somewhat captured. The basic pipe model allows the inlet temperature to pass directly through to the pipe outlet. With the addition of any transient effects, the immediate transport will encounter a delay. Further investigation will reveal if the models need to be developed together to create one dual-purpose model.

In conclusion, three numerical heat transfer models will be developed which use the Kusuda and Achenbach soil temperature prediction method, and do not include an actual transport delay aspect. These three models will be compared against a verification model discussed in chapter 3, and a decision will be made to implement one of the models weighing accuracy vs. computation time.

## CHAPTER 3

### Fluent Reference Model

#### 3.1 Fluent Model Description

When creating or testing any model, there must be a method of ensuring the model is operating properly. In some cases, analytic solutions may be available which can be used as a validation source. Another way of performing validation is through experimental results. If one can create an experimental apparatus or facility to which the model can be applied, the results can be compared to prove the model's validity. In the current case, experimental data is not available, and so direct validation is not possible. In some limiting cases, analytic means are used in this work to prove model operation. These cases require substantial assumptions to allow an analytic solution to be developed. For the majority of this current work, verification will be performed. In verification, the model is compared against a more robust, or previously validated model. Fluent CFD software is employed for the current situation. In most cases, Fluent is used to simulate fluid flow in diverse situations. However, the finite volume engine within Fluent is powerful enough to simply switch off the momentum equations, and only solve the conservation of energy equation in solid regions. This allows conduction to be modeled easily within Fluent, along with convection flow in a tube, all in the same model.

Another benefit of using Fluent is the flexibility of boundary conditions. There are features within Fluent that allow users to input their own functions that can be spatially or temporally dependent, and applied to any boundary of the model. The functions are written in the C programming language, can be easily hooked to a

model, and can access many internal variables to Fluent's solver. This is very useful when simulating, for instance, the annual variation of ground surface temperature. The user defined function can reach within Fluent, retrieve the current simulation time step, and return a value of surface temperature for that particular hour of the year. For some situations where the boundary condition is spatially dependent, such as the Kusuda and Achenbach boundary (a function of time and depth), the function can reach into Fluent and get the depth coordinate in order to return the appropriate earth temperature for that time and depth. The other boundary conditions can all be applied as needed, some symmetric, some known boundary temperature. The exact configuration will depend on the model being verified.

Figure 3.1 shows a typical Fluent model for this work. The buried pipe channel along with the relevant boundary conditions, are shown. The boundary conditions will vary depending on the current model being tested.

Throughout this work, a number of simplified models will be compared to Fluent models that have been carefully generated to closely match the simplified model. The details of these comparisons are discussed in each individual model chapter.

### **3.2 Fluent Model Grid Refinement**

In order to develop a valid Fluent model, an independent grid must be demonstrated. By using the gambit journal file, it is easy to reproduce models quickly. An example of the journal files used in this study can be found in appendix B. In order to ensure that the grid is independent, the grid was reproduced several times, each with increasing refinement of the grid. The grid was refined in both the pipe and soil regions, each with its own given node spacing value. For the grid independence check, a steady state situation was utilized, with simple boundary conditions. The ground surface was held at 310K, while the other spatial boundaries were adiabatic. The pipe inlet was air at a uniform 1 m/s and 260K. The entire domain was initialized to the conditions

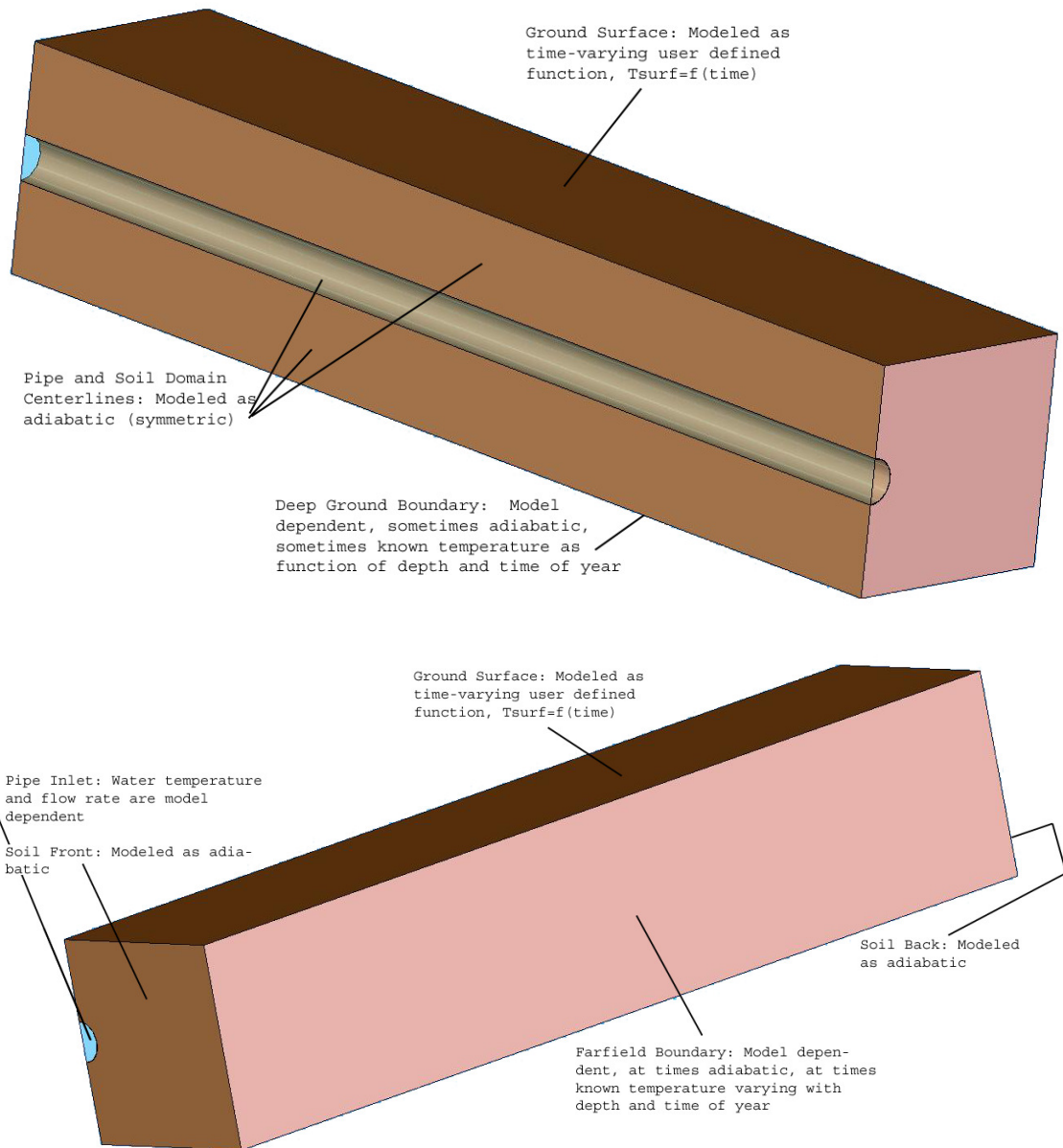


Figure 3.1: Generic Fluent Buried Pipe Model

Table 3.1: Results of Grid Independence Study

Pipe Mesh Spacing	Soil Mesh Spacing	Pipe Nodes	Soil Nodes	Iterations to Convergence	Pipe Wall Heat Transfer Rate	% Change ( new-old /old)	Approximate Run Time
[m]	[m]	[-]	[-]	[-]	[W]	[-]	[min]
0.500	1.000	50	1350	82	847.5729		1
0.250	0.500	400	11300	251	1052.578	24.187%	3
0.125	0.250	2000	88600	730	1109.659	5.423%	10
0.100	0.125	3250	407500	1358	1097.354	1.109%	45

at the pipe inlet, and the simulation ran to convergence. Convergence was kept at the default residual values (1E-03 for most variables, 1E-06 for energy equation). After convergence was attained and the results were checked for satisfactory convergence (no oscillation, etc.), the total heat transfer rate on the pipe wall was calculated by Fluent. This was used as the grid independence monitor. The grid was simulated for four different mesh conditions, and table 3.1 shows the results of the runs.

Table 3.1 shows that the results are in fact converging on a solution as the mesh becomes more and more refined. The table also shows that the time required for the simulation to run is becoming much larger. In order to provide quality results in a reasonable time frame, a compromise must be made between accuracy and computation time. For further computations, the mesh for case 3 (10 minute run time) is selected. This simulation gives quite good results with only about 5% improvement over the previous run. The mesh is shown in figure 3.2.

The grid independence is one of the most important checks to make when performing finite difference studies. Other studies to verify the Fluent model under different circumstances will be performed on a model-by-model basis throughout this work.

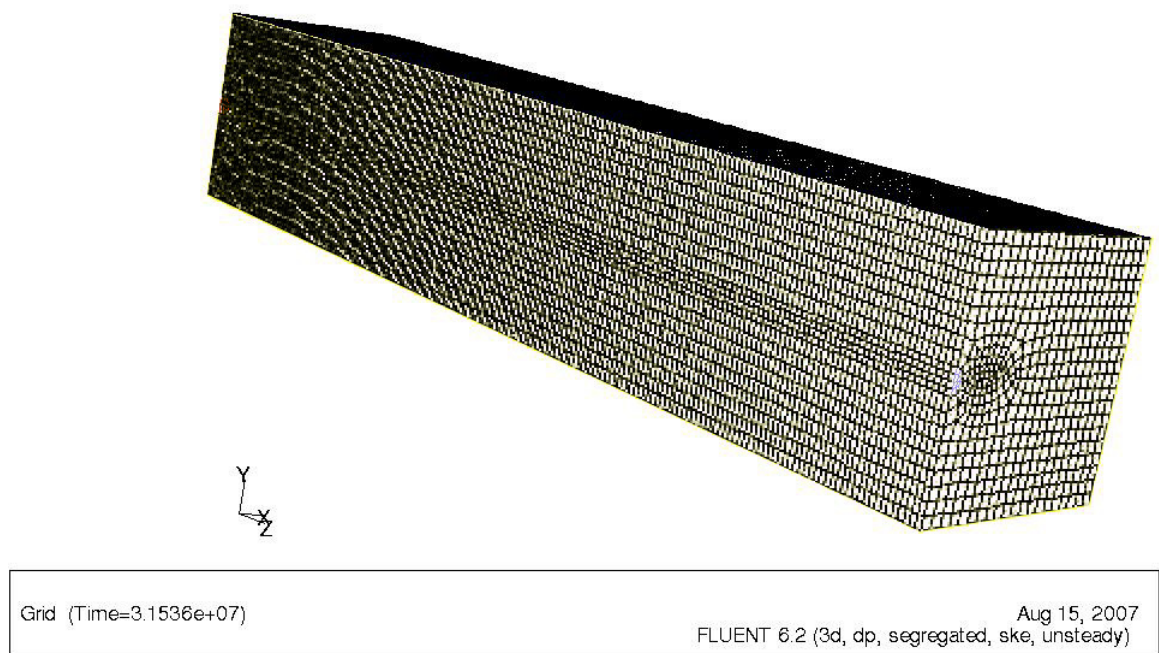


Figure 3.2: Fluent Model Mesh

## CHAPTER 4

### Earth Tube Model

#### 4.1 Earth Tube Model Description

One of the models which is used to predict ground heat transfer from a buried pipe was developed for an Earth Tube system (Lee & Strand 2006). In this earth tube system, ventilation air is brought into an underground duct from a certain distance away from the zone or conditioning system, and the air is tempered, either pre-heated or pre-cooled depending on the season, and then brought into the zone or through the conditioning equipment. This pre-treatment of the air helps to reduce the overall heating and cooling equipment loads while satisfying fresh air requirements. The model makes many assumptions, but requires minimal input data and has a very short computation time. These features lend themselves well to first stage design work in an annual simulation program. Because of the many assumptions, this model seems to be one of the simplest models to apply to a buried pipe.

As with many models, one must begin by understanding the underlying assumptions, in order to ensure that the model is valid for a particular system, and not oversimplified.

- The first assumption is that fluid flow within the pipe is thermally and hydrodynamically developed. This assumption can be easily made when the length of the pipe is much greater than the diameter. Developing flow will only occur within a short initial section of the pipe, and will not greatly influence the thermal behavior when the pipe is long. This assumption allows a single correlation



to be used for any given fluid and flow regime.

- The next assumption is that soil temperature in the pipe vicinity can be calculated using the model developed by Kusuda & Achenbach (1965). This earth tube model makes use of the soil temperature model to calculate a soil temperature one annulus from the center of the pipe.
- The temperature in the soil near the pipe is not affected by the pipe itself. This assumption allows the soil temperature to be uniform along the entire axial length of the pipe. This allows the solution of the system to be greatly simplified, but may impact the accuracy.
- The soil is homogeneous and maintains constant thermal properties (thermal conductivity) throughout any time step, although at each time step, the properties can be adjusted to a new temperature dependent value and held constant yet again.
- The fluid is axisymmetric at any cross section, and the pipe maintains a constant cross sectional area in the axial direction.
- At any given time step, the heat transfer behavior can be modeled as steady state.

In order to be useful, the model inputs must be available. Typically, this requires simplifying the model to accommodate data that most people can access. This particular model requires input of properties such as system geometry, material properties, fluid flow properties (including a convection correlation), and annual surface temperature data. The full set of input data is described in table 4.1. The system geometry should be available to a designer, and the fluid flow properties can be approximated based on design conditions. Soil properties and annual surface temperature data must be estimated. The soil properties will be variable based on moisture content,

Table 4.1: Earth Tube Model Inputs

Pipe Data	
Geometry:	Buried depth, Axial length, Radius, Wall thickness
Properties:	Pipe wall thermal conductivity
Soil Data	
Properties:	Thermal diffusivity, Thermal conductivity
Other:	Annual average surface temperature Annual surface temperature amplitude
Fluid Data	
Flow:	Flow rate, Convection correlation
Properties:	Density, Specific heat, Prandtl number Viscosity, Thermal conductivity

and the surface temperature data will be location specific. Soil properties may be determined from an on-site thermal conductivity test, and surface temperature data can be approximated from annual weather data.

Once the model has the required input data, it uses hourly outdoor air temperature and a series of equations to calculate the air temperature exiting the earth tube. These equations are described here.

The first equation calculates the ground temperature in the vicinity of the buried pipe. This equation is developed from the work by Kusuda & Achenbach (1965), but arranged to fit the attributes of this particular model:

$$T_{gnd,z} = T_s - A_s * e^{-z * \sqrt{\frac{\pi}{365 * \alpha}}} * \cos \left[ \frac{2 * \pi}{365} * \left( t - t_{shift} - \frac{z}{2} * \sqrt{\frac{365}{\pi \alpha}} \right) \right] \quad (4.1)$$

The variables used in equation (4.1) are defined in table 4.2.

Table 4.2: Variable Descriptions for Eq. 4.1

Symbol	Description
$T_{gnd,z}$	Ground temperature at pipe depth [C]
$T_s$	Annual average surface temperature [C]
$A_s$	Annual surface temperature amplitude [C]
$z$	Pipe burial depth [m]
$\alpha$	Ground thermal diffusivity [m <sup>2</sup> /day]
$t$	Simulation Run Time [day]
$t_{shift}$	Day of minimum surface temperature (i.e. 0 = 1-Jan) [day]

With the ground boundary temperature found at the pipe depth, focus can be switched to the fluid. To define the fluid to pipe interface, a convection coefficient is required. The correlation (not listed here) is a function of the working fluid (air, water) and the flow regime (laminar, turbulent). For typical fluids such as air and water, there are many correlations available in common heat transfer and fluid flow textbooks. Whichever correlation is used, the outcome is the convection coefficient,  $h$ , which can then be used in further calculations.

The soil data, pipe data, and fluid data have now all been initialized and steps can be taken to compute the exiting fluid temperature. First, the thermal resistances of each material and interface are calculated, then the total resistance, and therefore the total conductance, can be calculated with the following equations.

$$\text{Convection resistance} : R_c = \frac{1}{2\pi r_1 h} \quad (4.2)$$

$$\text{Pipe wall resistance} : R_p = \frac{1}{2\pi k_p} * \ln \left( \frac{r_1 + r_2}{r_1} \right) \quad (4.3)$$

$$\text{Soil resistance} : R_s = \frac{1}{2\pi k_s} * \ln \left( \frac{r_1 + r_2 + r_3}{r_1 + r_2} \right) \quad (4.4)$$

$$\text{Total resistance} : R_t = R_c + R_p + R_s \quad (4.5)$$

$$\text{Total conductance} : U_t = \frac{1}{R_t} \quad (4.6)$$

The paper then applies a heat balance to a differential length of pipe, where the heat transfer to the air is equated to the heat storage within the air. Because of the simplifications that previously resulted in a uniform temperature along the length of the pipe, the outlet air temperature is a simple expression which is a function of conductance, fluid properties, entering fluid temperature, ground temperature near the pipe, and pipe length. For simplification, the paper defines an intermediate term that can be calculated, which simplifies the final exiting temperature expression, and is given as equation (4.7).

$$A = \frac{\dot{m}_f C_f * \ln |T_{f,i} - T_{gnd,z}| - U_t * L}{\dot{m}_f C_f} \quad (4.7)$$

The variables used in equation (4.7) are described in table 4.3.

Table 4.3: Variable Descriptions for Eq. 4.7

Symbol	Description
$\dot{m}_f$	Mass flow rate of fluid
$C_f$	Specific heat capacity of fluid
$T_{f,i}$	Entering fluid temperature
$T_{gnd,z}$	Ground temperature near pipe
$L$	Pipe length

Using this intermediate term from equation (4.7), the outlet temperature can be calculated based on different scenarios regarding entering fluid temperature,  $T_{f,i}$ , and ground temperature,  $T_{gnd,z}$ , as described in table 4.4.

As this description shows, this model is a very simple model to implement, and lends itself well to annual simulation programs, where it may be called thousands

Table 4.4: Calculation of Earth Tube Outlet Temperature

Situation	Equation
$T_{f,i} > T_{z,t}$	$T_{f,ex}(L) = T_{z,t} + e^A$
$T_{f,i} < T_{z,t}$	$T_{f,ex}(L) = T_{z,t} - e^A$
$T_{f,i} = T_{z,t}$	$T_{f,ex}(L) = T_{z,t}$

of times during one simulation. When implementing this model in a spreadsheet environment, the annual simulation at an hourly time step took less than one second to complete. The simplicity does come at a price, however, and that price is accuracy. The assumption that the ground temperature near the pipe is not affected by the presence of the pipe goes against what most ground source heat pump developers count on, and that is heat storage in the ground. This model will be tested against more rigorous models to determine how much accuracy is lost in the assumptions and simplifications made.

## 4.2 Model Comparisons: VBA Earth Tube vs. Fluent

The earth tube model, as implemented in VBA, requires the inputs found in table 4.1. To reproduce the model in Fluent, modifications to the Fluent model discussed in chapter 3 are required. Geometrical constraints such as pipe diameter, depth, length, and thickness are all very similar. In the VBA implementation, there is no finite difference solution, so the domain is simply the pipe along with a representative soil temperature with which the pipe interacts. For the Fluent model, however, the geometric constraints must include distances to apply boundary conditions in the 3D domain. These distances represent the width and height of the soil that is modeled. The soil is modeled underneath the pipe, and around the side of the pipe. The VBA earth tube model does not take into account any heat transfer from these regions. In an effort to produce the most direct comparison of the two models, the most

appropriate way to implement these boundary conditions in the Fluent model is to use adiabatic boundary conditions on these faces. The soil and fluid properties may be directly placed within both models, which helps ensure agreement between the two. The fluid to pipe convection coefficient will cause some difference between the models. For the earth tube model, a heat transfer correlation is used which is based on Reynolds number, and therefore based on bulk flow rate through the pipe. In Fluent, the local velocity and boundary layer will be simulated, and so a uniform convection coefficient will not be modeled. The last item that changes is the soil temperature prediction. The earth tube model uses annual average surface temperature data to produce a single correlation as a function of depth and time. This then produces a temperature in the soil near the pipe at each time step of the simulation. In Fluent, this would over specify the problem, since the soil is being modeled as a solid volume, not just the near pipe vicinity. The inputs to the earth tube model are the annual average surface temperature and the annual surface temperature amplitude. These two inputs can also be used in Fluent to develop a user-defined transient boundary condition. Some details on user-defined functions are presented in section 3.1. The surface temperature can be approximated as a sine wave throughout the year with the same given average and amplitude. In summary, the models can be made very similar, but with three significant differences:

1. The soil is modeled from the surface to a distance below the pipe and in the region to the side of the pipe in Fluent. The 'deep ground' and 'far-field' boundaries will initially be modeled as adiabatic to account for the fact that the VBA earth tube model ignores heat transfer interaction with these regions.
2. The air flow through the tube is modeled as a finite element mesh in order to predict heat transfer behavior from the air in Fluent. In the earth tube model, a correlation is used based on bulk flow through the tube.

3. The soil surface boundary condition will be a user-defined sine wave approximation of a yearly cycle with a given average and amplitude in Fluent. In the earth tube model, the same average and amplitude are used in a correlation to predict the temperature of the soil in the near-pipe vicinity, which then becomes the boundary condition for the model. In other words, the earth tube calculations only use the surface temperature to pre-calculate the soil temperature at the pipe depth for any given day of the year, and the surface is not directly modeled.

Note that the VBA implementation was not directly verified against the EnergyPlus implementation. A paper by Lee & Strand (2006) covers the development of the model and implementation of the model in EnergyPlus. The work in this paper was used as the guideline for the current VBA model implementation. One major difference that may occur between the VBA and EnergyPlus implementation is the time step management; the VBA implementation uses a constant one hour time step, while EnergyPlus varies the time step as needed throughout the simulation. The model is updated with the current ground temperature and the earth tube is simulated. Based on a verification of the governing model equations, the model presented in the paper and the VBA model should produce the same results.

### **4.3 Model Comparison Results: VBA Earth Tube and New Fluent Earth Tube**

With the proper mesh developed for the Fluent model, the earth tube model as implemented in VBA and the Fluent model can be directly compared. The detailed differences between the models can be found in Section 4.2. The inputs used which are common to both models are given in Table 4.5.

The inputs which are not shared between the models are summarized below. For each input, the method used by each model is given.

Table 4.5: Common Input Data For Earth Tube Models

Input Description	Value	Units
Pipe Data		
Burial Depth	2.5	[m]
Length	25.0	[m]
Radius	0.25	[m]
Thickness	0.01	[m]
Thermal Conductivity	200	$[\frac{W}{m-K}]$
Soil Data		
Thermal Conductivity	1.5	$[\frac{W}{m-K}]$
Fluid Data		
Working Fluid	Air	[–]
Flow rate	0.785	$[\frac{m^3}{s}]$
Simulation Data		
Surf Temp Avg	15	[C]
Surf Temp Ampl	5.6	[C]

- Ground Surface Temperature

- VBA Earth Tube: Use average surface temperature and amplitude data along with equation (4.1) to generate soil temperature near pipe.
- Fluent Earth Tube: Use average surface temperature and amplitude data as a transient sine wave:  $T_{surf}(t) = T_{surf,avg} + T_{surf,ampl}\sin(A * t)$ . The A coefficient is modified to fit the time unit conventions in Fluent. This equation is similar to the full Kusuda & Achenbach (1965) correlation, but does not require the exponential because the depth is zero at the ground surface.



- Deep Ground Heat Transfer
  - VBA Earth Tube: This model does not take into account any heat transfer interaction to deep ground or heat transfer to the side of the pipe.
  - Fluent Earth Tube: Soil surrounding pipe is modeled, but all surfaces are set as adiabatic to mimic current earth tube behavior.
- Fluid Properties
  - VBA Earth Tube: This model uses constant values of air properties such as density and specific heat.
  - Fluent Earth Tube: Fluent contains libraries of material properties, some of which are constant, and some of which are calculated by equations of state (such as ideal gas).
  - Note: For this model comparison, the air will not see drastic temperature or property changes, so this change is not a significant source of error.

The main output of the VBA earth tube model is the outlet temperature from the tube. The earth tube model inherently assumes steady state behavior. During an annual simulation, the ground temperature and inlet temperature are updated, and a new steady state solution is found. For both models, a time step of one hour is used. The simulation is then operated for 8760 time steps to include a full annual simulation. In the earth tube model, hourly weather data is read directly. For the Fluent model, the entering air temperature is a boundary file, which consists of 'if-then' structures to select the outdoor dry bulb temperature for any given hour of the year. The weather data used is from Atlanta, GA.

Although Fluent can be used to output any data desired, the variable of most interest is the exiting fluid temperature. This is what will be compared to the earth tube model. The goal of this comparison is to determine how well the earth tube

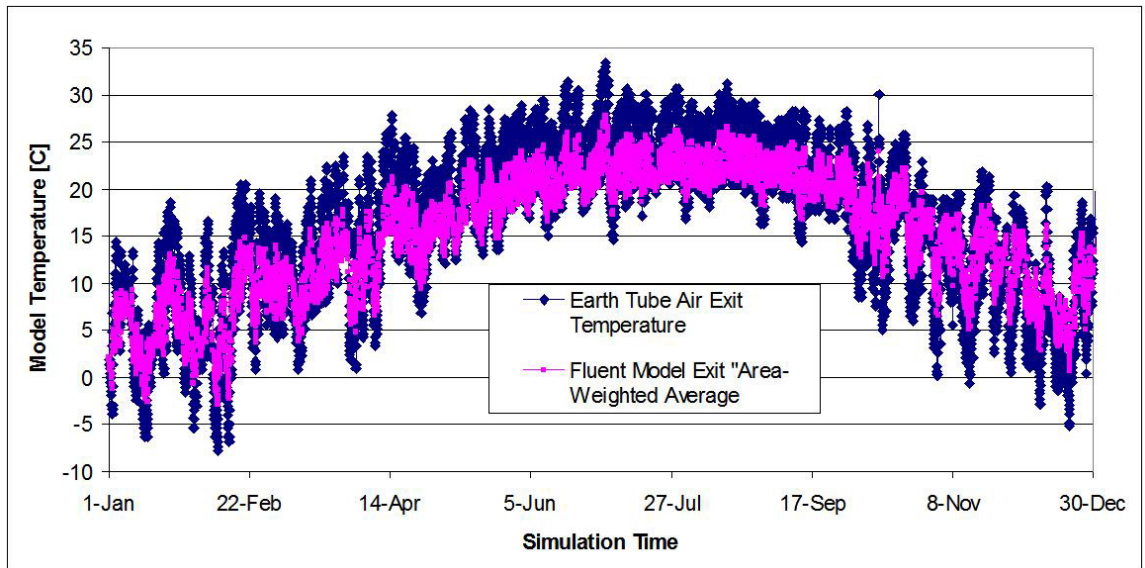


Figure 4.1: Earth Tube Models: Exit Air Temperatures

can predict ground heat transfer, compared to the more robust and thorough Fluent model. Other comparisons are performed as needed.

The exiting air temperatures are plotted for the entire simulation year in Figure 4.1. The numerous simplifications inherent in the earth tube model result in some disagreement with the Fluent model. The deviations between the models are plotted in figure 4.2. The earth tube model is a steady state model at each time step, while Fluent solves the transient equations of momentum and energy for each time step. At the beginning of the simulation, Fluent initializes the entire domain to a steady condition based on the values at the initial time step. For the entire year, the trends of both models agree, but the actual values do not. For most of the year, the models deviate by about 5°C. In the summer, the Fluent model shows better pre-cooling capabilities, while in the winter, it shows better pre-heating capabilities. The earth tube model appears to be in error, but in a conservative manner. This seems to be due to the better ground heat storage modeling in Fluent.

Another way to characterize the error between the two models is to show the different heat transfer rates predicted. This is similar to presenting the pipe delta

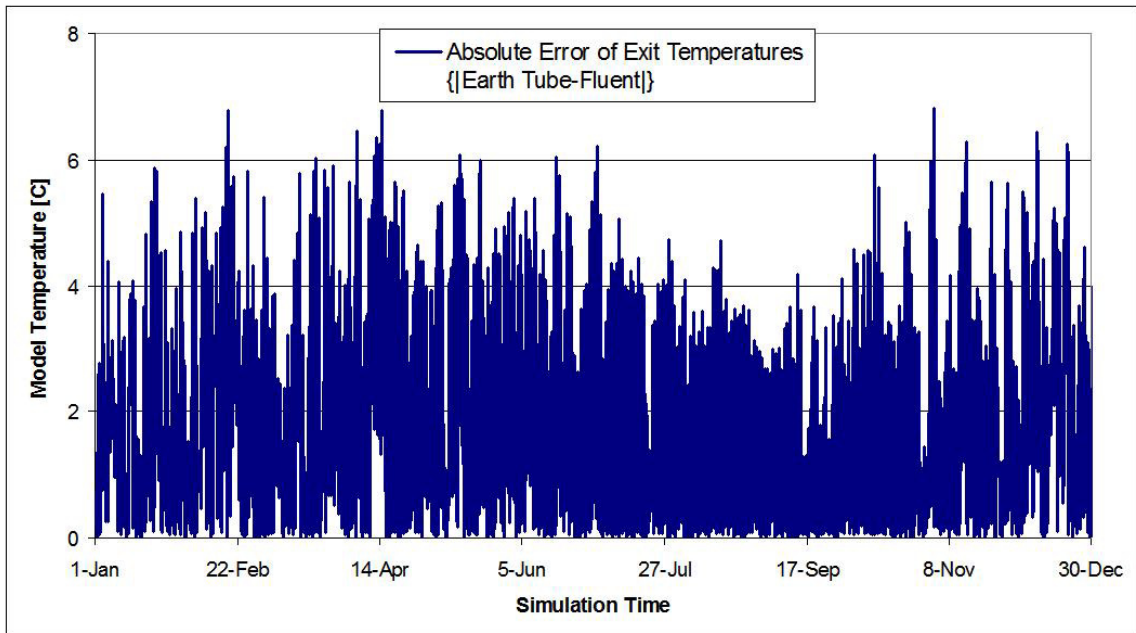


Figure 4.2: Earth Tube Models: Exit Air Temperature Deviations

temperature (inlet to output), but gives a more applicable aspect to the results. Most designers will care more about the heat transfer rate than predicted temperatures. Figure 4.3 shows the heat transfer rates predicted by the two models.

The heat transfer rates between the two models show the same basic trends, but differ drastically in actual values. Through the simulation, the heat transfer rate predicted by Fluent is up to four times as high as the earth tube model prediction. The model predicts higher heat transfer rates in both heating and cooling conditions. This shows that the earth tube model is, in fact, a conservative model. When a designer is using the earth tube model in EnergyPlus within a simulation, it should be noted that the earth tube may actually perform better than the model predicts.

Although the earth tube model does deviate from the Fluent model, the extreme increase in simplicity for model implementation and computation speed still make it a possible candidate to become a buried water pipe model. A Fluent model will also be developed to verify the model accuracy when the earth tube is converted to a buried pipe model. This model development is described in section 4.4.

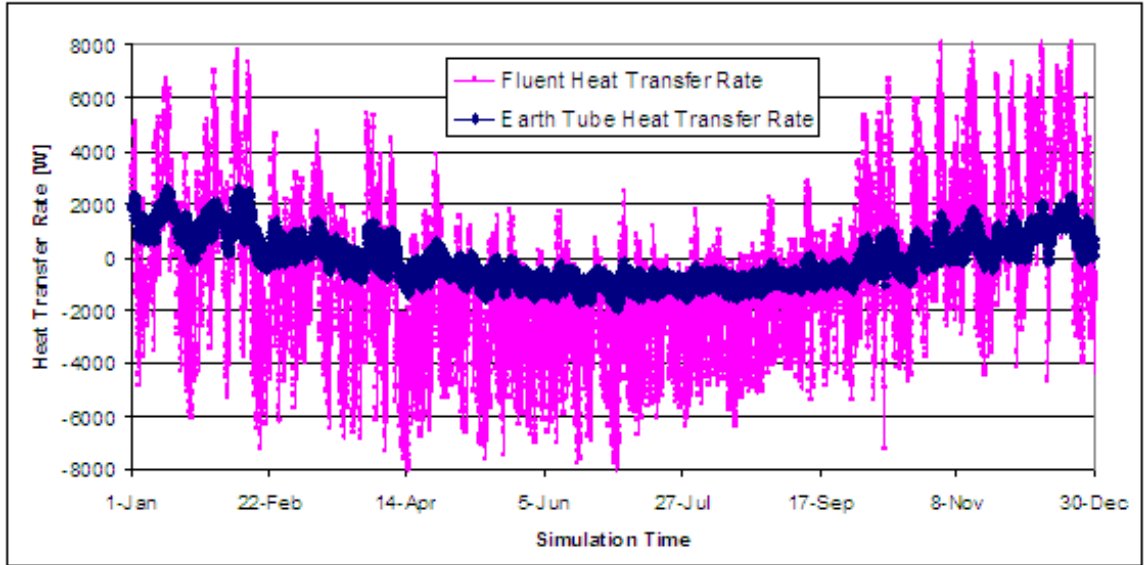


Figure 4.3: Earth Tube and Fluent Heat Transfer Rates

#### 4.4 Earth Tube Conversion to Pipe Model

This section describes the changes made to the earth tube model in order to simulate a buried pipe with water flow. For simplicity in this study, many simulation parameters will remain constant. The surface temperature will still be modeled by a sinusoidal wave in Fluent, using the same average and amplitude as the earth tube model. The pipe depth will remain constant, although the pipe diameter will change. The new pipe will be a 0.1 [m] nominal diameter pipe. The other boundary conditions will remain constant except for the inlet conditions. For this, a new set of boundary values based on ground source heat pump water temperatures will be used. This data was recorded at the Oklahoma State University Heat Pump Laboratory. The data is the entering water temperature to a set of vertical boreholes, so the data cannot be used as validation for a horizontal heat exchanger loop. However, the data does provide a semi-realistic input to the model. There is one key issue with simulating a short section of pipe and not an entire loop. The error in exiting temperature will have a tendency to propagate through the entire loop, and the entering water tem-

perature will be a function of the exiting water temperature. By using this entering temperature as the boundary condition, the small amount of error in the loop is corrected each new hour. If the full loop were run along with a heat pump model, this error may accumulate. This simulation is out of the context of the Fluent reference model, and requires long term validation data to account for these long term effects. However, as the current model is only for a buried pipe, using this entering water temperature data will ensure that the simulation is performed in the most realistic manner possible without drastic changes to the model itself. The values are summarized in appendix C, and the same values will be used in the Fluent model and the earth tube model. The water flow rate will also be different from the air flow rate. The water velocity will be decreased from 1.0 m/s to 0.15 m/s. For a pipe of 0.1 m diameter, this is on the order of 0.0012 m<sup>3</sup>/s, or 19 GPM. For typical standard conditions, this results in a Reynolds number of approximately 12,000. For the water flow, Fluent will automatically solve the momentum and boundary layer equations using water data instead of air data once this is selected as the working fluid. For the earth tube model, a new convection correlation will be required. With this Reynolds number known, the convection correlation can be specified in equation (4.8), with the correlation applicable over the range specified in Table 4.6, as found in Incropera & DeWitt (2002).

$$Nu_D = 0.027 Re_D^{4/5} Pr^{1/3} \left( \frac{\mu}{\mu_s} \right)^{0.14} \quad (4.8)$$

For the case of this simulation, the minimal property variations will not have a drastic effect on the results because the temperatures throughout the entire simulation vary only within a small range. This assumption should allow the last term in equation (4.8),  $\left( \frac{\mu}{\mu_s} \right)^{0.14}$ , to be neglected, thus simplifying the simulation.

With this convection correlation in place, the simulation can be performed. For an annual simulation with the given data, the resulting temperatures are shown in figure

Table 4.6: Convection Correlation Information for Circular Pipe Flow

Conditions:	Turbulent Flow Fully Developed $0.7 \leq \text{Pr} \leq 16,700$ $Re_D \geq 10,000$ $L/D \geq 10$
Variable	Description
$Re_D$	Reynolds number based on diameter
Pr	Fluid Prandtl number
$\mu$	Viscosity at fluid bulk temperature
$\mu_s$	Viscosity at film temperature

4.4. There are three curves shown: Pipe Inlet Temp, Pipe Outlet Temp, and Temp Deviation. The inlet and outlet are basic flow temperatures, although on this plot, the differentials are actually hard to see. With this simulation, the temperature difference from inlet to outlet is small, on the order of  $1^\circ\text{C}$ . This is why the differentials are also plotted. The temperature difference is plotted on a different scale to make it easier to visualize. As can be seen on the plot, the temperatures fluctuate widely. This is simulating the heat pump demand during the week, and then off on the weekends. The model predicts about  $1^\circ\text{C}$  of pre-cooling in the summer, and  $0.5^\circ\text{C}$  of preheating in the winter.

The Fluent model was also modified, as discussed previously. The main change in the mesh involves a smaller pipe diameter. This smaller pipe requires a tighter mesh as well, but this is a simple task to perform once a baseline journal file has been created for Gambit. The new pipe mesh was placed in Fluent, and the same simulation that was performed for the earth tube was repeated, with two changes: Pipe inlet temperature and working fluid. The simulation was initialized to data

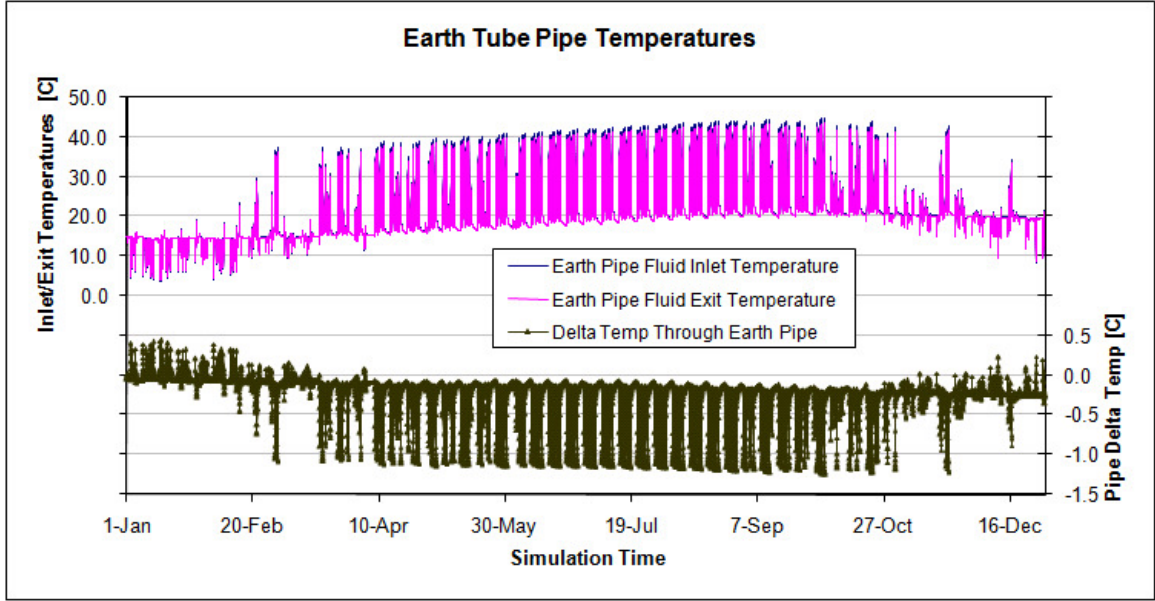


Figure 4.4: Earth Tube Pipe Model Results

at the first time step until steady state, and then the transient annual analysis was performed. The exit temperatures for both the Fluent pipe model and the earth tube pipe model are shown in figure 4.5.

Figure 4.5 shows that the Fluent model predicts a much higher pre-cooling rate during the summer, and a significant but lower pre-heating rate during the winter. To better visualize the differentials, the absolute value of the deviations is plotted in figure 4.6.

This difference means that, as with the earth tube model comparison, the earth tube is a conservative simulation. If used as a design tool, it appears that the actual performance will be higher. This is most likely due again to the Fluent model capability to better model heat storage in the ground. For the earth tube, the air has an effect on ground temperatures near the pipe, but this effect is small relative to the effect from a water pipe. For this water pipe, the heat storage in the ground is more prominent. Improper modeling of the ground capacity along with previously discussed model assumptions led to poor results from the modified earth tube model.



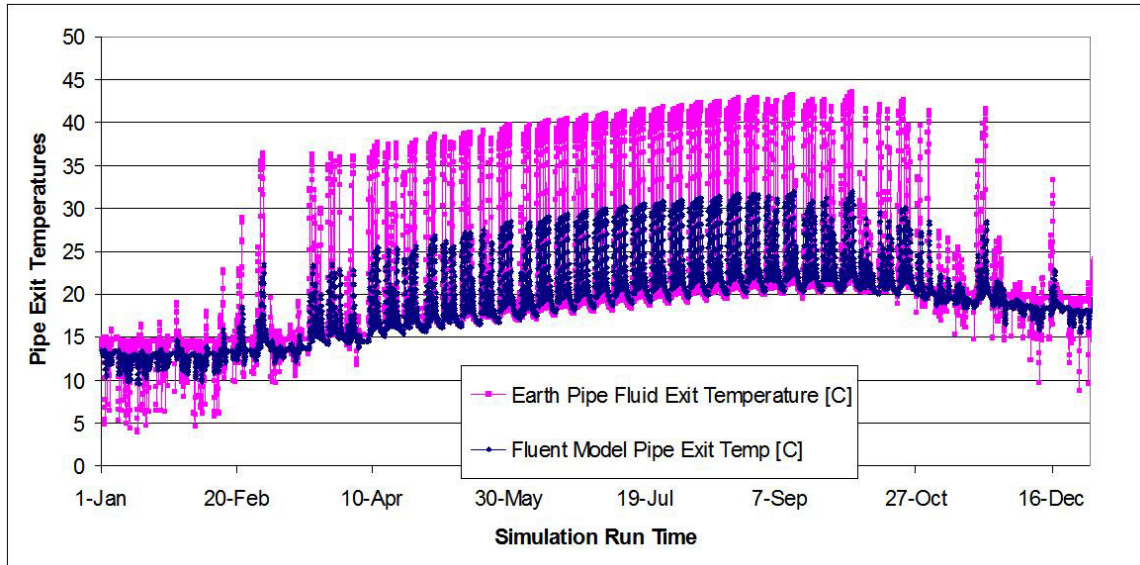


Figure 4.5: Fluent and Earth Tube Pipe Model Exit Temperatures

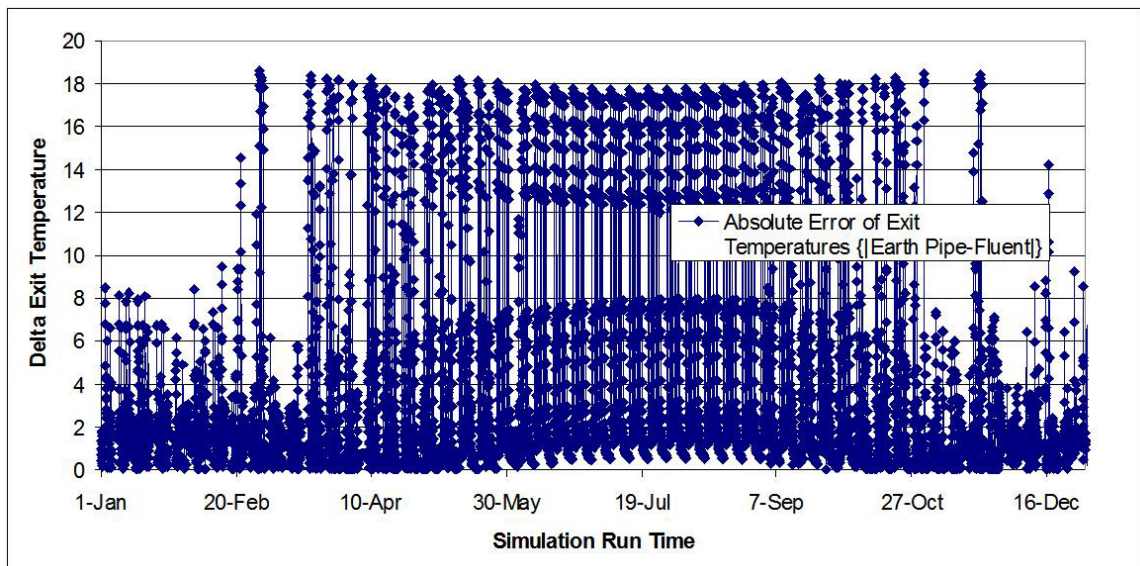


Figure 4.6: Fluent and Earth Tube Pipe Model Delta Exit Temperatures



## 4.5 Earth Tube Model Guidance

The results of the pipe study show that the earth tube model does not give good results when using water as the working fluid. One reason for this is the added thermal storage in the system. In a typical earth tube, the air flows through quickly, and the effects of the air are not as prominent in the ground as a flow of water. The model creates a steady state simulation at each time step, assuming a constant temperature in the ground near the pipe. With water, the ground absorbs and rejects significant heat which causes the variation in temperature along the length of pipe to be more intensified. An improvement to this model could be found in the calculation of the ground temperature in the near pipe region. Currently, surface temperature data is used in a correlation and this results in a temperature at the pipe depth, which is used as a boundary condition to the model. This temperature, however, is too close to be considered a far-field boundary. A serial model is not robust enough, and there should be some feedback from the pipe when generating a ground temperature. This is a difficult improvement when the model remains steady state.

The earth tube model is built upon deep underlying assumptions. Although the model has limitations, some general guidance is provided for situations where the earth tube model should provide higher accuracy. Due to the constant temperature assumption along the length of the pipe, the earth tube model accuracy should be improved in designs where the earth tube will not encounter major temperature variations through the ground along the length of the tube. This is similar to the statement that the earth tube model will be more accurate for cases where ground temperatures are dominated by ground-surface interaction rather than ground-pipe interaction.

- Minimal earth tube pipe length: The shorter the tube, the less chance there is for a temperature variation within the tube, and therefore within the ground.

When a shorter tube is in place, however, the entrance effects are much more definitive. The heat transfer coefficient will be higher in this entrance region due to the developing boundary layer, but overall, the heat transfer will be reduced.

- Increased flow rate: When the flow rate is reduced, the temperature difference in the fluid will be greater. This axial variation poses an opportunity for inaccuracy in the model. Therefore, it may be inferred that the model will increase accuracy with higher flow rate.
- Soil properties: With the earth tube model assuming steady state behavior at every time step, higher accuracy should be found in simulations that better approximate steady behavior. Higher values for soil conductivity and diffusivity lead to faster heat diffusion through the soil. This will in turn reduce the possibility for temperature variation in the soil. This will become a case that performs similar to a steady situation. With regard to soil properties, the higher diffusivity used should result in the higher accuracy model.

In addition to the model input guidance given above, a parametric study was performed with the earth tube model within the EnergyPlus simulation program to determine which of the model inputs have a significant impact to the simulation output. For the inputs with higher sensitivity, more time should be spent increasing the quality. If an input shows negligible sensitivity, time will be wasted trying to improve its quality. A simple earth tube model was set up for the annual simulation. The simulation contains a full building simulation, and the earth tube is applied to a single zone. The representative output for the model is selected as the furnace heat transfer rate. One at a time, the variables shown in table 4.7 were adjusted, and the change in coil energy requirements were recorded. The sensitivity was non-dimensionalized according to equation (4.9) with inputs  $X$  and outputs  $Y$ . The subscripts refer to

either 0 for the base case simulation or i for the simulation of case i.

$$\text{Sensitivity} = \frac{\frac{|Y_i - Y_0|}{Y_0}}{\frac{|X_i - X_0|}{X_0}} \quad (4.9)$$

With equation 4.9, the study revealed the data in table 4.7.

Table 4.7: Earth Tube Model Sensitivity Study Results

Case	Variable	Baseline	New Inp	Input Chg	Output Chg	Sensitivity
0	Baseline	-	-	-	-	-
1	Flow (m <sup>3</sup> /s)	1	1.25	0.25	0.0007	0.0028
2	Radius (m)	0.3048	0.4048	0.3281	0.0003	0.0008
3	Length (m)	50	75	0.5	0.0063	0.0127
4	Depth (m)	3	4.5	0.5	0.0002	0.0003

In addition to testing the sensitivity of the model, influence coefficients can provide another level of meaning to how the model responds to different inputs. Application of influence coefficients to building simulation are discussed in Spitler et al. (1989). These coefficients are similar to the sensitivity discussed previously. However, the estimated percent error is developed which includes the estimated error (uncertainty) in the input value. Equation (4.10) is used to define the type 2 dimensional influence coefficients, and equation (4.11) is used to define the percent error.

$$\text{Influence Coefficient} = \frac{\frac{Y_0 - Y_1}{Y_0}}{X_0 - X_1} \quad (4.10)$$

$$\text{Percent Error} = \text{Influence Coefficient} \cdot \text{Estimated Error in Input} \cdot 100 \quad (4.11)$$

The influence coefficients defined here are dimensional as they contain the inverse units of the input parameter. When the percent error is calculated, the estimated

error in input carries the input units also, which results in a dimensionless percent error, as expected. The four case results are presented in Table 4.8 in terms of influence coefficients and percent error. The uncertainty of the inputs was set to 5%.

Table 4.8: Earth Tube Model Influence Coefficients and Percent Error

Case	Variable	Influence Coefficient	Percent Error
1	Flow ( $\text{m}^3/\text{s}$ )	-0.00276	-1.378%
2	Radius (m)	-0.00251	-1.253%
3	Length (m)	-0.00025	-0.127%
4	Depth (m)	-0.00012	-0.058%

This influence coefficient study shows that the percent error in results is highest in the flow rate and pipe radius. The sensitivity of the model was shown above to be higher in the flow rate and pipe length input parameters. With this information, it is assumed that the highest possibility for model improvement is in the flow rate estimation. The simulation indicates that the earth tube model is sensitive to the flow rate, and a small uncertainty in the input parameter produces a percent error of about 1.4%.

## 4.6 Earth Tube Model Conclusions

The results of this chapter indicate that the earth tube model, as it operates currently, is not a suitable candidate for the buried pipe model. Other models will be compared throughout this study, most of which include a more substantial set of input data and require significantly more computation time. If none of these seem suitable, the earth tube model may become the basis of a new model that better handles heat storage in the soil and pipe.

## CHAPTER 5

### Mei Model

#### 5.1 Model Description

Mei (1986*a*) developed a model to predict heat transfer around a buried horizontal pipe. This model uses an explicit finite difference scheme, and develops update equations, which are used in a pseudo-3D environment along the pipe. As one would expect, this model uses symmetry to split the soil region in half, centered along the pipe. This model is considered simple due to a single cylindrical coordinate system. This gives a less complex algorithm within the code compared to other models which may mix coordinate systems. The original code, however, seems more complex, as the model was programmed using older FORTRAN conventions. This model was translated to VBA and tested in the Excel environment.

There are actually numerous advantages when using this model. One, already mentioned, is the single coordinate system. This simplifies the heat transfer equations in the domain. Another advantage this model has is that it allows for a backfill material to be used around the buried pipe. This ability is already in the code, so the only items a user must input are the material properties of the backfill material, and how thick the material is, and the program will automatically simulate the region accordingly. In this same manner, if no backfill material is used, this region can simply be set to the outer soil properties, and the program will run as normal, with soil filling the backfill region.

There are also some disadvantages of this model. The single radial coordinate system is centered on the centerline of the pipe, and extends the radius to the ground

surface (although the domain can be fully underground). The model layout can be seen in figure 5.1. This layout indicates that there will be a single node at the ground surface at each cross section. This does not seem to be as effective as spreading out nodes along the ground surface. However, testing may indicate that a single node is suitable for representation. Another disadvantage may be the distribution of grid points. This model does allow the grid points to be non-uniform in the radial direction in the soil, with fixed spacing in each of the backfill and pipe wall regions. However the variation in grid spacing can lead to stability problems.

The radial coordinate system is applied to nodes in different ways throughout the domain. The water at any given pipe cross section is represented as a single node. The pipe wall is represented by radial nodes; variations in the angular ( $\theta$ ) direction are ignored. This correlates to the assumption that the heat transfer up to the outer pipe wall is axisymmetric. Therefore, at a given cross section and radius, the pipe temperature is assumed constant for all angles. Moving outward radially, the pipe outer wall interfaces with the backfill region. The code has an interesting effect through this backfill region. There are nodes set up as if a full 2D (radial and angular) grid was set up, but the heat transfer only passes in the radial direction. This is analogous to breaking the domain up into a 3D grid, but ignoring the heat transfer along the axial direction. This allows a first-stage analysis of heat transfer varying with angle and therefore depth. Moving outward the next section is the main soil section. In this region, the domain is fully 2D, both angular and radial heat transfer effects are modeled. To better illustrate this grid, figure 5.1 describes the various domains and figure 5.2 shows the layout of the finite difference grid.

As mentioned previously, there are a number of assumptions that are used by the model, in order to develop a tractable solution. Some of these may turn out to be invalid in certain situations. The main assumptions used, as presented by Mei, are summarized as follows:

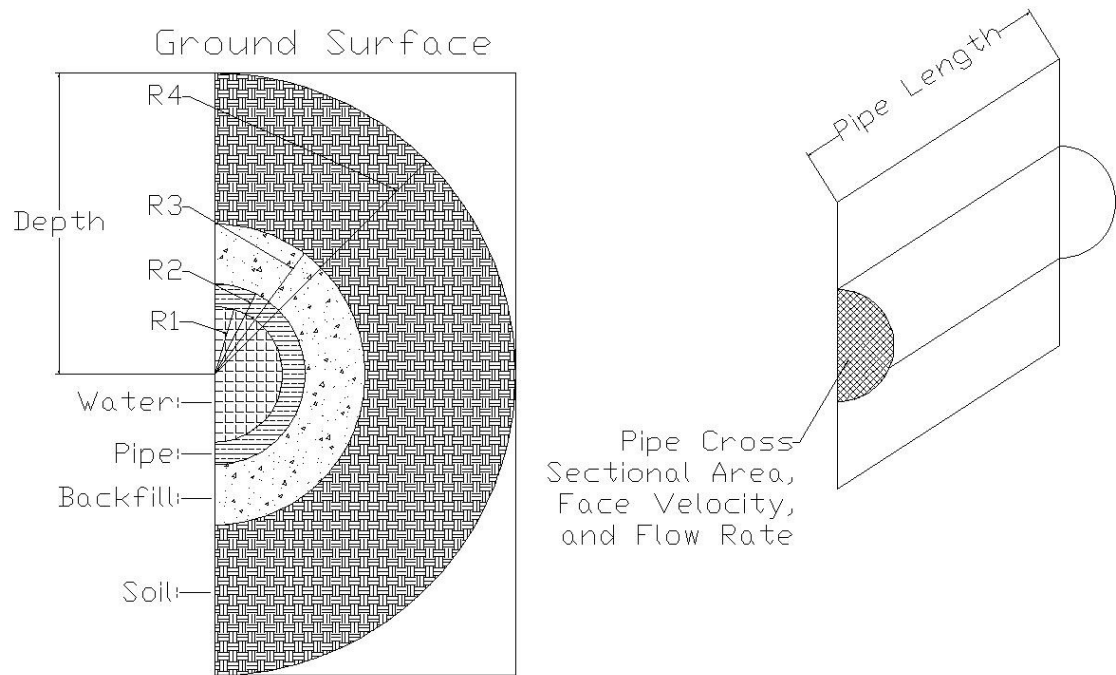


Figure 5.1: Mei Model Domain Description

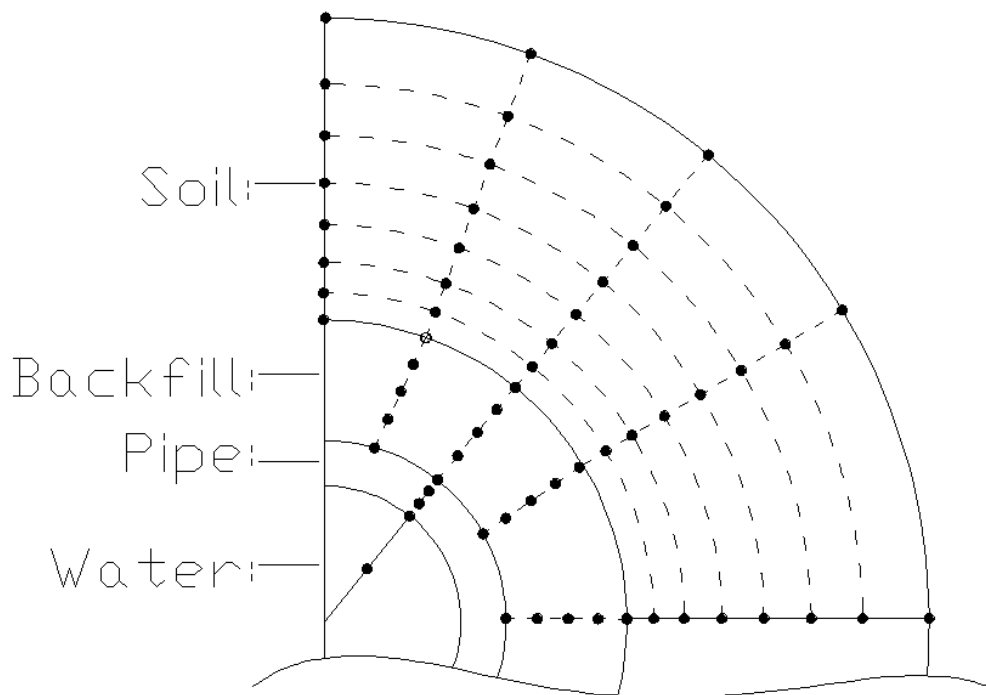


Figure 5.2: Mei Model Finite Difference Grid

- Homogeneous soil, which allows constant properties within the soil region. However, with the addition of the backfill region, a secondary homogeneous material (either a second soil type or pipe insulation) can be supplied for the analysis.
- Fluid temperature and velocity are constant at any cross section. This allows a single node to represent the fluid temperature and velocity within the pipe at any axial point.
- Pipe depth is great enough that the domain boundary can be considered a far-field boundary. This assumption allows the model to ignore surface heat transfer effects directly.
- There is only one pipe in the ground in the given domain.
- Heat transfer within the pipe up to the pipe wall is axisymmetric. This allows the heat transfer within this region to be 1D radial.

The model operates on a dual time step. The pipe wall and water nodes run at a shorter time step in an attempt to ensure convergence, while the backfill and soil nodes run at a much longer time step. This allows the accuracy and stability of a short time step only in the regions where it is required. In the backfill and soil regions, where the temperature gradients are smaller, a longer time step is more suitable.

As one would expect, since the model is broken down into four different regions (water, pipe wall, backfill, and soil), there are four different temperature arrays which hold the data. The water temperature array is defined in the program as  $U(\text{Length}, \text{Time Step})$ . The pipe wall temperature array is defined as  $T(\text{Radius}, \text{Length}, \text{Time})$ . In the backfill region, the heat transfer is modeled as pseudo 2D; the temperature can vary angularly, but the heat transfer along the angular direction is ignored. The array will therefore have four variables, and is defined as  $F(\text{Radius}, \text{Length}, \text{Angle}, \text{Time})$ . The final temperature array is the soil temperature



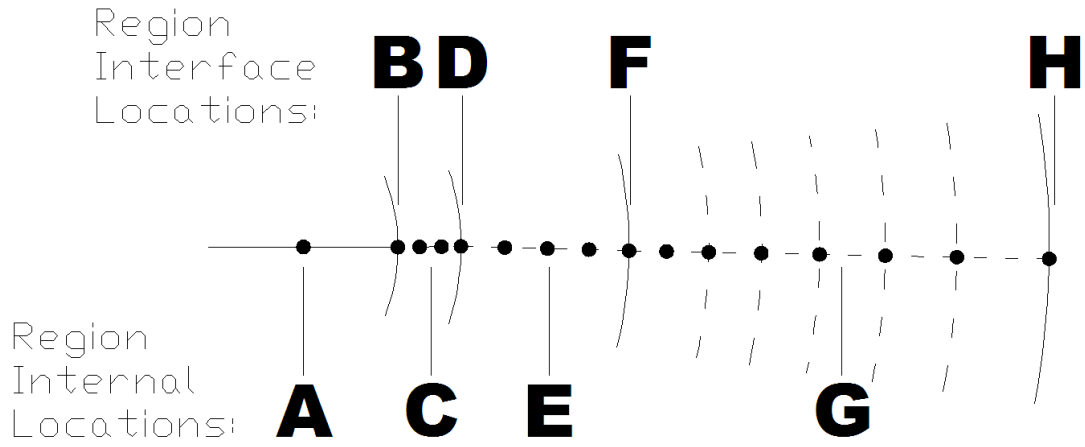


Figure 5.3: Mei Model Update Equation Locations

array. It is defined as  $S$  (Radius, Length, Angle, Time). These arrays are updated sequentially, according to specific update equations for the simulation domain and model conditions.

The flow of the model in its entirety is similar to other models. The model reads parameters supplied by the user, initializes the domain, starts the transient iterations, updates boundary temperatures, updates the water and pipe wall temperatures on the smaller time step and then updates the soil and backfill regions on the larger time step, writes output at each larger time step, and repeats until the simulation is complete. More detail is given later in this section as required.

The update equations differ based on the region and conditions. For instance, the pipe wall to water interface equations change depending on whether the flow is on or off. The different locations to which an update equation might be applied are shown in figure 5.3. Table 5.1 references the locations shown in figure 5.3, describes the conditions, and references the equation number of the update equation discussed in the following paragraphs.

In the equations, the independent variables have been simplified. The time step is not listed as a subscript as are the other variables. Instead, the convention has been

Table 5.1: Mei Model Update Equation Organization

Location (Figure 5.3)	Number (in text)	Description (Conditions)
A	5.1	Water Node, Flow ON, J=1
A	5.4	Water Node, Flow OFF, All Other J
B	5.3	Inner Pipe Wall, Flow ON
B	5.5	Inner Pipe Wall, Flow OFF
C	5.6	Internal Pipe Wall Node, All Conditions
D	5.7	Outer Pipe Wall, All Conditions
D	5.8	Inner Backfill Node, All Conditions
E	5.9	Internal Backfill, All Conditions
F	5.10	Outer Backfill, $\theta = 0$
F	5.11	Outer Backfill, $0 < \theta < \pi$
F	5.12	Outer Backfill, $\theta = \pi$
G	5.13	Soil, $\theta = 0$
G	5.14	Soil, $0 < \theta < \pi$
G	5.15	Soil, $\theta = \pi$
H	4.1	Far-field, All Conditions

Table 5.2: Mei Model Nomenclature

Parameters and Subscripts	Region Extents
Pipe Length	Inlet to Outlet
J	1 to NZ
Angular Location	Top to Bottom of Domain
M	1 to NRAD
Pipe Wall Radial Location	Pipe Centerline to Outer Pipe Wall
I	1 to NPIPE
Backfill Radial Location	Outer Pipe Wall to Outer Backfill
I	1 to NFZ
Soil Radial Location	Outer Backfill to Outer Domain Boundary
I	1 to NSOIL
Example Variable	Description
$U_J$	Water Temp at Length J
$T_{I,J}$	Pipe Wall Temp at Radius I, Length J
$F_{I,J,M}$	Backfill Temp at Rad I, Length J, Angle M
$S_{I,J,M}$	Soil Temp at Radius I, Length J, Angle M

applied which uses the prime ' notation to denote the updated time step. Aside from the time step, the independent variables are given in table 5.2.

As mentioned, the variables in this section represent both the updated temperatures and the temperature from the previous time step. The updated temperatures are denoted with a prime, such as  $F'_{I,J,M}$ . Note that with this dual time step program, the main outer time step, which runs the soil and backfill regions, is denoted  $\Delta t_1$ . The inner time step, which runs the coil wall and water nodes, is denoted  $\Delta t_2$ . These variables will appear throughout these equations.

In this domain, there are a number of radii which are very specific. The general

radius term is denoted  $r_I$ , and can be used within any of the regions. There are also four specific radii that represent specific interfaces in the domain. These, along with the last variables of interest in these equations, are denoted and defined in the following:

- $r_1$ : Inner Pipe Wall Radius
- $r_2$ : Outer Pipe Wall Radius / Inner Backfill Radius
- $r_3$ : Outer Backfill Radius / Inner Soil Radius
- $r_4$ : Outer Soil Radius / Far-field Boundary Radius
- $h$ : Water to Pipe Convection Coefficient
- $\vec{V}$ : Flow Velocity
- $\Delta r$ : Radial spacing: This variable has a constant value in the pipe wall and backfill regions, but is non-uniform in the soil region. Therefore, the radial spacing is dependent on the current radius.

The first set of equations presented here are applied to the water and inner pipe wall nodes when the flow is on.

$$U'_1 = \left(1 - \vec{V} \frac{dT}{dz} - \frac{2h\Delta t_2}{\rho_f C_{p_f} r_1}\right) U_1 + \left(\vec{V} \frac{dT}{dz}\right) \text{E.W.T.} + \left(\frac{2h\Delta t_2}{\rho_f C_{p_f} r_1}\right) T_{1,1} \quad (5.1)$$

$$U'_J = \left(1 - \vec{V} \frac{dT}{dz} - \frac{2h\Delta t_2}{\rho_f C_{p_f} r_1}\right) U_J + \left(\vec{V} \frac{dT}{dz}\right) U_{J-1} + \left(\frac{2h\Delta t_2}{\rho_f C_{p_f} r_1}\right) T_{1,J} \quad (5.2)$$

$$\begin{aligned} T'_{1,J} = & \left(1 - \frac{\alpha_{\text{pipe}} \Delta t_2}{\Delta r_{\text{pipe}}} \left(\frac{2}{\Delta r_{\text{pipe}}} + \frac{1}{r_1}\right) - \frac{2\alpha_{\text{pipe}} \Delta t_2 h}{\Delta r_{\text{pipe}} k_{\text{pipe}}}\right) T_{1,J} \\ & + \left(\frac{\alpha_{\text{pipe}} \Delta t_2}{\Delta r_{\text{pipe}}} \left(\frac{2}{\Delta r_{\text{pipe}}} + \frac{1}{r_1}\right)\right) T_{2,J} + \left(\frac{2\alpha_{\text{pipe}} \Delta t_2 h}{\Delta r_{\text{pipe}} k_{\text{pipe}}}\right) U_J \end{aligned} \quad (5.3)$$

Equations (5.4) and (5.5) are used when the flow in the pipe is off.

$$U'_J = U_J + \frac{2k_{pipe} (T_{2,J} - T_{1,J}) \Delta t_2}{\rho_f C p_f r_1^2 \log \left( 1 + \frac{\Delta r_{pipe}}{r_1} \right)} \quad (5.4)$$

$$T'_{1,J} = U'_J \quad (5.5)$$

Once the simulation has left the inner pipe wall surface, the equations are no longer dependent on the flow being on or off. Therefore, all of the remaining equations in this discussion are applied for both flow on and flow off conditions. Equations (5.6) and (5.7) are for the rest of the pipe wall nodes, both interior nodes and outer pipe wall surface node, respectively. In equation (5.7), a term TAVG has been introduced. Within the pipe wall, there is a single set of pure radial nodes. Outside the pipe wall, there are multiple nodes in the angular direction, even though angular interaction is neglected. Therefore at the outer pipe wall interface, the grid turns from a single 1D radial grid to a number of radial grid points. The single interior node must interact with the multiple grid points outside the pipe wall. Therefore, it is assumed that the one outer pipe wall node interacts with the average of all innermost backfill nodes. This average of the backfill nodes which are directly adjacent to the pipe wall is called TAVG for brevity.

$$T'_{I,J} = \left( 1 - \frac{\alpha_{pipe} \Delta t_2}{\Delta r_{pipe}} \left( \frac{1}{\Delta r_{pipe}} + \frac{1}{r_I} \right) - \frac{\alpha_{pipe} \Delta t_2}{\Delta r_{pipe}^2} \right) T_{I,J} + \left( \frac{\alpha_{pipe} \Delta t_2}{\Delta r_{pipe}} \left( \frac{1}{\Delta r_{pipe}} + \frac{1}{r_I} \right) \right) T_{I+1,J} + \left( \frac{\alpha_{pipe} \Delta t_2}{\Delta r_{pipe}^2} \right) T_{I-1,J} \quad (5.6)$$

$$T'_{Npipe,J} = \left( 1 - 2 \frac{k_{fill}}{k_{pipe}} \frac{\alpha_{pipe} \Delta t_2}{\Delta r_{pipe} \Delta r_{fill}} - \frac{\alpha_{pipe} \Delta t_2}{\Delta r_{pipe}} \left( \frac{2}{\Delta r_{pipe}} - \frac{1}{r_2} \right) \right) \times T_{Npipe,J} + \left( 2 \frac{k_{fill}}{k_{pipe}} \frac{\alpha_{pipe} \Delta t_2}{\Delta r_{pipe} \Delta r_{fill}} \right) T_{AVG} + \left( \frac{\alpha_{pipe} \Delta t_2}{\Delta r_{pipe}} \left( \frac{2}{\Delta r_{pipe}} - \frac{1}{r_2} \right) \right) T_{Npipe-1,J} \quad (5.7)$$

When the simulation has reached this point, both the water and the pipe wall nodes have been simulated. This occurs at a time step of  $\Delta t_2$ . The simulation then moves on to the backfill region and simulates at a time step of  $\Delta t_1$ . There are three sub-regions in the backfill region, the inner node, interior nodes, and the outer node. Each of these are defined individually in equations (5.8) through (5.12).

$$F'_{1,J,M} = T'_{J,NPipe} \quad (5.8)$$

$$\begin{aligned} F'_{I,J,M} = & \left( 1 - \frac{\alpha_{fill} \Delta t_1}{\Delta r_{fill}} \left( \frac{1}{\Delta r_{fill}} + \frac{1}{r_I} \right) - \frac{\alpha_{fill} \Delta t_1^2}{\Delta r_{fill}} \right) F_{I,J,M} \\ & + \left( \frac{\alpha_{fill} \Delta t_1}{\Delta r_{fill}} \left( \frac{1}{\Delta r_{fill}} + \frac{1}{r_I} \right) \right) F_{I+1,J,M} + \left( \frac{\alpha_{fill} \Delta t_1^2}{\Delta r_{fill}} \right) F_{I-1,J,M} \end{aligned} \quad (5.9)$$

Once the simulation has reached the outermost backfill node, the grid has three possible equations based on the node location. Even though the update equations in the interior of the backfill region are only derived in the radial direction, the soil region is derived in both the radial and the angular directions. The grid points along the interface of the backfill and soil regions are derived to match the soil region. Because of the angular dependence, the grid points at the angular domain extents will encounter the adiabatic (symmetric) boundary. This leads to three different update equations, one for  $M=1$  ( $\theta = 0$  radians at the top of the domain), one for  $M=NRAD$  ( $\theta = \pi$  radians at the bottom of the domain), and one for the interior points. These locations are described in figure 5.4. The equations follow.

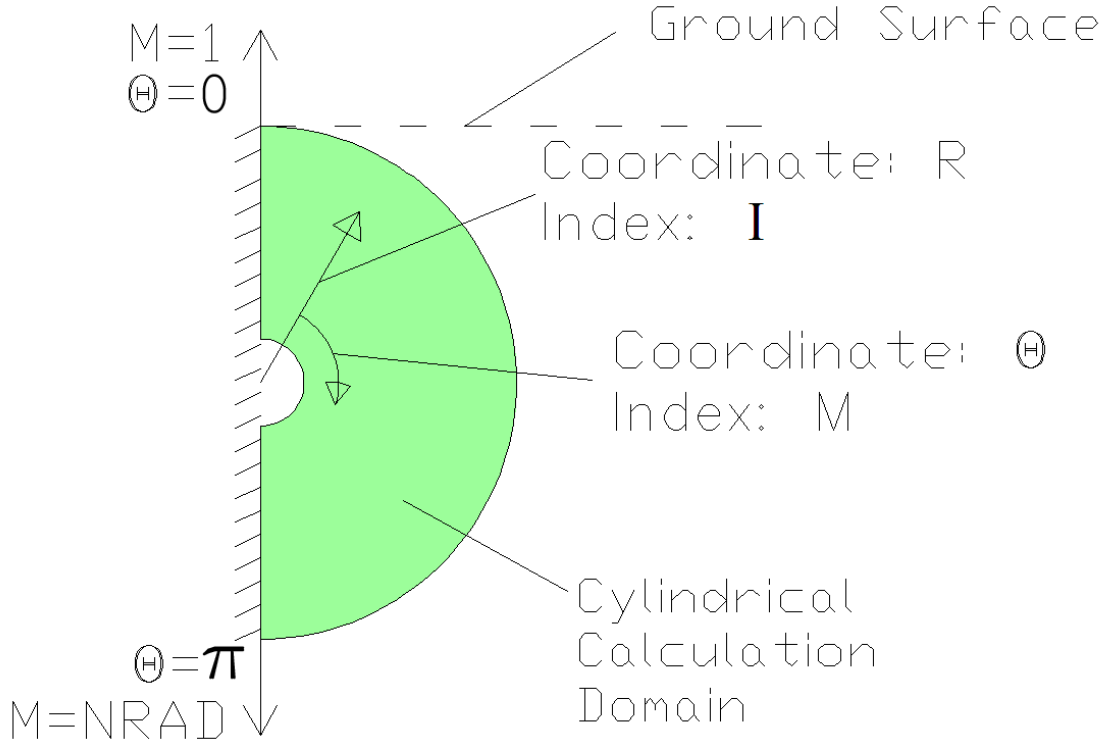


Figure 5.4: Mei Model Description: Angular Grid Locations

$$\begin{aligned}
 F'_{NFZ,J,1} = & \left( \frac{2k_{\text{soil}}\alpha_{\text{fill}}\Delta t_1}{k_{\text{fill}}\Delta r_{\text{soil},1}\Delta r_{\text{fill}}} \right) S_{2,J,1} \\
 & + \left( \frac{2\alpha_{\text{fill}}\Delta t_1}{\Delta r_{\text{fill}}} \left( \frac{1}{\Delta r_{\text{fill}}} - \frac{1}{2r_3} \right) \right) F_{NFZ-1,J,1} \\
 & + \left( \frac{\alpha_{\text{fill}}\Delta t_1}{(r_3\Delta\theta)^2} \right) 2F_{NFZ,J,M+1} + F_{NFZ,J,1} \\
 & \times \left( 1 - \frac{2k_{\text{soil}}\alpha_{\text{fill}}\Delta t_1}{k_{\text{fill}}\Delta r_{\text{soil},1}\Delta r_{\text{fill}}} - \frac{2\alpha_{\text{fill}}\Delta t_1}{\Delta r_{\text{fill}}} \left( \frac{1}{\Delta r_{\text{fill}}} - \frac{1}{2r_3} \right) - 2\frac{\alpha_{\text{fill}}\Delta t_1}{(r_3\Delta\theta)^2} \right)
 \end{aligned} \tag{5.10}$$

$$\begin{aligned}
F'_{NFZ,J,M} = & \left( \frac{2k_{\text{soil}}\alpha_{\text{fill}}\Delta t_1}{k_{\text{fill}}\Delta r_{\text{soil},1}\Delta r_{\text{fill}}} \right) S_{2,J,M} \\
& + \left( \frac{2\alpha_{\text{fill}}\Delta t_1}{\Delta r_{\text{fill}}} \left( \frac{1}{\Delta r_{\text{fill}}} - \frac{1}{2r_3} \right) \right) F_{NFZ-1,J,M} \\
& + \left( \frac{\alpha_{\text{fill}}\Delta t_1}{(r_3\Delta\theta)^2} \right) (F_{NFZ,J,M+1} + F_{NFZ,J,M-1}) + F_{NFZ,J,M} \\
& \times \left( 1 - \frac{2k_{\text{soil}}\alpha_{\text{fill}}\Delta t_1}{k_{\text{fill}}\Delta r_{\text{soil},1}\Delta r_{\text{fill}}} - \frac{2\alpha_{\text{fill}}\Delta t_1}{\Delta r_{\text{fill}}} \left( \frac{1}{\Delta r_{\text{fill}}} - \frac{1}{2r_3} \right) - 2\frac{\alpha_{\text{fill}}\Delta t_1}{(r_3\Delta\theta)^2} \right)
\end{aligned} \tag{5.11}$$

$$\begin{aligned}
F'_{NFZ,J,NRAD} = & \left( \frac{2k_{\text{soil}}\alpha_{\text{fill}}\Delta t_1}{k_{\text{fill}}\Delta r_{\text{soil},1}\Delta r_{\text{fill}}} \right) S_{2,J,M} \\
& + \left( \frac{2\alpha_{\text{fill}}\Delta t_1}{\Delta r_{\text{fill}}} \left( \frac{1}{\Delta r_{\text{fill}}} - \frac{1}{2r_3} \right) \right) F_{NFZ-1,J,M} \\
& + \left( \frac{\alpha_{\text{fill}}\Delta t_1}{(r_3\Delta\theta)^2} \right) 2F_{NFZ,J,M-1} + F_{NFZ,J,NRAD} \\
& \times \left( 1 - \frac{2k_{\text{soil}}\alpha_{\text{fill}}\Delta t_1}{k_{\text{fill}}\Delta r_{\text{soil},1}\Delta r_{\text{fill}}} - \frac{2\alpha_{\text{fill}}\Delta t_1}{\Delta r_{\text{fill}}} \left( \frac{1}{\Delta r_{\text{fill}}} - \frac{1}{2r_3} \right) - 2\frac{\alpha_{\text{fill}}\Delta t_1}{(r_3\Delta\theta)^2} \right)
\end{aligned} \tag{5.12}$$

With these equations applied at M=1 through M=NRAD, the backfill region outer interface is complete, and the simulation can move to the soil region. The soil domain is meshed into a full 2D polar grid. This mesh is similar to the interface of the backfill and the soil in that there will be three different update equations based on the angular location. These three equations account for the adiabatic surfaces at the top and bottom of the left side of the domain, as well as the internal points. This mesh structure can be visualized as before in figure 5.4. Equations (5.13), (5.14), and (5.15) are for M=1 points, Internal points, and M=NRAD points, respectively.



$$\begin{aligned}
S'_{I,J,1} = & \left( 1 - \frac{2\alpha_{\text{soil}}\Delta t_1}{\Delta r_{\text{soil},I}\Delta r_{\text{soil},I-1}} - \frac{\alpha_{\text{soil}}\Delta t_1}{\Delta r_{\text{soil},I-1}} \left( \frac{2}{\Delta r_{\text{soil},I-1}} - \frac{1}{r_I} \right) - \frac{\alpha_{\text{soil}}\Delta t_1}{(r_I\Delta\theta)^2} \right) \\
& \times S_{I,J,1} + \left( \frac{2\alpha_{\text{soil}}\Delta t_1}{\Delta r_{\text{soil},I}\Delta r_{\text{soil},I-1}} \right) S_{I+1,J,1} \\
& + \left( \frac{\alpha_{\text{soil}}\Delta t_1}{\Delta r_{\text{soil},I-1}} \left( \frac{2}{\Delta r_{\text{soil},I-1}} - \frac{1}{r_I} \right) \right) S_{I-1,J,1} \\
& + \left( \frac{\alpha_{\text{soil}}\Delta t_1}{(r_I\Delta\theta)^2} \right) 2S_{I,J,2}
\end{aligned} \tag{5.13}$$

$$\begin{aligned}
S'_{I,J,M} = & \left( 1 - \frac{2\alpha_{\text{soil}}\Delta t_1}{\Delta r_{\text{soil},I}\Delta r_{\text{soil},I-1}} - \frac{\alpha_{\text{soil}}\Delta t_1}{\Delta r_{\text{soil},I-1}} \left( \frac{2}{\Delta r_{\text{soil},I-1}} - \frac{1}{r_I} \right) - \frac{\alpha_{\text{soil}}\Delta t_1}{(r_I\Delta\theta)^2} \right) \\
& \times S_{I,J,M} + \left( \frac{2\alpha_{\text{soil}}\Delta t_1}{\Delta r_{\text{soil},I}\Delta r_{\text{soil},I-1}} \right) S_{I+1,J,M} \\
& + \left( \frac{\alpha_{\text{soil}}\Delta t_1}{\Delta r_{\text{soil},I-1}} \left( \frac{2}{\Delta r_{\text{soil},I-1}} - \frac{1}{r_I} \right) \right) S_{I-1,J,M} \\
& + \left( \frac{\alpha_{\text{soil}}\Delta t_1}{(r_I\Delta\theta)^2} \right) (S_{I,J,M+1} + S_{I,J,M-1})
\end{aligned} \tag{5.14}$$

$$\begin{aligned}
S'_{I,J,NRAD} = & \left( 1 - \frac{2\alpha_{\text{soil}}\Delta t_1}{\Delta r_{\text{soil},I}\Delta r_{\text{soil},I-1}} - \frac{\alpha_{\text{soil}}\Delta t_1}{\Delta r_{\text{soil},I-1}} \left( \frac{2}{\Delta r_{\text{soil},I-1}} - \frac{1}{r_I} \right) - \frac{\alpha_{\text{soil}}\Delta t_1}{(r_I\Delta\theta)^2} \right) \\
& \times S_{I,J,NRAD} + \left( \frac{2\alpha_{\text{soil}}\Delta t_1}{\Delta r_{\text{soil},I}\Delta r_{\text{soil},I-1}} \right) S_{I+1,J,NRAD} \\
& + \left( \frac{\alpha_{\text{soil}}\Delta t_1}{\Delta r_{\text{soil},I-1}} \left( \frac{2}{\Delta r_{\text{soil},I-1}} - \frac{1}{r_I} \right) \right) S_{I-1,J,NRAD} \\
& + \left( \frac{\alpha_{\text{soil}}\Delta t_1}{(r_I\Delta\theta)^2} \right) 2S_{I,J,NRAD-1}
\end{aligned} \tag{5.15}$$

Thus all interior points of the calculation domain have been acknowledged. The only points which do not have an update equation given here are along the outer far-field boundary. The depth of each boundary point in this radial domain is calculated

based on input geometry. With the current node depth and simulation time known, the Kusuda and Achenbach correlation which has been discussed previously in this work is used to update the node at each outer time step. The Kusuda correlation used here is very similar to equation (4.1). More detail is provided in section 5.3.4.

## 5.2 Modifications to Mei Model

After the initial implementation of the Mei model, some modifications were required to fit better with the current implementation language and some features were removed or modified. The structure of the original program was very difficult to understand because the programming did not include some common structures such as the 'Else-If' command. Without a structure such as this, the code must wind in and out with hundreds of 'GOTO' statements, rendering it quite difficult to follow. Thus the program was modified and updated with newer command structures whenever possible.

As for actual model features, there were two items which were modified: specification of the backfill region, and temperature arrays to store previous values of backfill and soil nodal temperatures. In the original program, the use of a backfill region was optional. This allowed a user to place the pipe in direct contact with the soil. However, this option introduces many additional equations. In order to simplify the program, the option was removed, and the backfill region is now in place all the time. This does not actually limit the program in any way. To simulate the pipe without a backfill region, one can simply specify the backfill properties to be the same as the soil properties. The second change involved the storage of values from previous time steps. Although it may have been a simple omission, the code in Mei's report never included storing the backfill and soil temperatures at the end of each time step. This was revealed during testing as discussed in section 5.3.3. The addition of storage resulted in a model that performed as expected.

### 5.3 Model Testing

After initially debugging the model, it appeared to be operating correctly. However, tests were performed to help reveal any underlying model problems. The first test was a simple test where the entering water temperature and all boundary conditions were set to the same temperature. If the model were operating correctly, there would be essentially no response from the model, just constant temperatures everywhere. For the second test, the inputs to the Mei model were adjusted to mimic a constant pipe wall temperature condition. This was set by carefully adjusting the conductivities and other parameters. In the third test, the model was run for different initial conditions to determine convergence characteristics and to ensure that the model was properly updating each temperature node. In the fourth test, the flow rate was increased to eliminate axial heat transfer effects and to assess the 2D effects calculated by the models.

#### 5.3.1 Fully Constant Model Testing

This test was designed to ensure that the model algorithm and update equations are defined properly. If the update equations are not implemented properly, heat transfer may be simulated through nodes when it should not, simply because of an error in a coefficient. During this test, the boundary temperatures and inlet water temperature were set to a constant value of 50°F. The model responded properly to these boundary conditions. This test served to establish some confidence in the model implementation.

#### 5.3.2 Constant Wall Temperature Testing

This test approximates an analytic solution. The analytic solution is simply a constant pipe wall temperature solution for exiting fluid temperature as a function of entering water temperature. A more detailed discussion of the analytic solution is

given in section 6.4.2. In this test, the Mei model was modified to approximate a constant pipe wall. The conductivities in the backfill region, soil region, and pipe wall were increased to the order of 999 Btu/hr-ft-F, and the outer boundary temperature was held constant. With the high conductivities, this boundary temperature should transfer quickly to the inner pipe wall. This test was performed with a boundary temperature of 50°F and an entering water temperature of 0°F. The test was repeated for several different pipe lengths to see the model behavior. At each run, the pipe inner surface temperature along the length of the pipe was recorded. With this numerical scheme, it is nearly impossible to get the pipe temperatures to exactly 50° while achieving model convergence. Therefore, an average surface temperature for each run was found, and this was used as the surface temperature in the analytic solution. The exiting water temperature for the numerical case was then compared to the analytic solution. The main analytic equation governing the exiting fluid temperature is given here as equation (5.16), but as mentioned, the full development is in section 6.4.2. As is also mentioned in that section, the analytic solution was applied to small segments of the pipe in order to improve the comparison with the Mei model.

$$T_2 = \frac{k0.023 \left( \frac{\rho DV}{\mu} \right)^{0.8} Pr^{0.4} \pi L \left( T_s - \frac{T_1}{2} \right) + \dot{m} C_p T_1}{\frac{k}{2} 0.023 \left( \frac{\rho DV}{\mu} \right)^{0.8} Pr^{0.4} \pi L + \dot{m} C_p} \quad (5.16)$$

The results of this study for the Mei model are given in figure 5.5. At the lengths reported, the models agree to within 5%. This test removes the soil modeling from the simulation, and with this high agreement, increases the confidence in the water modeling of the simulation.

The dual time step, which allows the soil to run at a long time step while the pipe wall and water node can run at a short time step, is required for convergence. With a thin pipe, the pipe node spacing becomes very small. When these small nodes are

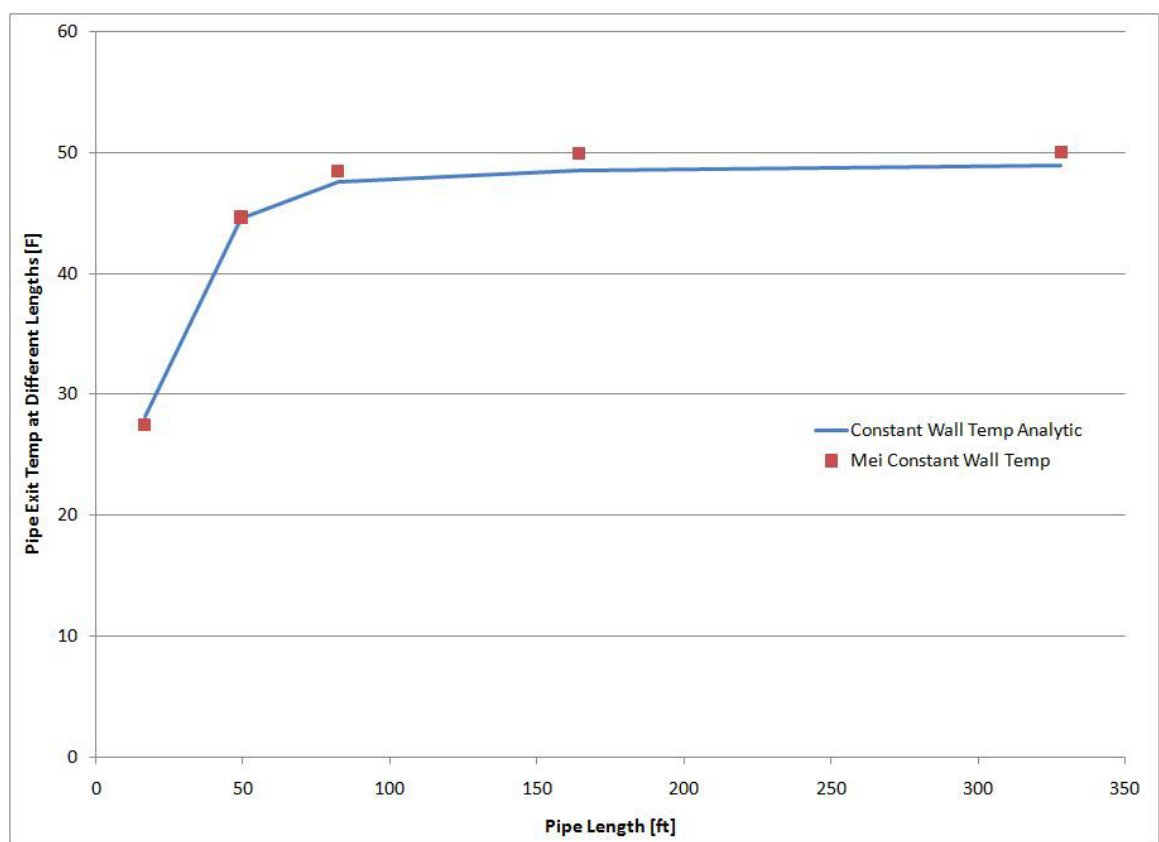


Figure 5.5: Mei Model Test Results: Constant Wall Temperature

encountered, a substantially short time step must also be used. During this specific test of constant wall temperature, conductivity values were set above realistic values. This was required in order to quickly translate the boundary temperatures to the pipe wall. The conductivity plays a role in the update equation coefficients, and when these values were increased, the model had serious convergence problems. In order to achieve convergence, the model was run at a 30 minute outer time step, and a .001 minute inner time step. For normal conductivities, initial tests revealed that for an outer time step of one hour, an inner time step of 0.1 minute was required for convergence. The minimum system time step in EnergyPlus is one minute. In order for this model to be implemented in EnergyPlus, an outer structure would be required to simulate this model a number of times during a single EnergyPlus time step. This stability limit does not completely eliminate the possibility of implementing the Mei model in EnergyPlus, but it does introduce another level of complexity to the model and the implementation.

### **5.3.3 Initial Condition Independence Testing**

In order to ensure that the model was properly updating the temperatures at each node, a series of initial conditions were placed on the model. The model was then run for a period until the results converged. Figure 5.6 shows the results. In the first test, an initial condition of 0°F was placed on every node in the model domain. In the second test, the entire model domain was initialized to the Kusuda and Achenbach predicted temperature at the pipe burial depth. In the third test, the model domain was initialized to 100°F. Figure 5.6 shows that even with the extreme initializations of tests one and three, the model converges, though over two weeks worth of simulation time was required!

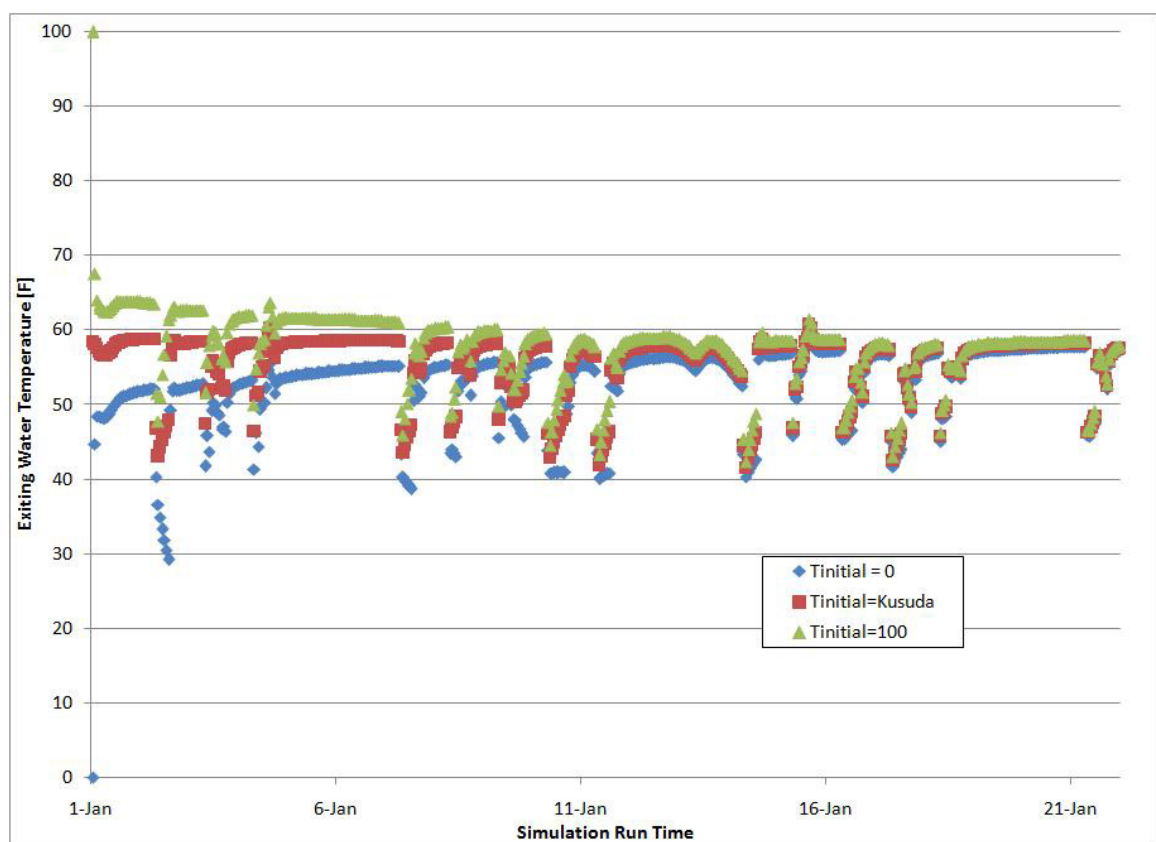


Figure 5.6: Mei Model Test Results: Initial Condition Independence

### 5.3.4 High Flow Rate Testing (2D Model Simulation)

The Mei model does not account for the axial heat transfer effects in the soil or pipe wall. The water in the pipe is the only region which carries heat along the length of the pipe. The Fluent model, however, includes heat transfer in all dimensions. Because of this difference, it is necessary to perform a test which can simulate the ability of the models to simulate in just two dimensions (eliminating the axial dependence). This is performed by substantially increasing the flow rate through the pipe. With this higher flow rate, the fluid will experience almost no temperature change along the entire length of the pipe. If the boundary conditions also do not change along the length of the pipe, two dimensional heat transfer will result.

This test marks the first comparison between the Mei model and the Fluent verification model. The Mei model is a cylindrical domain. The Fluent verification model is a rectangular based domain. For many of the boundary conditions, this will not have an effect. In the far-field boundary condition, however, a deviation will occur between the two models. Both models will use the Kusuda and Achenbach correlation to develop the boundary temperatures. In order to create a pseudo steady-state model, the simulation time will be set to zero so that this Kusuda temperature field will not change throughout the iterations. The Fluent model will use the Kusuda and Achenbach directly on the ground surface (no outdoor air interaction), and the far-field (side wall) boundary, and the deep ground boundary. The Mei model will use the Kusuda and Achenbach correlation directly on the cylindrical perimeter of the model. The Mei model does not differentiate between the deep ground and side boundaries, because it is one outer surface boundary in cylindrical coordinates. Figure 5.7 shows the boundaries for both models.

While increasing the flow rate, a value will be reached where the axial effects are



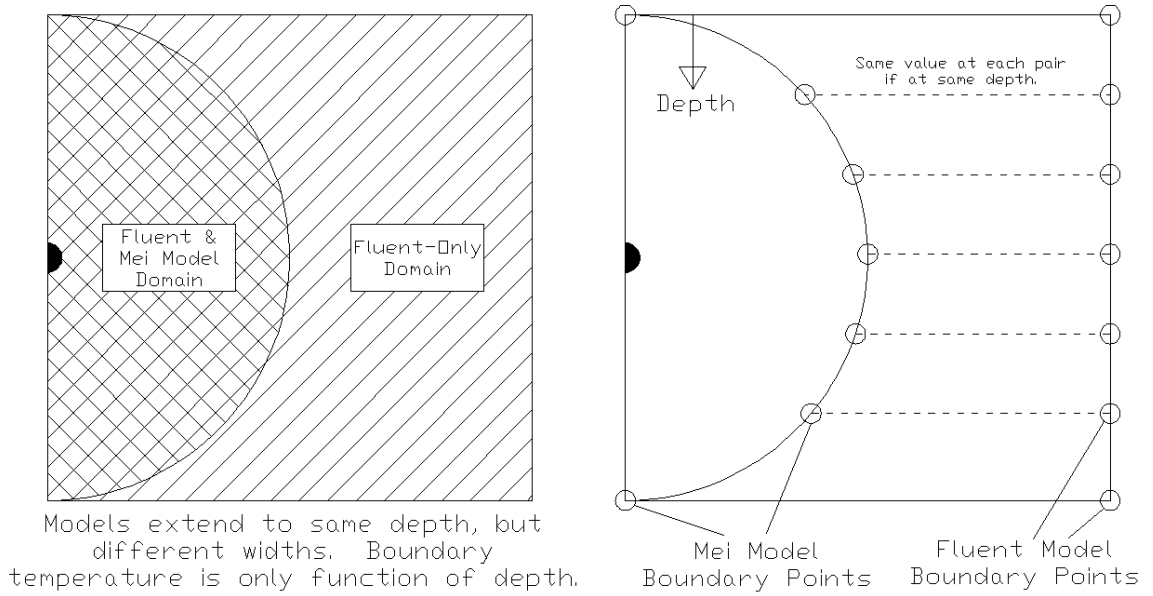


Figure 5.7: Mei and Fluent Model Boundary Differences

negligible. In the Mei model, the fluid enters at  $37^{\circ}\text{C}$ , with a flow rate of  $0.24 \frac{\text{m}^3}{\text{s}}$ . The flow was increased similarly in the Fluent model. The removal of axial heat transfer from the model should help to reveal two things: whether the models agree when only 2D heat transfer effects are concerned, and if the different boundary type seem to have an effect on overall model agreement.

Both of these models are transient in nature, and therefore include the effects of heat storage in the soil and other regions where appropriate. In order to perform this analysis, the models were run until a steady condition was achieved. In the Fluent model, one could turn the model to a steady behavior by switching model parameters, and letting it run until convergence. However, in the interest of comparing these two models in their base configurations, they were both left as transient. To monitor for steady conditions, some variables had to be recorded. For the Mei model, representative temperatures at numerous locations throughout the domain were printed at each time step. In the Fluent model, temperature output is not as convenient, so the overall heat transfer from the pipe wall was recorded, and monitored for steady

behavior.

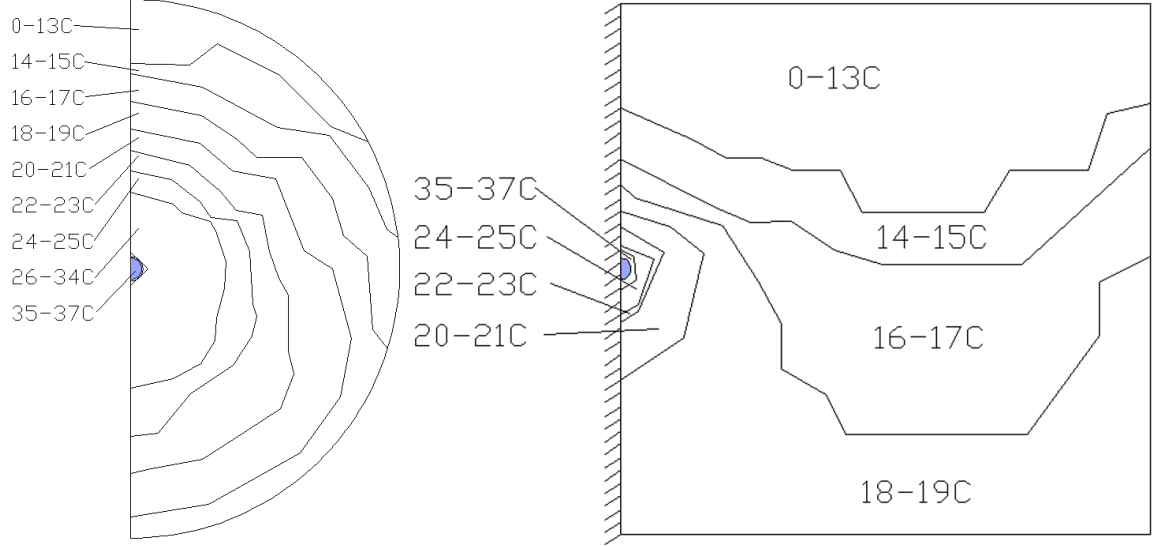


Figure 5.8: High Flow Test: Mei and Fluent Cross Section Temperature Profiles

Figure 5.8 shows the temperature distributions for both models. As the figure shows, the temperature distributions do not agree well. The temperature distribution along the far-field boundary follows a behavior that would be expected from the Kusuda and Achenbach correlation, but the rest of the domain shows deviations. The Mei model has already shown problems with initial condition independence and stability. The inaccuracy of the 2-D calculation is another serious limitation of the Mei model.

#### 5.4 Mei Model Conclusions

The Mei model was introduced as a model with intermediate complexity. The single cylindrical coordinate system indicated a model which could produce quality results while balancing the computation time that may be encountered with a more complex model. However, throughout the initial testing, the model did not produce qual-

ity results and encountered several problems which eliminate it as a candidate for implementation within EnergyPlus:

- Stability
- Accuracy
- Ground Surface Interaction
- Initial Condition Independence

The first problem, stability, is a result of two things: an explicitly formulated model, and widely varying grid spacing. This varying grid spacing is partially accounted for by the dual time step method used. However, in the initial testing there were several simulations that were unusable because instability caused divergence. This is the main problem of the Mei model. The second problem involves the accuracy of the model. This first set of initial tests, where the domain is idealized in one form or another, show that the Mei model does not agree well with the verification model. The results are expected to worsen as the domain is placed back to its default state where the boundary conditions are both spatially and temporally dependent. The third problem is that the model does not directly interact with the ground surface. The far-field boundary condition of the model is simply a correlation of depth and time. The problem with this is that the model never takes into account the short time scale behavior of the outdoor air. With the other problems encountered during testing, a solution for this problem was not investigated. The fourth problem is that the model showed a very slow independence from initial conditions. The model took almost fourteen days to 'forget' the initialization of the model. A 'warm-up' period would be required for the model in addition to the base warm-up periods that EnergyPlus uses.

These problems indicate that the Mei model is not currently the ideal model for implementation into EnergyPlus. In chapter 6, the Piechowski model will be evaluated,

and depending on these results, chapter 7 will reveal which model is implemented into EnergyPlus. Also, if no model is suitable in its current state, a decision will be made regarding major modifications to one of the models in order to improve the quality, so that it can then be implemented.

## CHAPTER 6

### Piechowski Model

#### 6.1 Model Description

Piechowski (1996) developed a quasi-3D finite difference buried pipe heat transfer model. Although a set of 3D grid points is generated, the effects of heat transfer from one section of pipe length to the next is only modeled within the fluid. In other words, the soil and pipe material do not model axial heat transfer. Piechowski assumes that the larger heat transfer gradients occur in a radial direction away from the pipe surface, with relatively smaller gradients in the axial direction. Therefore, at each pipe cross section, a 2D grid is developed. The grid is based on a cartesian coordinate system, with boundaries at the ground surface, a deep ground depth, and along the far-field surface on the side. The domain splits the pipe along the middle of the cross section in order to accommodate symmetry. Within this cartesian grid, there is one singular node at each cross section that includes the soil near the pipe, the pipe, and the fluid within the pipe. This layout is shown in figure 6.1. Using a single node alone to represent the pipe would not provide sufficient accuracy, and so a secondary coordinate system was developed, centered upon this representative node. This secondary domain is in radial coordinates. In this radial system, where the grid spacing is more refined than in the outer cartesian system, both heat and mass transfer are calculated, while in the larger grid, only sensible heat transfer is accounted for. The smaller grid layout is shown in figure 6.2.

Within the program, there are three distinct temperature arrays. Each of these accounts for a different section of the simulation domain. The first temperature array

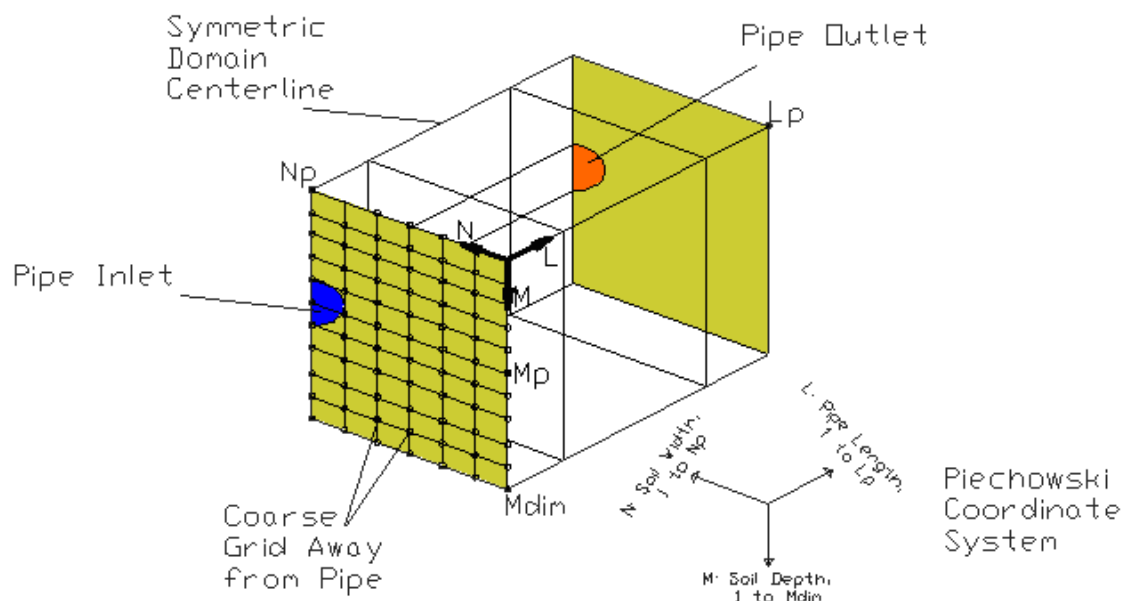


Figure 6.1: Large Scale View of Piechowski Domain Cutaway

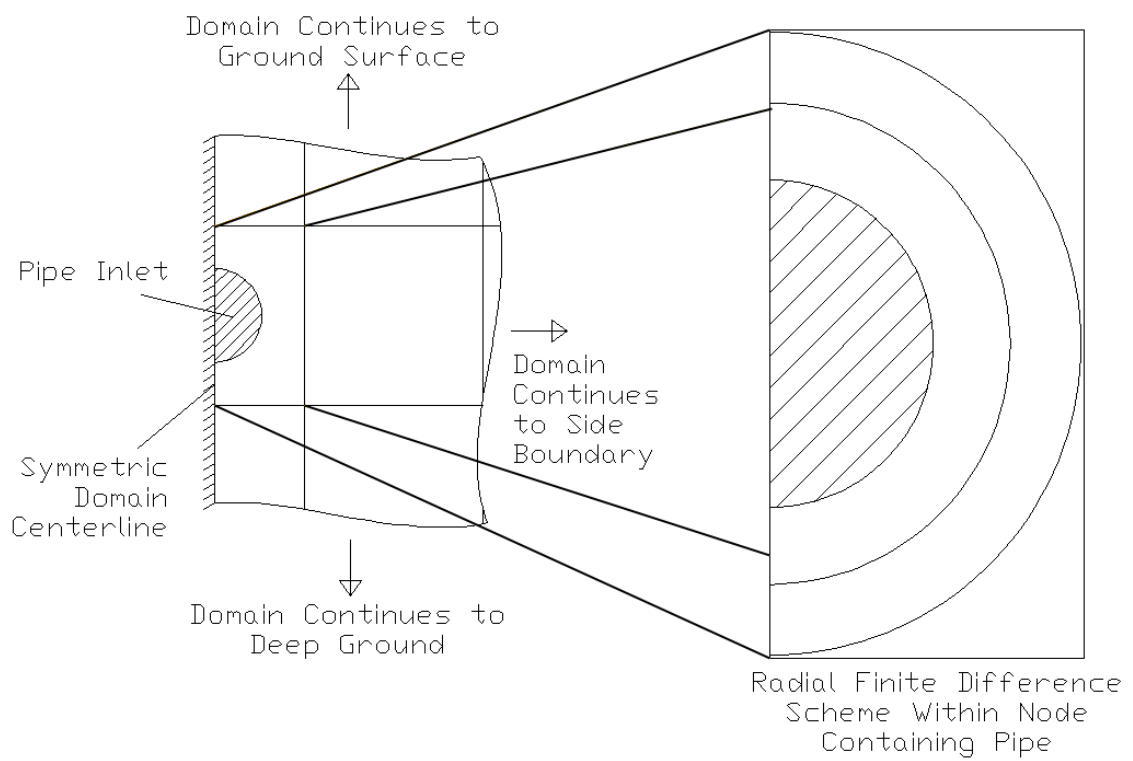


Figure 6.2: Small Scale View of Piechowski Domain Cutaway

is  $T(\text{TimeStep}, \text{Pipe Length}, \text{Soil Depth}, \text{Soil Width})$ . This temperature array has a value for the entire Cartesian soil domain. In this region, the grid is a 3D Cartesian coordinate system, and includes a representative value for the rectangular node which contains the pipe. This node will be discussed further in a later section. The second temperature array is held in the variable  $T_R(\text{TimeStep}, \text{Pipe Length}, \text{Radius})$ . This temperature array represents the values within the radial near-pipe region. In this section, the heat transfer is assumed to be axisymmetric, and the grid is therefore 1D (radial) throughout each cross section. When this region is analyzed in the program, the results are converted into an effective temperature, which can then be used in the Cartesian far-field analysis. In this way, the pipe effects are 'hidden' from the main routine, which simplifies the entire analysis. The third temperature array is  $T_W(\text{TimeStep}, \text{Pipe Length})$ . This array holds all the water temperatures along the pipe length at each time step.

The program follows a simple process all controlled by the MAIN subroutine:

- Calculate coefficients: pipe convection, moisture coefficients, soil properties
- Initialize arrays: water temperature, radial nodes, Cartesian nodes
- Loop through all simulation days and perform the following tasks:
  - Update side boundary soil temperature as a function of depth, time, etc.
  - Update surface temperature and deep ground surface temperature.
  - Retrieve cycle on-time for current period in order to provide a stopping point for the simulation.
  - Retrieve entering pipe water temperature.
  - Call routine to simulate near-pipe radial system and produce an 'effective' pipe node temperature for the far-field Cartesian system.

- Call routine to develop equation coefficients based on correlations and input data.
- Loop through all pipe length cross sections and perform the following tasks:
  - \* Loop through all nodes at the current cross section and update all nodal temperatures based on different conditions: Adiabatic on symmetric centerline, constant temperature boundaries on surface, side and deep ground

This process is performed with the following required inputs: Material properties, entering water temperatures, pipe on-cycle time per day, geometric data, and correlations. Some of the other key features of this simulation from a programming standpoint are the use of a function that can update a boundary temperature for both adiabatic and constant temperature boundaries. Using the same function simplifies the programming, and cleans up the code. For the entering water temperature, the same hourly boundary data was used as in the earth tube model, and is summarized in Appendix C.

In Piechowski's full program, the effects of moisture are modeled in the radial grid system. For this investigation, the effects were removed as described in section 6.2.

The heart of the program is the set of algorithms used for updating the temperatures of each node at every time step. The program is designed so that at each time step, a subroutine is called which pre-calculates coefficients. Thus the actual final equations are simplified. There are several different equations, depending on the location of the node, whether it is on the surface boundary, adiabatic boundary, near the pipe, or in the middle of the domain. These algorithms are contained in the GLOOP subroutine, and because they represent the Cartesian temperature field, they are denoted by the simple symbol,  $T(K,L,M,N)$ . The definitions of these independent variables  $K$ ,  $L$ ,  $M$ , and  $N$  are given previously. Four different update equations, (6.1,



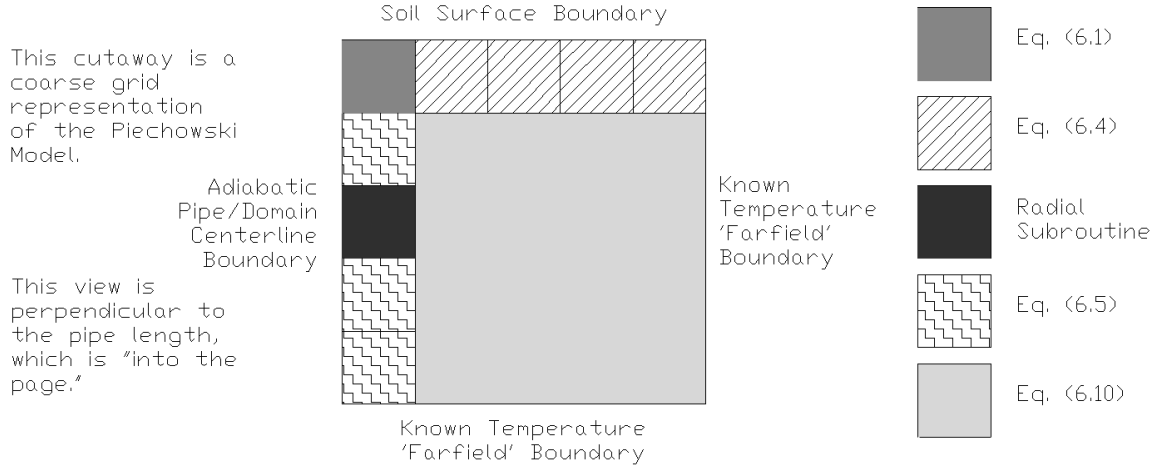


Figure 6.3: Case Layout and Node Descriptions for Piechowski Model

6.4, 6.5, and 6.10), as well as the radial near-pipe subroutine are applied throughout the solution domain, as shown in figure 6.3.

The program first updates the temperatures along the boundary of the soil and the ambient air. Even in this section, there are two different types of nodes. One node will be at the adiabatic centerline of the domain as shown in figure 6.3. Because of this symmetry condition, the update equation, (6.1), for this node will be slightly different from the other regular nodes along the surface.

$$T_{K, L, M, N} = 2 \cdot S_1 \cdot (T_{K, L, m+1, n} + T_{K, L, m, n-1}) + S_2 \cdot T_{AMB} \quad (6.1)$$

Where the coefficients are defined as:

$$S_1 = \frac{1}{(2 \cdot (H_{AMB} \cdot dX / K_s + 2))} \quad (6.2)$$

$$S_2 = \frac{H_{AMB} \cdot dX}{(H_{AMB} \cdot dX + 2 \cdot K_s)} \quad (6.3)$$

The other nodes along the surface are bounded by other nodes on the sides and the bottom. The top boundary will be a simple convection boundary. The update equation is equation (6.4).

$$T_{K, L, M, N} = S_1 \cdot (2 \cdot T_{K, L, m+1, n} + T_{K, L, m, n-1} + T_{K, L, m, n+1}) + S_2 \cdot T_{AMB} \quad (6.4)$$

The program then switches from scanning across the ground surface and begins traversing down the adiabatic boundary of the domain. This boundary is lined up with the centerline of the pipe, and simulates an adiabatic condition, which will be a good approximation as long as the ground is consistent with no other pipes or heat sources or sinks nearby.

When the program reaches the node where the pipe is located, the program calls a separate subroutine, RADIAL, as shown in figure 6.3. This subroutine sets up a radial grid within this Cartesian node. The result is an 'effective temperature' which can then be used by the nodes in the Cartesian array. This is beneficial because the complexity of the pipe domain is 'hidden' from the main program. This subroutine is called with the following command:

Call RADIAL(LOOPStatus, L, M<sub>p</sub>, N<sub>p</sub>, CB<sub>1</sub>, CB<sub>2</sub>, CB<sub>3</sub>, NR)

As can be seen from the command, there are several variables passed to this radial solver. These include the current status of the water loop (on/off), the number of radial nodes to generate, and the soil coefficients CB<sub>1</sub>, CB<sub>2</sub>, CB<sub>3</sub>, which are defined later in this section.

Aside from the surface node, and the pipe node, the nodes on the adiabatic boundary will be bounded by regular nodes above and below, as well as toward the interior of the domain. The other boundary will be the adiabatic condition. For these nodes, equation (6.5) is used to update the temperature.

$$T_{K, L, M, N} = A_1 \cdot (T_{K, L, m+1, n} + T_{K, L, m-1, n} + 2 \cdot T_{K, L, m, n-1}) + A_2 \cdot T_{K-1, L, m, n} \quad (6.5)$$

Where the coefficients are defined as:

$$A_1 = \frac{Fo}{(1 + 4 \cdot Fo)} \quad (6.6)$$

$$A_2 = \frac{1}{(1 + 4 \cdot Fo)} \quad (6.7)$$

It is always important to note the development of dimensionless quantities. In the case of this simulation, the Fourier number plays a large role, and is defined in equation (6.8). The thermal diffusivity of the soil is embedded in the Fourier number, and so it is defined here also, in equation (6.9).

$$Fo = \alpha_S \cdot \frac{dt}{(dS^2)} \quad (6.8)$$

$$\alpha_S = \frac{K_s}{(\rho_s \cdot C_s)} \quad (6.9)$$

All the other nodes in the domain are bounded by four other regular nodes or known temperature boundary conditions. The update equation is given as equation (6.10), and is simply an average of the neighboring nodes along with a time-lagged term from the previous time step at the current grid point.

$$T_{K, L, M, N} = A_1 \cdot (T_{K, L, m+1, n} + T_{K, L, m-1, n} + T_{K, L, m, n+1} + T_{K, L, m, n-1}) + A_2 \cdot T_{K-1, L, m, n} \quad (6.10)$$

At the point when the program reaches the node with the pipe, the RADIAL subroutine is called. The main goal of this routine is to develop the temperature of the node which can be used in the main Cartesian grid. In the radial domain, the temperature variable of interest is  $T_R$  (time, pipe length, radius). There are two equations, one for interior nodes, and one for the outer boundary of the radial domain. The nodal distribution can be seen in figure 6.4.

Table 6.1: Symbols and Variables used in Piechowski Model

Variable	Description	Equation Occurrences
$T_{AMB}$	Ambient Air Temperature	(6.1)
$H_{AMB}$	Ground Surface Convection Coefficient	(6.2, 6.3)
$K_S$	Soil Thermal Conductivity	(6.2, 6.3, 6.9)
$\rho_S$	Soil Density	(6.9, 6.18, 6.19, 6.20)
$C_S$	Soil Specific Heat	(6.9, 6.18, 6.19, 6.20)
dt	Time Step	(6.8)
dX	Grid Spacing: Width	(6.2, 6.3)
dS	Grid Spacing: Depth	(6.8)
dR	Grid Spacing: Radial	(6.18, 6.19, 6.20)
$R_{NR}$	Current Radial Node	(6.18, 6.19, 6.20)
$R_{NR-1}$	Radial Node Minus One Increment	(6.18, 6.19, 6.20)
$C_x$	Intermediate coefficient	(6.12)
IX	Radial Node Counter	(6.16, 6.12)

For interior nodes, the equation is given in equation (6.11).

$$\begin{aligned}
T_R(K, LX, i) = & A_T * (T_R(K, LX, i-1) - T_R(K, LX, i+1)) + \\
& B_T * (T_R(K, LX, i-1) - T_R(K, LX, i+1)) + \\
& C_T * (T_R(K, LX, i-1) - T_R(K, LX, i+1)) + D_T * T_R(K-1, LX, i)
\end{aligned}
\tag{6.11}$$

Where the coefficients are defined as:

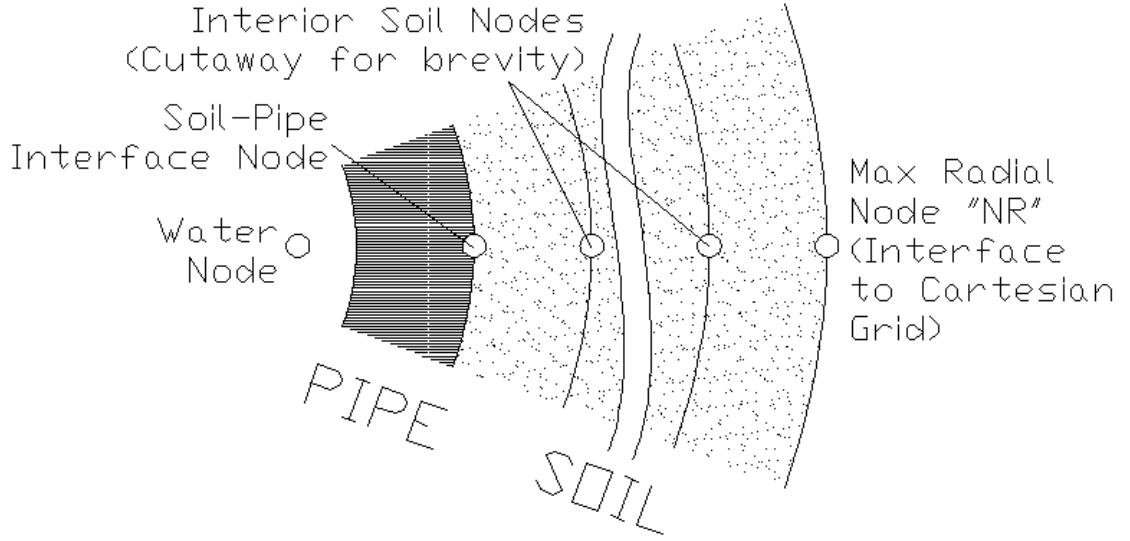


Figure 6.4: Piechowski Radial Grid Distribution

$$A_T = \frac{K_S (IX + 1) - K_S (IX - 1)}{4 * C_x * dR^2} \quad (6.12)$$

$$B_T = \frac{K_S (IX)}{2 * C_x * R (IX) * dR} \quad (6.13)$$

$$C_T = \frac{K_S (IX)}{C_x * dR^2} \quad (6.14)$$

$$D_T = \frac{\rho_S * C_S}{C_x * dt} \quad (6.15)$$

The intermediate coefficient  $C_x$  is defined as:

$$C_x = \frac{\rho_S * C_s}{dt} + \frac{2 * K_S (IX)}{dR^2} \quad (6.16)$$

For the outer boundary of the radial domain, the node is influenced by not only the radial section, but also by the Cartesian neighboring nodes. This can be seen in the update equation for the outermost radial node (6.17). The CB coefficients are defined in equations (6.18)-(6.20).

$$\begin{aligned}
T_R(K, LX, i) = & CB_1 * T_R(K, LX, NR-1) + CB_2 * [T(K, LX, Mp+1, Np) + \\
& T(K, LX, Mp-1, Np) + 2 * T(K, LX, Mp, Np-1)] + \\
& CB_3 * T_R(K-1, LX, i)
\end{aligned} \tag{6.17}$$

Where the coefficients are defined as:

$$CB_1 = \frac{1}{1 + \frac{4}{\pi} \cdot \ln\left(\frac{R_{NR}}{R_{NR-1}}\right) \cdot ((dS^2 - \pi \cdot (R_{NR-1} + dR/2)^2) \cdot \rho_s \cdot C_s)} \tag{6.18}$$

$$CB_2 = \frac{1}{\frac{\pi}{\ln\left(\frac{R_{NR}}{R_{NR-1}}\right)} + 4 \cdot ((dS^2 - \pi \cdot (R_{NR-1} + dR/2)^2) \cdot \rho_s \cdot C_s)} \tag{6.19}$$

$$CB_3 = \frac{(0.5 \cdot dS^2 - \pi \cdot (R_{NR-1} + dR/2)^2) \cdot \rho_s \cdot C_s}{\frac{\pi \cdot K_s \cdot dt}{\ln\left(\frac{R_{NR}}{R_{NR-1}}\right)} + 4 \cdot (K_s \cdot dt) \cdot ((dS^2 - \pi \cdot (R_{NR-1} + dR/2)^2) \cdot \rho_s \cdot C_s)} \tag{6.20}$$

Once the radial distribution is calculated, the effective temperature for use in the Cartesian grid can be approximated by the outermost radial node temperature. Also, if the loop is in the 'off' status, the water temperature is approximated by the innermost radial node temperature. These two conditions are given in equations (6.21) and (6.22).

$$T(K, LX, M_p, N_p) = T_R(K, LX, i) \tag{6.21}$$

$$T_W(K, LX) = T_R(K, LX, 1) \tag{6.22}$$

However, if the loop is in the 'on' status, the water temperature is updated by equation (6.23).

$$T_W(K, LX) = C_1 * T_W(K, LX - 1) + C_2 * T_R(K, LX, 1) + C_3 * T_W(K - 1, LX) \tag{6.23}$$

Table 6.2: Piechowski Model Symbol Definitions

Symbol	Definition
H	Fluid to Pipe Convection Coefficient
$R_{P,i}$	Inner Pipe Radius
$R_{P,o}$	Outer Pipe Radius
$K_p$	Pipe Conductivity
V	Fluid Velocity
$\rho_f$	Fluid Density
$C_f$	Fluid Specific Heat

The coefficients in equation (6.23) are defined next. In equations (6.24) to (6.27), the symbols that have not been previously defined are given in table 6.2.

$$U = \frac{1}{\frac{1}{H} + \frac{R_{P,i}}{K_p} \cdot \text{Log} \left( \frac{R_{P,o}}{R_{P,i}} \right)} \quad (6.24)$$

$$C_1 = -\frac{\frac{-V \cdot dt}{dX}}{1 - \frac{-V \cdot dt}{dX} + \frac{2 \cdot U \cdot dt}{\rho_f \cdot C_f \cdot R_{P,i}}} \quad (6.25)$$

$$C_2 = \frac{\frac{2 \cdot U \cdot dt}{\rho_f \cdot C_f \cdot R_{P,i}}}{1 - \frac{-V \cdot dt}{dX} + \frac{2 \cdot U \cdot dt}{\rho_f \cdot C_f \cdot R_{P,i}}} \quad (6.26)$$

$$C_3 = \frac{1}{1 - \frac{-V \cdot dt}{dX} + \frac{2 \cdot U \cdot dt}{\rho_f \cdot C_f \cdot R_{P,i}}} \quad (6.27)$$

## 6.2 Simplified Piechowski Model

The model described in the previous section is a modified version of the full Piechowski model. In Piechowski (1996), it was found that although moisture did at times play a significant role in overall model accuracy, the pipe temperatures achieved in most systems were not high enough to cause significant moisture migration. The lack of significant moisture migration lessens the need for a dynamic mass transfer

algorithm. Due to the need to create a model that would fit in an annual simulation program, the model was modified to only include sensible heat transfer effects, and moisture was not modeled. Therefore, the selection of soil thermal conductivity plays a more important role in determining the accuracy, as this one value will be used throughout the simulation. The inaccuracies caused by this will not be clear during the verification, since the Fluent model is currently a sensible heat transfer model as well.

The removal of the moisture simulation did require some changes in the computer program code. With the moisture transfer originally only modeled in the small section near the pipe, the removal of this feature in the model is contained in a small set of code. Some of the finite difference equations are formulated in Piechowski (1996), and the moisture effects are kept separate from the temperature driven effects. The equations were then shortened, with the moisture coefficients removed.

Another item that was modified from the original program was the use of cycle on-time. In the original program, the daily heat pump on-time was an input, and the program would begin each simulation day by running the ground heat exchanger with fluid flow 'on' for that period of time. The program would then run the heat exchanger with fluid flow 'off' for the rest of the day. This would repeat for all days of the simulation. This procedure may give reasonable results when looking at overall energy consumption, but is definitely not a valid approach for a full energy simulation program model. With the addition of hourly weather, temperature, and cycle on-off flags, the program could choose at each hourly time step whether to turn the flow 'on' or 'off'. This addition is expected to have a significant impact on the overall accuracy of the model.



### 6.3 Analysis of Piechowski Model Grid Dependence Parameters

There are a number of input parameters which can affect the overall accuracy of the Piechowski model simulation. These parameters are the time step, radial grid spacing, number of nodes in the Cartesian 2D domain, and the number of nodes along the length of the pipe. The objectives of this section are to determine the limit at which the model results are independent of further refinement of the simulation domain grid as well as to find optimum values of the grid density which balance the improvement of accuracy with computation time.

A series of tests were performed using the Piechowski model, each varying one or more grid parameters. The results are mostly as expected: as one increases the number of nodes, computation time increases accordingly. Three grid parameters were varied: the number of grid points along the length of the pipe,  $dX$ ; the grid spacing for the Cartesian system at each cross section,  $dS$ ; and the number of grid points within the radial section near the pipe,  $NR$ .

First a very coarse grid spacing was used throughout, then one by one, the grid parameters were improved until convergence was reached. A reminder here that convergence simply indicates that an improvement in a model parameter does not result in a similar change in results. This investigation was performed in three major steps:

1. With a rough Cartesian and radial grid distribution, the grid spacing along the length of the pipe was refined from an initial grid spacing of 2.5m to a grid spacing of 1.0m, and finally to a grid spacing of 0.5m. For a 25m long pipe, this means the number of grid points along the length rose from 10 to 25 to 50.
2. While keeping this increased accuracy in the grid along the length of the pipe, the Cartesian grid was refined. The grid spacing went from 0.5m to 0.25m. For a 5m by 5m Cartesian domain at each cross section, this means the number of

grid points went from 100 to 400. There was no significant change in results, so throughout further improvement was studied, and this higher accuracy was maintained.

3. With this refined length and Cartesian grid spacing, the radial spacing was then improved from 10 nodes to 150 nodes. The initial increase from 10 to 25 produced a fairly significant deviation, but then the results began converging.

Table 6.3 summarizes the individual cases that were performed during this investigation. The cases are labeled C through J, and these case labels carry over to the temperature results in figure 6.5. As a parameter increases the density of the mesh, the computation time also increases for all but 'trial h'. For this trial, which was repeated several times, increasing the grid density decreased the computation time. One reason for this may be that a convergence check is made in the radial subroutine. With these additional nodes, convergence of the radial model may now be achieved faster at each time step, thus reducing the overall computation time of the model. This will have to be considered when choosing the number of radial nodes to use in the verification testing.

An important note here is that the computation times given were for a spreadsheet implementation of this model, where a large number of data points were being passed to and from the spreadsheet, and a plot was updated in the process. For a compiled version of the model, as would appear in the EnergyPlus distribution, the speed would be drastically improved. The important aspect for now is the relative improvement in time. As table 6.3 shows, the time required to simulate this period doubles throughout the trials.

The results of this parametric study are shown in figure 6.5. As refinements are made to the grid, the results appear to be converging. In addition to the exiting water temperature, the entering water temperature (EWT) and the ground temperature near the pipe are shown. These two temperatures bound the exiting water

Table 6.3: Piechowski Input Variable Tabulated Results

	dX - Axial	dS - Cartesian	NR - Radial	Time
Trial	Spacing [m]	Spacing [m]	Nodes [-]	[s]
C	2.5	0.5	10	4
D	<b>1</b>	0.5	10	5
E	<b>0.5</b>	0.5	10	5
F	0.5	<b>0.25</b>	10	15
G	0.5	0.25	<b>25</b>	25
H	0.5	0.25	<b>50</b>	17
I	0.5	0.25	<b>100</b>	28
J	0.5	0.25	<b>150</b>	45

temperature as expected.

Figure 6.5 shows several different series, one for each trial. Although it may be difficult to see in the plot, there are actually four series almost completely overlaying each other. This indicates that the effect of these parameters on the exiting water temperature was minimal. These are trials C, D, E, and F, which involved the parameters for axial grid spacing and Cartesian grid spacing.

Figure 6.5 also shows that exiting water temperature is very sensitive to the radial grid density. The original case had 10 radial nodes, which intuitively seemed like a reasonable number. However, as these tests show, the results are very sensitive to the number of radial nodes. Changing the radial grid from 10 nodes to 25 nodes resulted in upwards of  $0.5^{\circ}\text{C}$  deviation from the previous trial at one point. Then changing the grid from 25 to 50 nodes made an even more drastic change, nearly  $1.0^{\circ}\text{C}$ . As the grid was improved to 100 nodes, and then to 150 nodes, the results converged nicely.

In conclusion, it appears that only the radial node density was significant. The results of table 6.3 and figure 6.5 indicate that while the fully refined grid does appear

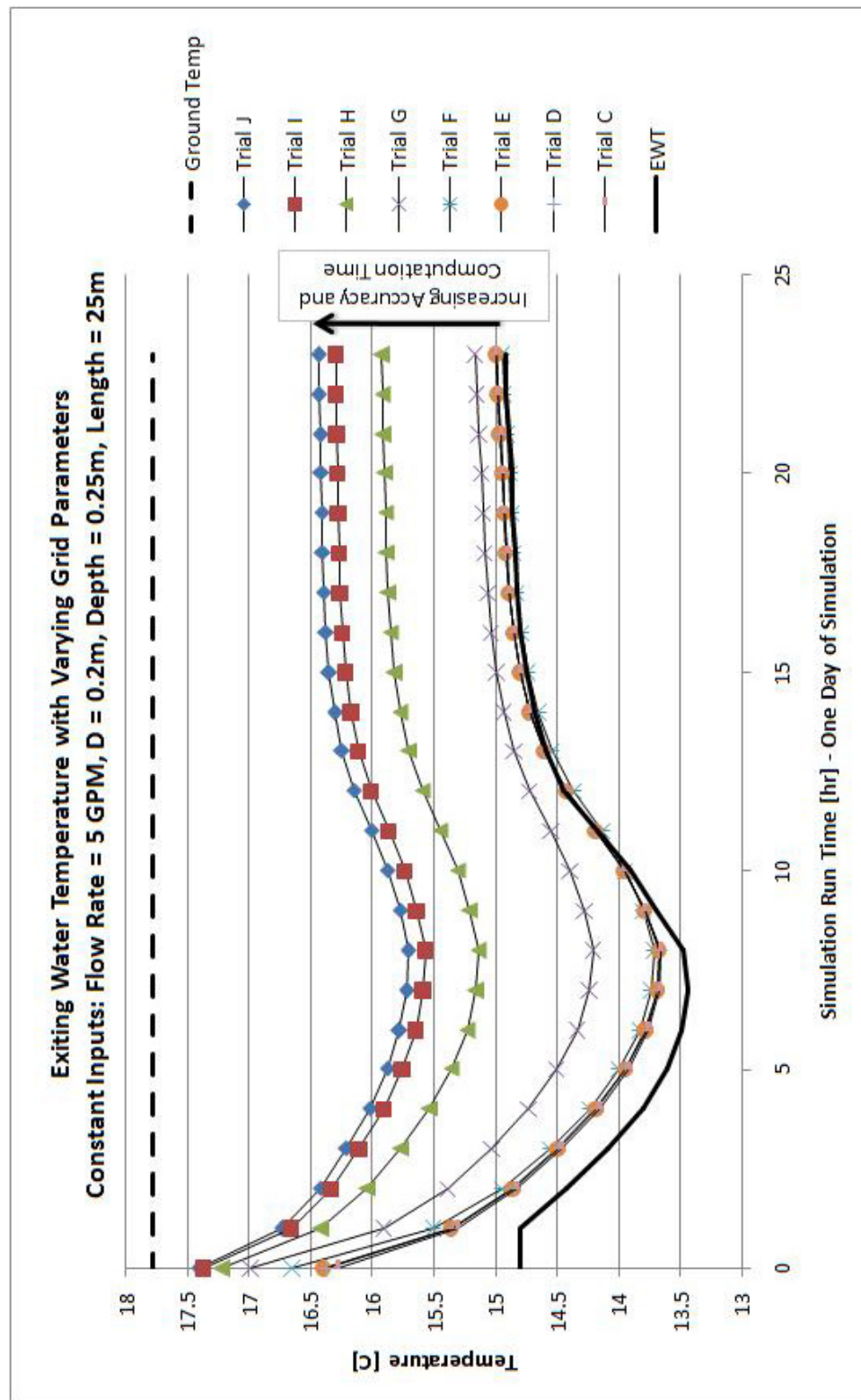


Figure 6.5: Piechowski Input Variable Study Results

to produce higher quality results, the increase in computation time is significant. For testing purposes, the trade-off between accuracy and computation time led to the selection of the following grid:

- Number of radial nodes = 100
- Cartesian grid spacing = 0.25 m
- Axial grid spacing = 0.5 m

However, when the model is implemented in EnergyPlus, an algorithm will be developed to determine the number of nodes required. In this meshing technique, the number of nodes will be specified based on the geometry of the model. Specifying the number of nodes is more general than specifying the grid spacing if the technique must be applied to any given length of pipe.

## 6.4 Initial Model Testing

It is not sufficient to simply assume the model is operating properly, even if the data shows good behavior. Due to the long time scale of ground heat transfer simulations, small perturbances may be hidden by the full, long, simulation time steps. In this section, some of the initial tests that were performed to provide evidence of proper operation are discussed. These tests include:

1. A code integrity test, where all boundary conditions and entering water conditions are set equal. This test is designed to reveal major errors in the finite difference equation coefficients or algorithms.
2. A steady state test, where the simulation is modified to provide a constant pipe temperature. The results can be compared to an analytic solution for this idealized case.

3. An initial-condition independence test is performed where the same operating conditions are simulated with varying initial conditions. At steady conditions, the solution should be the same.
4. A high flow rate test where the 3D effects are eliminated from the model in order to verify that the 2D processes are operating properly. This is the first stage comparison to a simplified Fluent model.

#### **6.4.1 Code Integrity Test**

This test involves setting all the boundary temperatures, and the entering water temperature equal. The expected behavior will be zero heat transfer between any two nodes. This test was used to reveal errors within the update equations. Once the bugs in the model were corrected, the temperatures throughout the domain were constant at the initial temperature, and as expected, there was no heat transfer. The exiting fluid temperature was equal to the entering fluid temperature for all iterations.

#### **6.4.2 Steady State Test**

By eliminating the ground heat transfer, a simple analytic solution can be written to check the pipe flow computation of the model. There are two major assumptions which can be used to develop this analytic solution: Constant Pipe Wall Temperature or Constant Pipe Wall Heat Flux. Either of these provide a means of integration, assuming a bulk temperature can be used to describe the fluid condition at any cross section. The constant pipe wall test is selected and performed based on the following assumptions:

1. Constant Wall Temperature: the ability to simulate this behavior in the model by Piechowski is described further, later in this section.
2. Constant Properties: the density, specific heat, and thermal conductivity are

assumed independent of temperature to simplify the solution.

3. Thermally and Hydrodynamically Fully Developed: this ignores the entry effects, which allows a single Nusselt correlation to describe the heat transfer along the full length of the pipe.
4. Turbulent Fluid Regime: this defines what correlation is used to calculate the Nusselt number, this correlation is the same as the default in the original Piechowski model.

The development of the analytic solution begins with applying two heat transfer equations: one (6.28) is the heat gain from the pipe surface temperature to the average bulk temperature in the pipe, and the second (6.29) is the heat gain of the fluid throughout the length of the pipe.

$$\dot{q} = h\pi DL \left( T_{\text{surface}} - \frac{T_{\text{entering}} + T_{\text{exiting}}}{2} \right) \quad (6.28)$$

$$\dot{q} = \dot{m}C_p (T_{\text{exiting}} - T_{\text{entering}}) \quad (6.29)$$

Equation (6.28) appears to be applied to the entire pipe in one step. Contrary to the assumption of the equation, temperature in a pipe is not linear, so further development was performed to accommodate the non-linearity. This non-linear effect is further discussed later in this section.

For steady conditions, the heat transfer from the pipe must be equivalent to the heat gain of the fluid flowing through it. Equating the heat transfer rates in equations (6.28) and (6.29), gives equation (6.30). Throughout the rest of this development, the entering fluid temperature and exiting fluid temperature will be denoted as  $T_1$  and  $T_2$ , respectively.

$$\dot{m}C_p (T_2 - T_1) = h\pi DL \left( T_{\text{surface}} - \frac{T_1 + T_2}{2} \right) \quad (6.30)$$

In this development the desired result is a formula of  $T_2$  in terms of  $T_1$ . Rearranging equation (6.30) to fit this form results in equation (6.31).

$$T_2 = \frac{\dot{m}C_p T_1 + h\pi DL \left(T_s - \frac{T_1}{2}\right)}{\dot{m}C_p + \frac{h\pi DL}{2}} \quad (6.31)$$

In equation (6.31), the convection coefficient is based on a correlation. This correlation should fit the assumptions given previously. The correlation currently used in the Piechowski Model, and as found in Holman (1981), is shown as equation (6.32).

$$h = \frac{k}{D} 0.023 \left(\frac{\rho DV}{\mu}\right)^{0.8} Pr^{0.4} \quad (6.32)$$

When this is substituted into equation (6.31), the result is a developed equation giving the exit fluid bulk temperature in terms of geometry, entering conditions, properties, and surface temperature, and is shown in equation (6.33).

$$T_2 = \frac{k 0.023 \left(\frac{\rho DV}{\mu}\right)^{0.8} Pr^{0.4} \pi L \left(T_s - \frac{T_1}{2}\right) + \dot{m}C_p T_1}{\frac{k}{2} 0.023 \left(\frac{\rho DV}{\mu}\right)^{0.8} Pr^{0.4} \pi L + \dot{m}C_p} \quad (6.33)$$

At this point, a series of tests can be performed comparing the simulation results to the analytic solution. It should be noted that this test only validates the simulation of the pipe fluid heat transfer. Interaction with the ground is not addressed.

The Piechowski Model boundary conditions were modified to fit the assumptions of the analytic solution. In order to simulate a constant pipe wall temperature, the Piechowski model boundary temperatures were set to 15°C and a very high soil thermal conductivity was specified. This resulted in nearly the same temperature at every pipe wall node. Even with the use of high soil conductivity, the temperature at the pipe node is slightly off of the boundary temperature. On average, the pipe wall temperature was within 0.05°C of the outer boundary temperature for all of the Piechowski model tests.



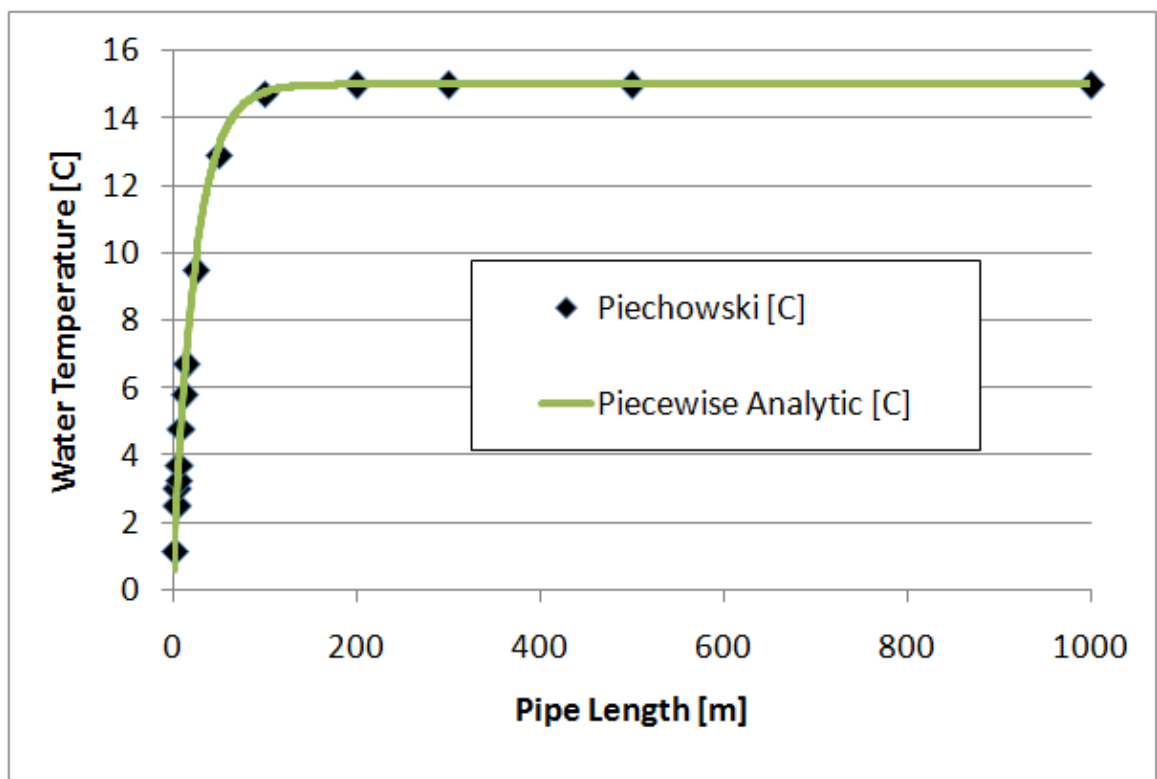


Figure 6.6: Constant Wall Temperature Model Results

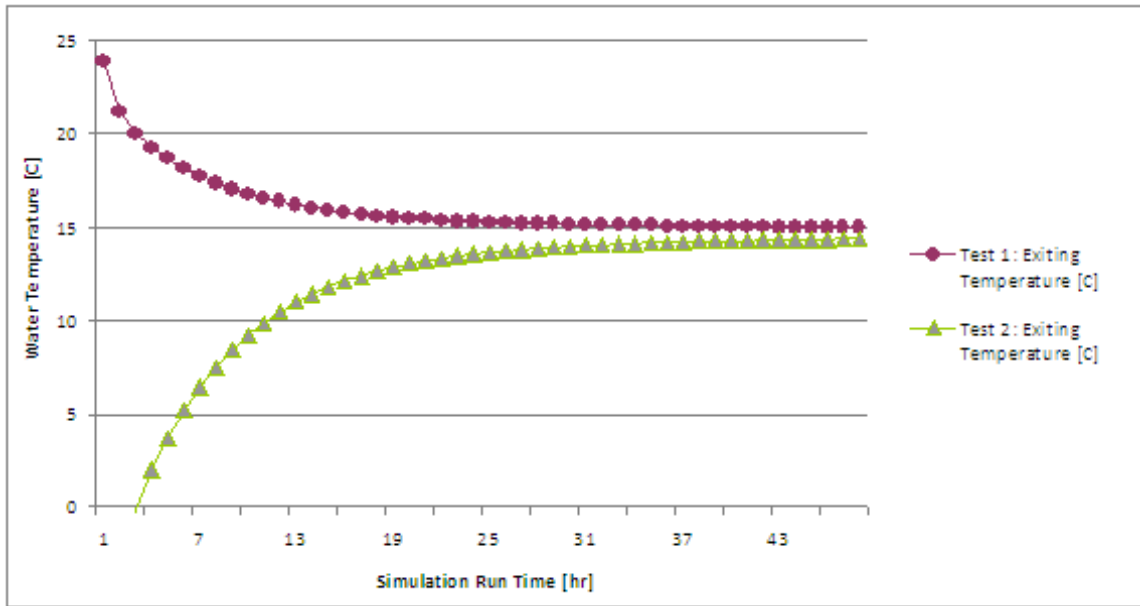


Figure 6.7: Piechowski Initial Condition Independence Results

The analytic solution was applied to small pipe segments beginning at the pipe inlet and continuing sequentially to the pipe exit. This piecewise application of the analytic solution matched the Piechowski model predictions as shown in figure 6.6.

#### 6.4.3 Initial Condition Independence Testing

A robust model should converge on the same steady state solution regardless of initial conditions. A brief study was performed where the solution domain was initialized to two different values:  $-30^{\circ}\text{C}$  and  $30^{\circ}\text{C}$ . The three boundary conditions (entering water temperature, Kusuda and Achenbach far-field boundary, and outdoor dry bulb) were set to constant values of  $15^{\circ}\text{C}$ . Figure 6.7 shows that within 48 hours, the simulations converge to within 5%.

#### 6.4.4 High Flow Rate Test

The Piechowski model does not include axial heat transfer in the soil or pipe wall. Although it is expected that this will have minimal effects on the results, testing

should be performed for verification. There is a simple method which one can use to essentially 'remove' the axial third dimension from the analysis. When the water flow rate is high enough in the model, the temperature difference along the length of the pipe will diminish. With all other boundary conditions uniform in the axial direction, each cross section should have the same temperature distribution. This alone would not provide any quantitative information, only a view of the temperature distribution in the Piechowski model. Therefore, a similar Fluent model is introduced here.

When performing this simulation, the Kusuda and Achenbach correlation was removed from both models, and the far-field side wall and deep ground boundaries were constant wall temperature boundaries of  $16.85^{\circ}\text{C}$  and  $11.85^{\circ}\text{C}$ , respectively. The ground surface temperature was kept as a convection boundary, but the outdoor free stream temperature was held constant at  $21.85^{\circ}\text{C}$ . The entering pipe temperature was set warm to  $36.85^{\circ}\text{C}$  and the flow rate was increased to 25 m/s. Thus all the boundary conditions were constant in both the the axial direction and in time. This allowed the model to essentially reach steady state conditions. Once steady conditions were reached, the temperatures could be compared. The steady state condition was determined by temperature convergence and overall pipe heat loss convergence.

The resulting temperature distribution is shown for the Piechowski simulation and the Fluent simulation in figures 6.8 and 6.9, respectively. The node distribution is different in the two models, and so the temperature distributions are slightly different. However, they do agree quite well.

## 6.5 Comparison to Verification Model

The Fluent verification model for this simulation is quite similar to the verification model for the Earth Tube Pipe Model in section 4.4. One major deviation is the introduction of convection at the ground-air interface. In the previous model, a simple average surface temperature and average temperature variation were used in

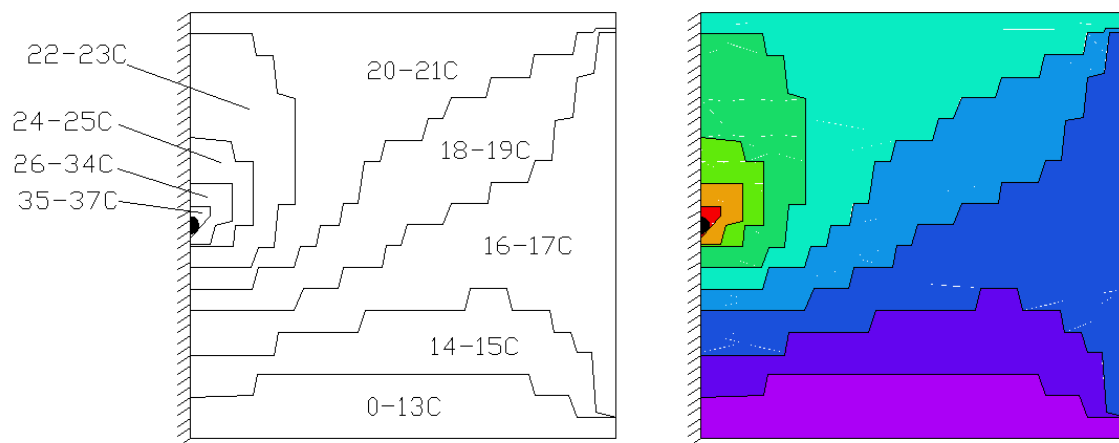


Figure 6.8: High Flow Rate Test Results: Piechowski Model Cross Section Temperature Distribution

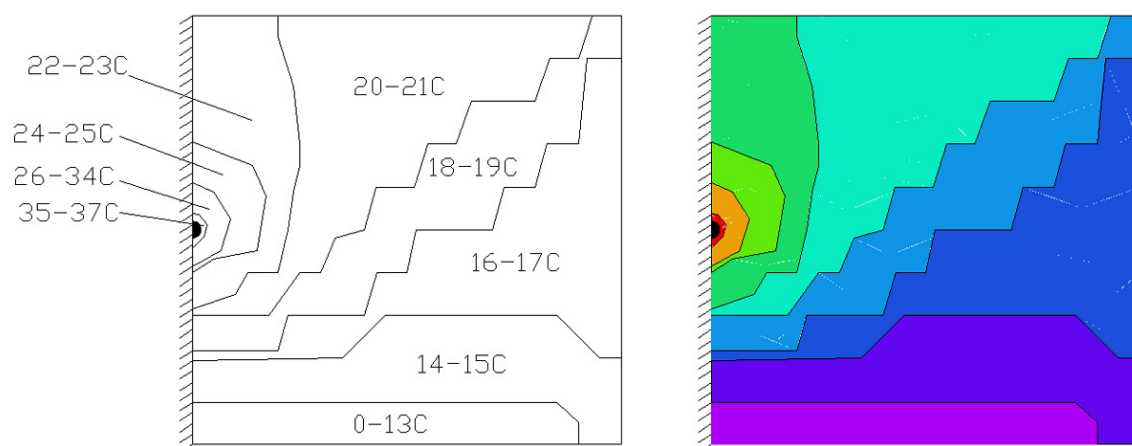


Figure 6.9: High Flow Rate Test Results: Fluent Model Cross Section Temperature Distribution

order to develop a sinusoidal varying surface temperature throughout the year. In the Piechowski model, the convection at the surface is easily modeled at the surface grid points with the use of a special update equation. The original Piechowski model used a single average outdoor air temperature. During development, an hourly set of outdoor air temperatures were placed within the model. This should increase the accuracy of the baseline model. This addition is also encouraged when considering the implementation in EnergyPlus. Within EnergyPlus, the outdoor air temperature will be available throughout the simulation. It seems reasonable that the model under test should have the same capabilities. The Fluent model is also modified to include the outdoor air at every hour, and both models use a constant convection coefficient for the ground surface. It is expected that there would be no drastic increase in accuracy if a full convection correlation were imposed, as wind speed data is at an hourly time step, and does not account for the small time scale changes in wind speed.

The rest of the model comparison details are very basic. The situation is a buried horizontal pipe, of internal radius 0.1m and thickness 0.01m, buried 2.5m underground. The pipe is 25m long. Due to symmetry, only half of the pipe is modeled, and the pipe centerline is part of the adiabatic surface in the models. For both models, the entire domain stretches 5m deep, 5m wide, and 25m long. The fluid within the pipe is water and constant properties are used in both models. For time steps where the flow rate is greater than zero (for example, when the heat pump system has triggered the circulation pump), the flow is assumed constant, and is set to  $4.39\text{E-}4$  m<sup>3</sup>/s, which works out to about 7 GPM with a velocity of  $1.4\text{E-}2$  m/s. For time steps when the flow rate is zero, the Piechowski model will set the water temperature to the pipe temperature, and find a solution throughout the domain. The Fluent model will operate the same as when flow is on; it will just find a solution where zero flow is in the pipe. It should be noted that switching between flow and no flow conditions drastically increased the computation time for the Fluent model. When the flow was

Table 6.4: Simulation Parameters for Piechowski Verification

Parameter	Value	Units
Soil Conductivity	0.36	W/mK
Soil Density	2000	kg/m3
Soil Specific Heat	1200	J/kgK
Soil Diffusivity	5.475E-5	m2/hr
Pipe Conductivity	3	W/mK
Piechowski Time Step	1	hr
Fluent Time Step	1	hr
Run Period	8760	hr
Avg Soil Surf. Temp.	18.333	C
Avg Surf. Temp. Amp.	11.667	C

constant, the flow equations were very similar from time step to time step and so the inner iterations were minimal. In this case where the flow fluctuates on and off, the flow equations can change significantly from one time step to the next. This results in a large number of iterations on time steps where the flow velocity changes. The Piechowski model was developed with this in mind, and by representing the water flow by one node at each cross section, this flow behavior does not affect the computation time significantly. The rest of the properties used in this calculation are given in table 6.4.

In both models, the same inlet water conditions were given, so the first major comparison looks at how well the outlet temperatures matched between the two models. Figure 6.10 shows the exiting water temperature results for both models. The data is broken up into quarters of the year to increase clarity. The figure shows that throughout the first and second quarters of the year, the models agree. In the fourth quarter, the model agrees after about November 15th. The third quarter shows more

deviation between the models. This behavior can be quantified somewhat with the use of a root-mean-square analysis as shown in equation (6.34)

$$\Delta_{\text{Error,ExWT,RMS}} = \sqrt{\frac{1}{n} \sum \left( T_{\text{Fluent,ExWT}} - T_{\text{Piechowski,ExWT}} \right)^2} \quad (6.34)$$

The result of applying this equation to each of the four quarters of the year and then for the whole year is summarized in table 6.5.

Table 6.5: Piechowski Verification: Exiting Temperature RMS Error

Simulation Period	RMS Error	Units
1st Quarter	0.97154	°C
2nd Quarter	0.77977	°C
3rd Quarter	2.77909	°C
4th Quarter	1.61480	°C
Full Year	1.72357	°C

The increase in error during the third quarter of the year is not completely clear. One theory is that the heat storage prediction is different between the models. In this case, the temperature delay in the ground would be more lagged behind in one model, causing a different temperature gradient around the pipe, and therefore different heat transfer characteristics and different exiting temperatures. However, it would be expected that this type of error would continue to 'build' on itself the longer the model operated. In the current case, the error starts getting smaller into the fourth quarter of the year.

While the heat storage may play some role in the deviations, the results may differ simply due to the different model characteristics. In the Piechowski Model, the Cartesian system is quite coarse, and the computation time is substantially less when compared to the Fluent model, and yet, the RMS error of exiting fluid temperature

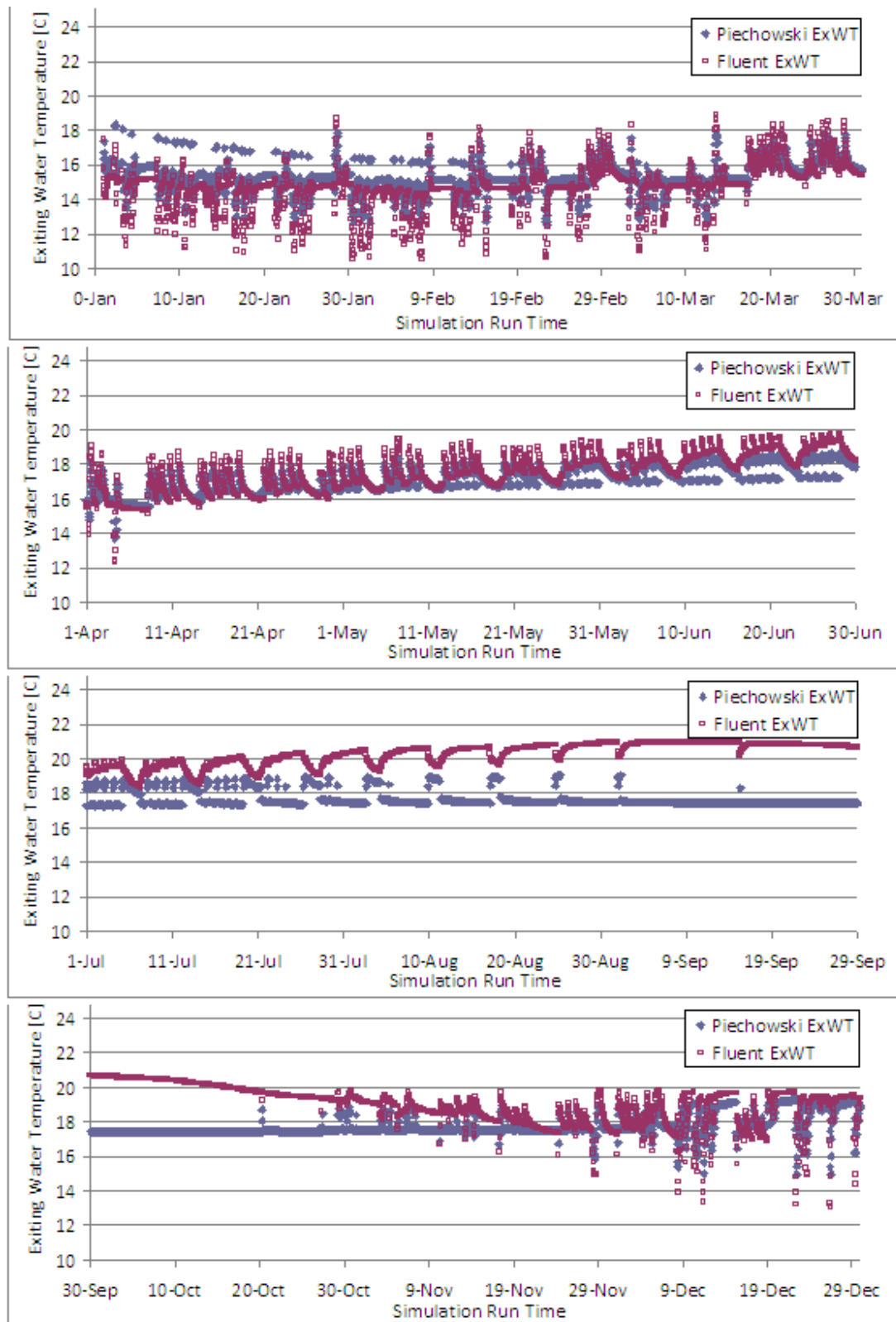


Figure 6.10: Piechowski Verification: Exiting Water Temperature Results



is less than 1.75 degrees for an entire annual simulation.

There are two other significant model differences that could play a part in the deviation. As previously discussed, the Piechowski model does not model heat transfer in the axial direction, except in the water flow. In addition, the Piechowski model uses a single water node at each axial point. The entire cross section of the pipe interior is modeled with a single bulk temperature. In the Fluent model, the water is broken into finite volumes along with the rest of the domain. The transient flow and energy conservation equations are then solved at hundreds of nodes in order to reach the solution. Therefore the temperature and velocity within any cross section can vary within Fluent, while the entire behavior is captured in one representative node in Piechowski. In Fluent, the exiting fluid temperature is found by taking an area-weighted average fluid temperature across the exiting surface. It appears that this is the greatest source of deviation between the two models.

While looking at exiting fluid temperature may be the one goal, the total heat transfer rate may be of more interest. The RMS error of the total heat transfer rate between the two models is calculated as with the exiting fluid temperature. The data is broken into the four seasons of the simulation year, and also an annual value is given.

Table 6.6: Piechowski Verification: Heat Transfer Rate RMS Error

Simulation Period	RMS Error	Units
1st Quarter	1758	W
2nd Quarter	1451	W
3rd Quarter	5102	W
4th Quarter	2968	W
Full Year	3163	W

The heat transfer rate error given in table 6.6 varies based on the season. The

total heat transfer rate error follows the same pattern as the exiting fluid temperature error, with low values in the first and second quarters, a peak in the third quarter, and then a medial error in the fourth quarter. The model differences that cause deviation in the exiting temperature are expected to carry through to produce similar errors in the heat transfer calculations.

## **6.6 Piechowski Model Conclusions**

Overall, the Piechowski Model performed well, with an average annual RMS error in exiting temperature of under  $1.75^{\circ}\text{C}$ . A number of tests were performed on the Piechowski model that show it expresses the expected behavior, but when compared to the verification model, some deviations arose. The most reasonable explanation of this deviation appears to be the way in which the water is modeled. In the Piechowski model the water is a single node at each axial position. In the Fluent model, the water is comprised of hundreds of finite volumes within the pipe. Throughout the model development, an attempt was made to bring the test and verification models close to the same boundary conditions, but this water modeling difference could not be improved without drastically changing the dynamics of the models. This model performs much better than either the earth tube pipe model developed in section 4.4, or the Mei model developed in chapter 5. The suitability of the Piechowski model for EnergyPlus implementation is discussed in chapter 7.

## CHAPTER 7

### Model Selection

#### 7.1 Individual Model Results Summary

Throughout this work, three individual models have been evaluated and tested for their accuracy and their suitability for EnergyPlus implementation. Transfer function methods were researched, but not developed. This brief chapter summarizes the benefits and liabilities of each model.

##### 7.1.1 Transfer Function Methods

Transfer function methods are used in numerous areas of building simulation. They are a convenient means to simulate transient heat conduction for wall constructions [Hittle (1979), Seem (1987)], for vertical borehole ground heat exchangers [Hellstrom (1991), Yavuzturk & Spitler (1999), Lamarche & Beauchamp (2007)], and for wall constructions which include a warm or cold pipe within the material layers [Strand (1995)]. Hellstrom's g-functions cannot be modified to accomodate buried horizontal pipes, but Strand's QTF's can theoretically be applied to horizontal buried pipes. When a pipe is buried in a shallow trench, the region of soil above the pipe is thin enough that transfer functions (QTF's) can be developed. However, when the construction is too heavy (thick concrete walls or a deep layer of soil), these standard transfer functions fail. With approximately one meter of soil, the EnergyPlus transfer function development routine cannot converge on a set of response factors. For this reason, transfer function methods based on Strand's QTF's could not be developed for the current work. However, this method does show great promise, as it is a very

fast and reliable method. It is recommended this method be investigated further in the future. The revised model may use multiple layers to handle the thick soil.

### **7.1.2 Earth Tube Pipe Model**

The earth tube pipe model was developed from a model that is currently implemented in EnergyPlus for the simulation of earth tube air ducts. The model is extremely simple due to numerous assumptions: the pipe's impact on surrounding soil, soil capacitance, and steady state behavior. With these assumptions, the model is essentially an analytic solution for the buried pipe, and therefore computation time is minimal. The input data for this model is also minimal, as no storage characteristics are needed for the soil or pipe wall. These simplifications come at a price, however, and that price is accuracy. When compared to the verification model, the earth tube and the earth tube pipe models both encountered significant deviations throughout the annual simulation. Due to the extreme simplifications of the model, it was anticipated that the improvements required for the model to produce quality results would require effort that was better utilized in developing the other models in the study.

### **7.1.3 Mei Model**

The Mei model was developed in an effort to create an intermediate model. The model uses a single cylindrical coordinate system that includes the effects of a variable boundary condition as well as the possibility of using a backfill region around the pipe. This model represented a significant improvement over the earth tube model in terms of accuracy, but had very significant stability that led to its rejection as a candidate EnergyPlus model. The model development revealed that a maximum time step of 0.1 minute was required for the pipe wall and water nodes. The minimum EnergyPlus time step is 1 minute. The process required to handle this instability practically eliminated the possibility of selecting the Mei model as the implementation model

in EnergyPlus. This instability in the Mei model was inherently a problem with the varying grid spacing and the explicit finite difference equations. In addition, the model did not show good agreement with the initial 2D comparison with the Fluent model largely because it did not encapsulate ground surface interaction. Finally, this model showed poor initial condition independence when compared to the Piechowski model.

#### **7.1.4 Piechowski Model**

The Piechowski model was developed more recently, and is a significant improvement over the Mei model. The Piechowski model uses a dual coordinate system, with a cartesian grid in the soil and a radial grid near the pipe. This was originally thought to be a complexity of the model, but this development actually allows the radial near-pipe conditions to be hidden from the outer main time step loop. This provides an overall simplification for the model. This model is also superior to the others due to stability and ground surface interaction. The implicit foundation of the finite difference equations led to stable simulations throughout testing. The model also uses a rectangular grid which has a boundary at the ground surface, so convection to the outdoor air is modeled. In the original model, only one outdoor temperature was used for the entire simulation period. This model was improved after initial development by including the hourly outdoor air as an input. The far-field boundary condition was also improved by applying the Kusuda and Achenbach correlation. Originally the model used a few days of measured soil temperatures. This is not a tractable option in an annual simulation program, so the Kusuda and Achenbach correlation was implemented to create a more general purpose model. The last improvement was in the on/off schedule of the pipe flow. Originally, the model would retrieve a fraction of on time for each simulation day. The model would simulate for that fraction of the day, and then turn off for the rest of the day. The model is now improved so

that at each time step, the model can run either off or on, based on a control signal. For long time steps, the pipe flow could still be simulated with an on/off fraction if necessary. Overall, this model performed extremely well under testing, with much higher accuracy than the other models in both the initial testing and the verification testing. In the idealized high flow rate 2D case, the temperature distributions agree well. All of these factors indicated that the Piechowski model was the best model for implementation in EnergyPlus.

## **7.2 Selection and Summary of Final Model**

From this summary, it is clear that the Piechowski model was the best choice for a model to implement in EnergyPlus. The model is implemented in the form described above, although the addition of insulation/backfill around the pipe is implemented. As a first approximation, the insulation heat storage is not modeled, but it is recommended as future work. Any implementation of a model in EnergyPlus requires extreme stability and minimal computation time, which are then balanced with the accuracy of the model. To accomplish this, the grid for each simulation will be generated by the model itself in order to better suit the situations at hand. The implementation chapter follows, and this work then ends with conclusions and recommended future work.

## CHAPTER 8

### Model Implementation in EnergyPlus

The model chosen for implementation in EnergyPlus is the Piechowski buried pipe model. This model was chosen based on its accuracy, computation time, and stability. The model was first translated to FORTRAN 90, with formatting and computer code that conforms with the EnergyPlus code standards. In addition to the main module code changes, there were changes within other EnergyPlus modules to accommodate the new model. There were other items involved in the implementation, including error handling, final testing, and EnergyPlus documentation.

#### 8.1 Buried Pipe Module Description

Figure 8.1 shows the flow of the main pipe simulation manager. This routine is called by upper level plant management routines. The 'Get Input' subroutine retrieves the input data from the input file. One note about input is the manner in which some data is entered. In order to simplify input, a large portion of the geometry is brought in by construction and material data. The material data needed for each layer (pipe, soil, insulation, etc.) is brought in with standard 'Material:Regular' objects in EnergyPlus. The thickness of each layer is inherent in these objects, so these actually define the thickness of the pipe wall, and the soil thickness, which is then converted into a pipe depth for further calculations. Using objects that are already implemented in EnergyPlus streamlines the implementation of the model and makes it easier for users of the new model.

The pipe initialization routine described in figure 8.2 is called by the pipe manager

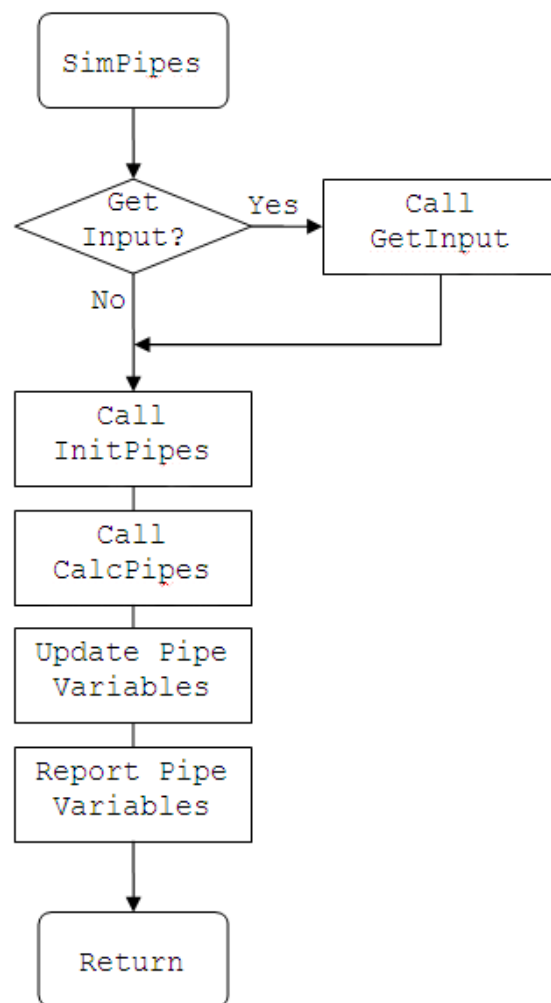


Figure 8.1: Main Pipe Simulation Manager Routine Flow



at each iteration. The 'Get Input' subroutine is called only one time.

The main pipe calculation routine shown in figure 8.3 actually controls all different types of pipe heat transfer, but only the buried pipe aspects are shown here. For the buried pipes, most of the calculations are kept in a separate routine, so this current routine is quite simple.

The routine in figure 8.4 manages most of the calculations for the buried pipes. When needed, calls are made to other routines. This calculation routine monitors the convergence of the temperatures in the cartesian outer domain.

The radial routine shown in figure 8.5 controls the simulation of the near pipe radial domain. At the pipe-water boundary, a separate routine is called. This calculation routine monitors the convergence of temperatures in the radial domain.

The routine described in figure 8.6 controls the inner-most pipe node and the water node at a given pipe cross section. The update equations are different based on pipe insulation existence.

This section has briefly covered the flow of the buried pipe section of the pipe heat transfer module in EnergyPlus. This section was intended to provide documentation once the model is fully implemented in the EnergyPlus distribution.

## **8.2 EnergyPlus Code Changes**

This section is a description of the changes made in the other EnergyPlus modules in order to accommodate the buried pipe model. This information is useful for keeping track of the changes in the software, an essential task when working with a team of developers.

### **8.2.1 Weather Manager**

The weather manager in EnergyPlus handles all of the atmospheric and weather conditions during the simulation. When this buried pipe model was added, a new program

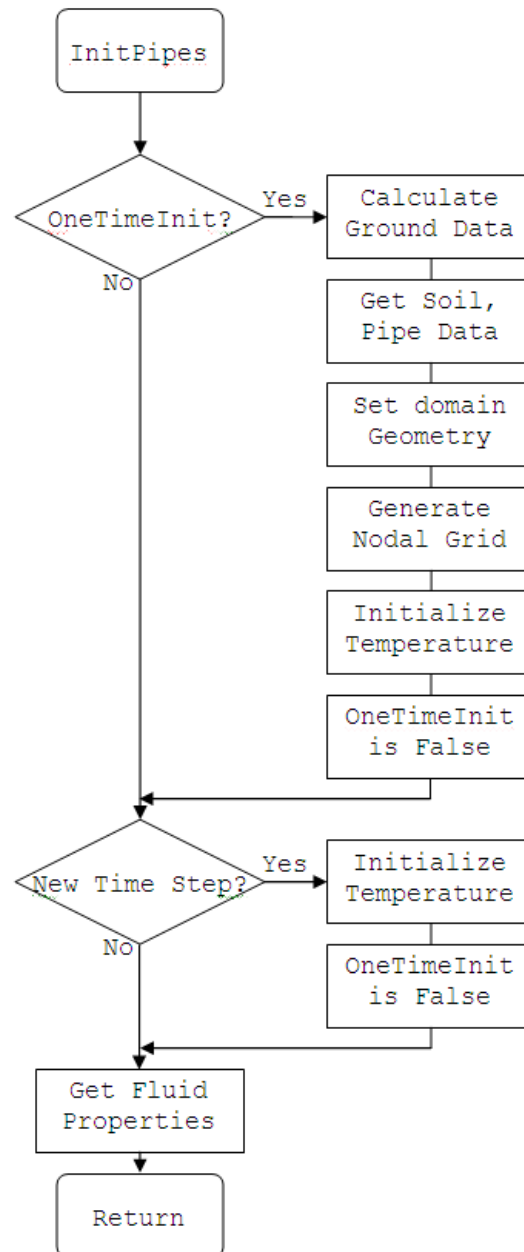


Figure 8.2: Pipe Initialization Routine Flow

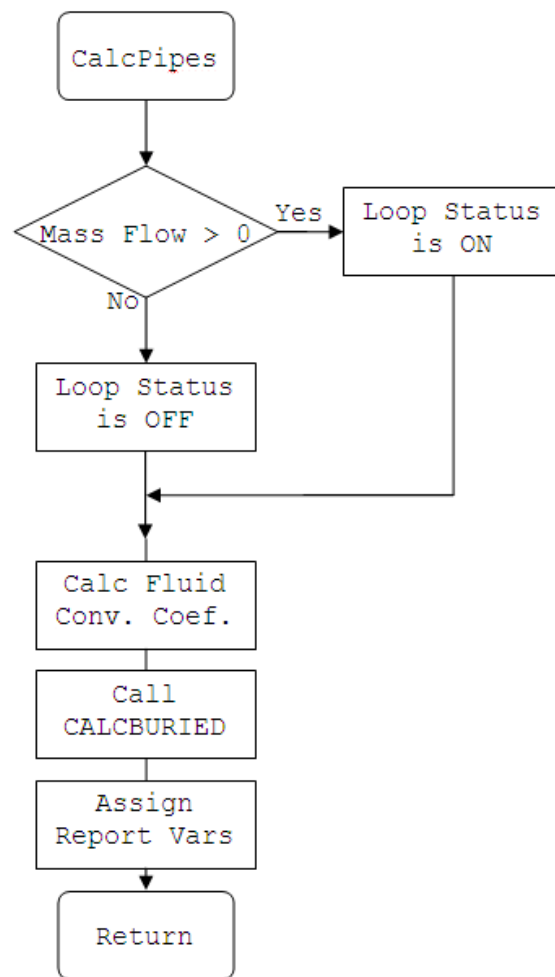


Figure 8.3: Main Pipe Calculation Routine Flow

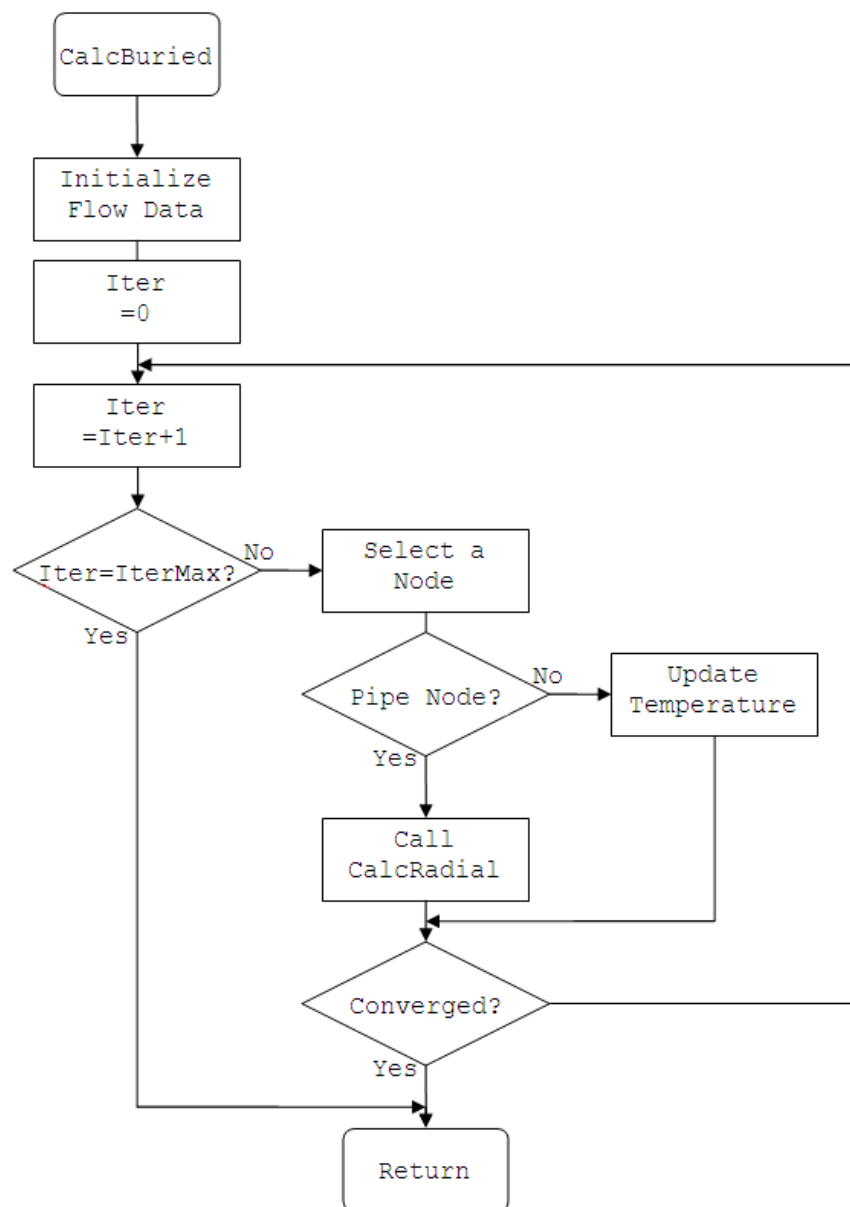


Figure 8.4: Buried Pipe Calculation Routine Flow

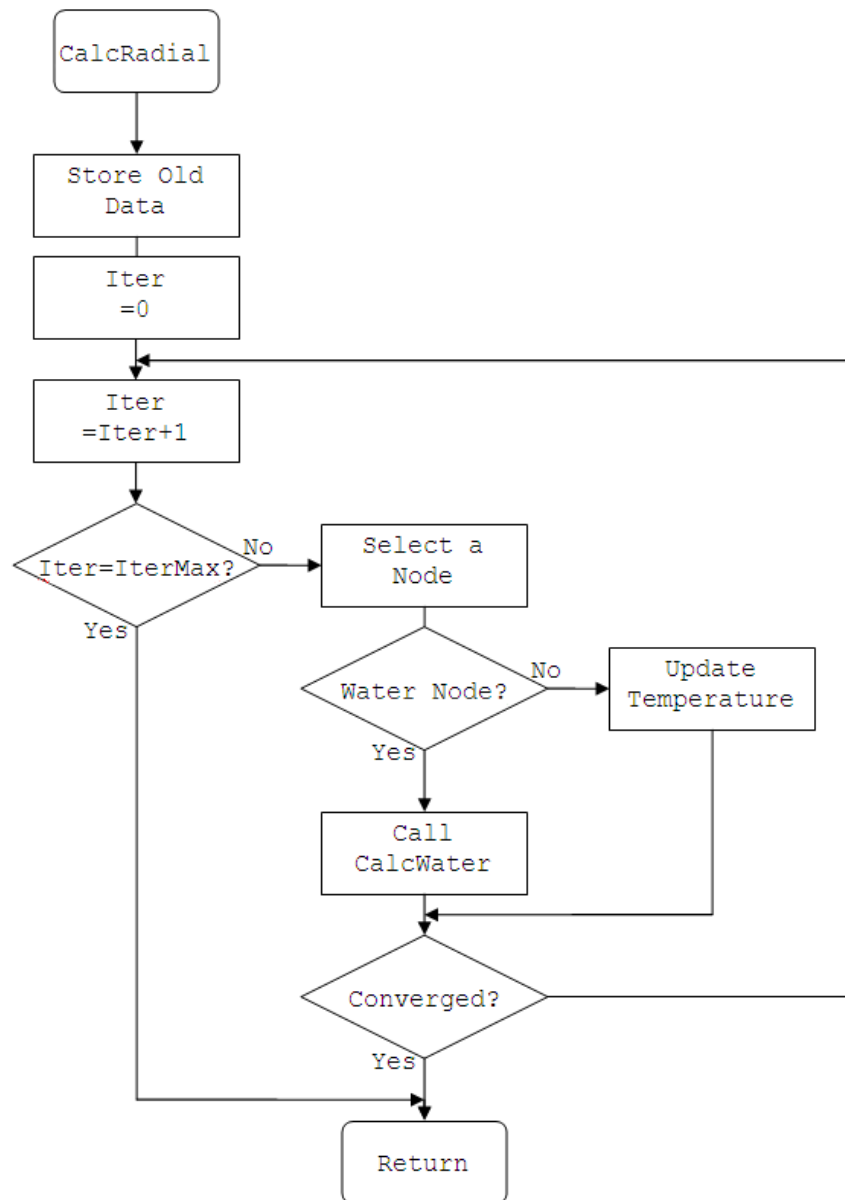


Figure 8.5: Buried Pipe Radial Region Routine Flow

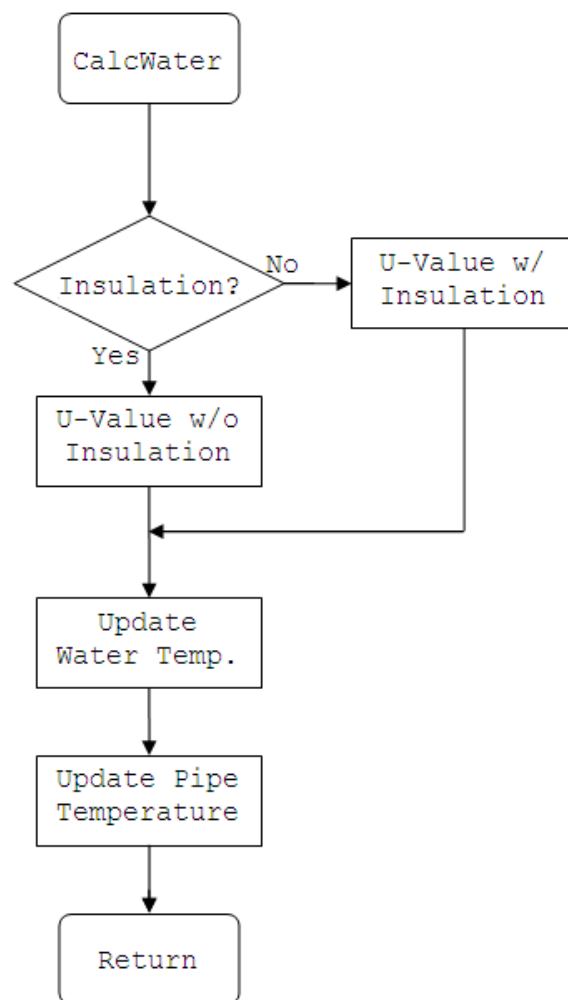


Figure 8.6: Buried Pipe Water Boundary Routine Flow

level variable was added which allows the annual ground surface temperatures to be retrieved at any time by the buried pipe module.

### **8.2.2 Plant Managers**

The plant manager handles the supply and demand loop managers. Through these modules, the underground pipe object was added in different manners. The plant manager is allowed to initialize the buried pipe model. The supply and demand side managers are simply modified to include the buried pipe objects. This is in addition to the outdoor pipe and zone pipe configurations.

### **8.2.3 Plant Loop Equipment**

The loop equipment module actually calls the pipe modules, so the loop equipment module code now has the ability to call the simulation routines for buried pipes.

## **8.3 Error Handling**

It is expected that there will be errors in an input file at some point during development of a building model. Errors could be as simple as a typo or it could be as critical as a stability issue. In this particular model, the implicit derivation should control the stability, but other errors may be encountered. The simulation catches typical errors that may be found during the input statements, such as a text phrase where a number is expected. The routine warns the user if excessive iterations are detected during the finite difference solution. If the user incorrectly inputs the soil/pipe/insulation construction, an error is reported. Surface ground temperatures are required for proper simulation, so if these objects are not found, an error is issued. EnergyPlus manager modules have error handling routines built in, so error traps were added by coding one line of code each, passing information such as the error message, the error type, and the pipe object name.

## 8.4 Preliminary Evaluation of the Model

Once the model was implemented in the EnergyPlus environment, testing was performed to ensure that the operation was as expected. As mentioned throughout this work, validation data is not available, so the original verification source is the Fluent model. This section discusses the input file used during testing. This input file includes a plant loop which contains the buried pipe model. The results of the simulation are then discussed; both temperature and heat fluxes over different periods of the year are evaluated. The model is then compared to the VBA implementation of the Piechowski model. The VBA version of the model was already verified against the Fluent model, and comparing the EnergyPlus implementation to the VBA model should ensure that the model was translated properly.

### 8.4.1 Input File Description

Required EnergyPlus inputs include, but are not limited to: simulation controls, material definitions, construction definitions, surface geometry, zone definitions, internal heat gains, output variable requests, pumps, coils, fans, boilers, chillers, mixers, splitters, and pipes. The input file must correctly define all loop topologies in order for the simulation to run correctly. The input file used in the testing in this section is a modified example file that comes with EnergyPlus. The original file is used to demonstrate the simulation of a pipe located within a zone and was modified to include a buried pipe.

The input file contains the information to simulate a 5,000 sq. ft. five-zone single floor building. All constructions follow standard industry practices. The simulation runs in Chicago for a full annual run period. The pipe which contains the new 'Pipe:Underground' object is titled: Pipe Heat Transfer Towers, and is located on the condenser supply cooling tower branch on the condenser loop.

In order to modify the file to include a buried pipe, the following tasks were



performed:

- Input Surface Ground Temperatures
- Input Material Definitions for Soil and Pipe Wall
- Input Construction object for buried pipe
- Modify a pipe within a condenser loop branch from type Pipe:Interior to type Pipe:Underground
- Comment out the Pipe:Interior object and Input a full Pipe:Underground object

With these steps completed, the file is ready to simulate for a fully annual period. The results are first analyzed alone, and then a comparison is made between this model and the VBA implementation of the Piechowski model.

#### **8.4.2 Discussion of Results**

A first check on model quality can be found from a look at the output alone. In a later section, the model results are compared to the VBA implementation of the model. For this self-test, the outlet temperatures and flow rates were recorded. In the original implementation of this model, it was trivial to control the reporting and iteration techniques. Once this model is implemented within the plant manager of EnergyPlus, the control becomes much more complex. During the periods of the simulation when the pipe is 'off' (i.e. no flow), the manager does not update the pipe temperatures. Because of this, the exiting temperature does not appear to 'float' like it does in the VBA implementation. However, this is merely a reporting difference between the models. The heat transfer to the fluid is properly accounted for while the flow is 'off'. The EnergyPlus implementation also catches freezing conditions, and outputs zero as the exiting temperature. This particular simulation was performed for two reasons: the root of the input file is that it is the example file for Pipe:Interior

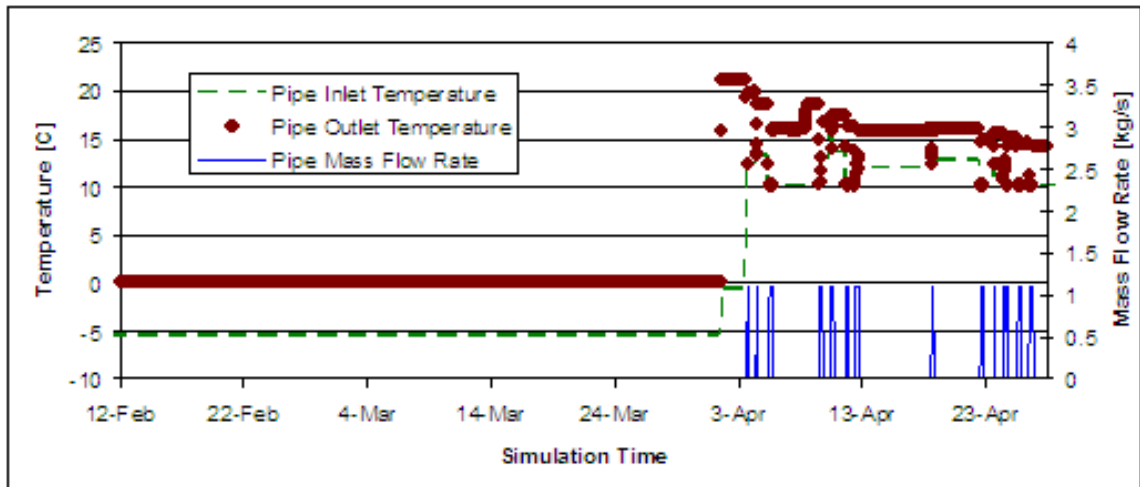


Figure 8.7: Results Section 1: 12-Feb to 28-Apr

objects, and also pipe freezing is encountered which ensures that model operates properly during these conditions. During the entire year of the simulation, the far-field boundary temperature at the pipe depth is approximately  $20^{\circ}\text{C}$ . This does not represent the exact temperature near the pipe, but it does provide a reference. For example, if the pipe entering water temperature is above this far-field temperature, the pipe will likely reject heat.

Figure 8.7 shows the model operation during the early part of the year. The main aspect of this plot is the transition from freezing conditions to normal operating conditions. In the first section of the plot (12-Feb to 1-Apr), the inlet temperature is approximately  $-5^{\circ}\text{C}$ , and freezing conditions exist. Because of this, the outlet temperature is held constant at  $0^{\circ}\text{C}$ . Once the pipe thaws, the model changes to normal operation; this effect is discussed in more detail in the following paragraphs.

Figure 8.8 shows a series of nine days, and reveals different aspects of the model behavior. Until about noon on 1-April, the pipe is frozen, and so the model gives zero as the outlet temperature. After this point, the pipe thaws, but the flow rate is still zero. During this time, the water temperature stays constant at the near pipe ground temperature. Around 4-April, the pump comes on, and the exiting temperature varies

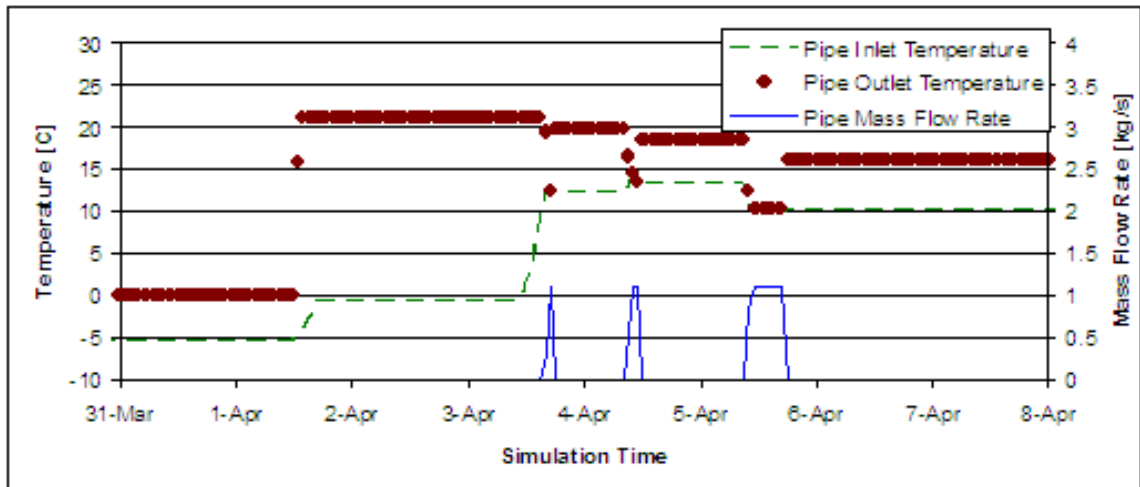


Figure 8.8: Results Section 2: 31-Mar to 8-Apr

for three hours. After this period, the exiting temperature is constant, but lower than before. This is simply because the cool water that flowed through the pipe cooled the ground temperature nodes near the pipe. Then during the pipe-off period, the EnergyPlus plant manager does not update the pipe exiting temperature at every time step. This continues during each on-off period over this time.

The month of April is represented in figure 8.9. During this time, the model operates as in figure 8.8, but shows the behavior on a larger scale. When looking at the whole month, it is easy to see the exiting temperature decreasing as the cool water flow decreases the ground temperature in the near-pipe region.

Figure 8.10 shows a two week period during the month of June. During this time, the pipe transitions from absorbing heat to rejecting heat. On 7-June, the entering water temperature moves above the ground temperature, and the pipe rejects heat. This increases the ground temperature near the pipe. This behavior is repeated in the second half of the plot.

The analysis in this section has shown that the model behaves reasonably from a qualitative standpoint. It is not possible to draw quantitative conclusions from this data alone, so in the next section, the EnergyPlus results are compared to verified

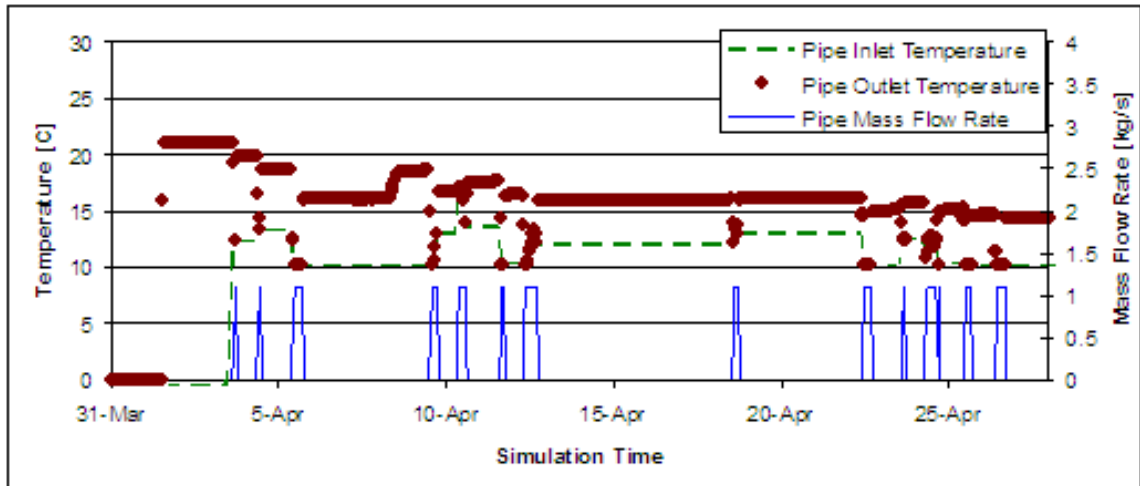


Figure 8.9: Results Section 3: 31-Mar to 28-Apr

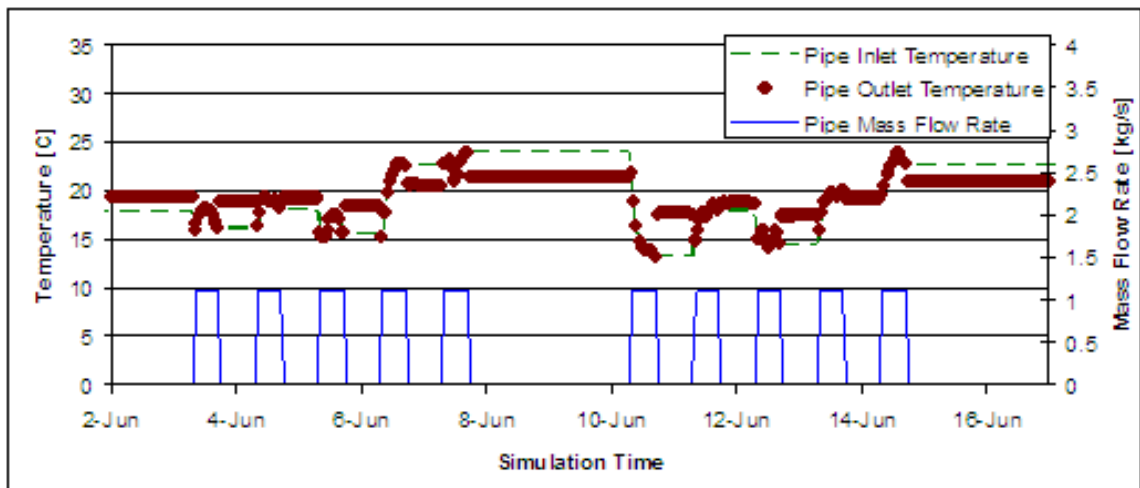


Figure 8.10: Results Section 4: 2-Jun to 17-Jun

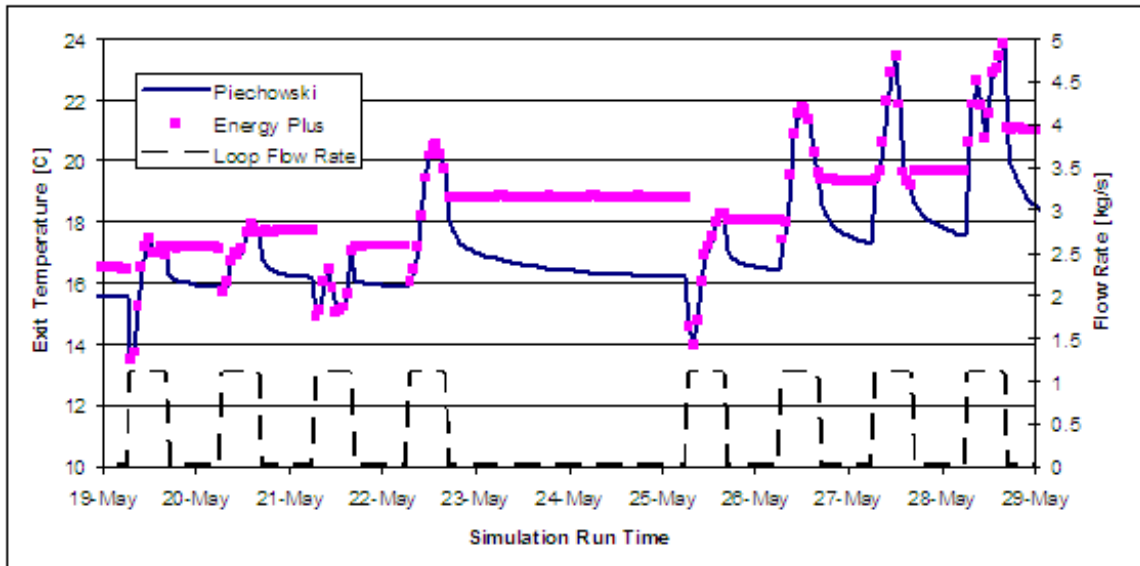


Figure 8.11: Implementation Comparison, EnergyPlus to VBA: Exiting Temperature

VBA model results.

### 8.4.3 Direct Implementation Comparison: EnergyPlus vs. VBA

One major difference between the EnergyPlus and the VBA implementations is the time step. In EnergyPlus, the plant manager routines adjust the time step constantly. In VBA, the time step is fixed. The model results may vary slightly due to this difference.

Figure 8.11 shows the outlet temperatures for both the models. The mass flow rate is also offered to understand the pipe on/off behavior. The models agree to within  $0.2^{\circ}$  during this period when the flow rate is greater than zero. As previously discussed, EnergyPlus does not report water temperatures when there is no flow in the pipe. However, the heat transfer rate is properly accounted for, so that for the very first time step after a 'no-flow' period, the water temperatures predicted by the two models agree.

Plotting temperatures alone can be deceiving, so typically the total heat transfer rate or the average heat flux are also plotted. This gives a representation of the delta

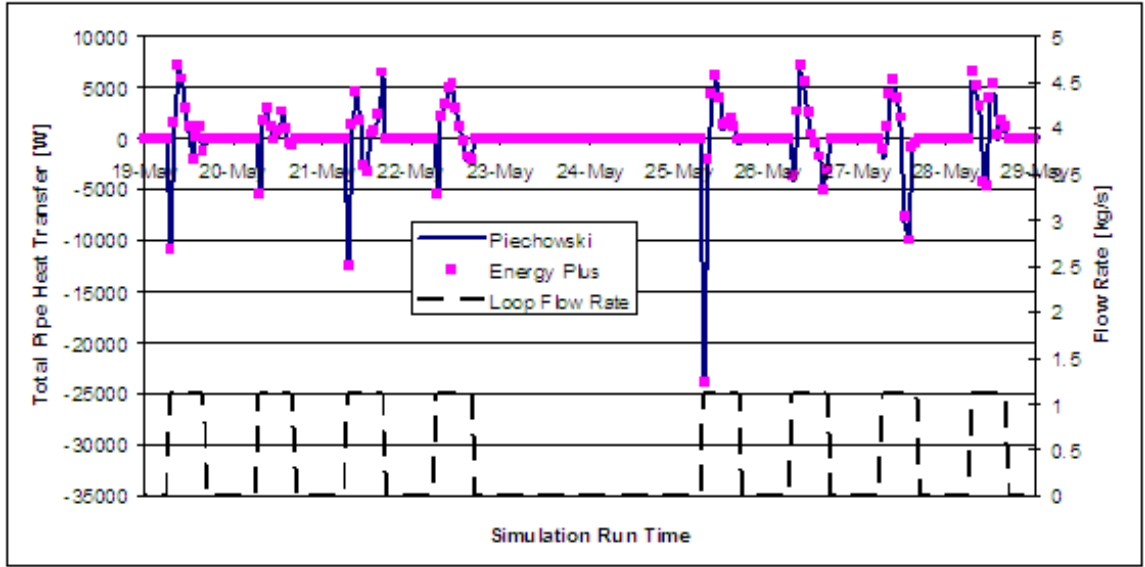


Figure 8.12: Implementation Comparison, EnergyPlus to VBA: Total Heat Transfer Rate

temperature through the pipe, which is more important when looking at overall model behavior. Figure 8.12 plots the total heat rate through the pipe which is calculated as shown in equation 8.1.

$$\dot{q} = \dot{m} \cdot C_p \cdot (T_{\text{out}} - T_{\text{in}}) \quad (8.1)$$

Figure 8.12 compares heat transfer rates predicted by the two models. When the EnergyPlus time step is shorter than the VBA time step, the data is averaged. The VBA simulation was performed with constant hourly time steps. As the figure shows, the heat transfer rates for both models agree almost exactly, however there are a few points which deviate slightly on 29-May. Errors such as this are expected to be a result of the time step management difference between the two models. From an annual standpoint, the heat transfer rates agree to within an RMS error of 750 W.

## 8.5 EnergyPlus Documentation

There are two documents that must be updated anytime a model is modified or implemented in EnergyPlus. The input/output reference document details the input syntax required by the model, as well as the output variables available for the model. The engineering reference document discusses how the model works, including its assumptions, capabilities and limitations. This section summarizes the contribution to each of these documents for the buried pipe model. These two document entries are included in appendices I and J.

## 8.6 Computation Time

One major factor when implementing a new model within a simulation program is computation time. For EnergyPlus, the simulations typically require anywhere from one minute to one hour to complete, based on model complexity and computer speed. For parametric studies, computation time plays a more significant role, as hundreds of simulations may be performed. A test was performed to see how different pipe models affect computation time for a full annual simulation. The three cases include a basic pipe model, an interior zone pipe model, and a buried pipe model. The basic pipe model sets the outlet conditions equal to the inlet conditions. The interior zone model utilizes a response factor method along with a convective boundary condition. The buried pipe model utilizes a finite difference grid along the length of the pipe and within the ground.

The buried pipe model is expected to increase computation time due to the large grid that is developed, and in fact, it does. However, the interior pipe model required less time than the simple pipe model. It is difficult to establish an exact reason for this behavior. In such a large program, every model utilized has an effect on the other models. The use of a buried pipe model may introduce a time-lagged effect in

Table 8.1: Computation Time Results

Pipe Model	Computation Time	Units
Simple Pipe	3.14	[minutes]
Interior Zone	2.91	[minutes]
Buried Pipe	3.24	[minutes]

the temperatures in the entire plant loop, which in turn causes a reduction in the number of iterations required by the plant manager. One aspect reveals itself from this study: the buried pipe model does not have a significant effect on computation time. If the number of buried pipes in an input file increases, the computation time will increase, and eventually, response factors may be required to accommodate this increased computation time.



## CHAPTER 9

### Conclusions

#### 9.1 Model Development

The objective of the investigation was to select a model for implementation in EnergyPlus. A reference model was developed as a basis for comparison since no experimental validation data was available. Three models were tested and compared to the reference model: the Earth Tube model, the Mei model, and the Piechowski model. The Earth tube pipe model was originally a regular earth tube model and was converted to a pipe model with a few changes as per section 4.4. Neither the Earth tube model nor the Earth tube pipe model performed well under thorough testing, with significant deviations of up to  $7^{\circ}\text{C}$  on the exiting temperature. This is due to the underlying assumptions of the model, which led to an inaccurate but very fast model. The Mei model was intended to provide an intermediate level of accuracy and computation time. After initial testing, the Mei model had significant drawbacks, mainly instability requiring a time step of 0.1 minute, which led to concluding the testing before the full verification was completed. The Piechowski model did not have the same stability problems as the Mei model due to the implicit formulation compared to the explicit formulation of Mei model.

The Piechowski model was selected for EnergyPlus implementation for reasons of stability and accuracy. The model, when compared to the Fluent verification model, produced an RMS error of exiting fluid temperature of less than  $1.75^{\circ}\text{C}$ , which resulted in an RMS error of total heat transfer rate of 3100 W. A number of improvements were made to the original Piechowski model:

- Ground surface interaction: The ground surface originally interacted with a single value of outdoor air, given as an input. The model now inputs hourly outdoor air temperature, which should provide a significant improvement on the small time scale accuracy.
- Far-field boundary condition: The far-field boundary is converted from a small set of days worth of ground temperature to the full Kusuda and Achenbach correlation. In the EnergyPlus system, this will serve better than a small set of experimental measurements.
- Flow on/off behavior: The on/off behavior of the model originally just ran the model for a period reflecting the run time for that day. Then for the rest of the day, the model simulates in the flow off condition. Currently the model can simulate in either flow off or flow on conditions at each individual time step. This should improve the accuracy of the model and how quickly heat can proceed to traverse through the soil.
- Pipe insulation: The pipe model was improved to include pipe insulation. For this current work, the pipe insulation is assumed, as with the pipe wall, to be steady state. The heat storage was not modeled in the insulation.

## 9.2 Final Model Implementation

Once the model was implemented in EnergyPlus, a series of tests were performed to ensure proper model operation. These tests revealed that during periods where the pipe is active (flow on), the model agrees with the VBA implementation with an RMS error of exiting water temperature of  $0.13^{\circ}\text{C}$  and an RMS error of total heat transfer rate of 750 W. These results came from a test where the peak heat transfer rate for the pipe length was over 20,000 W. These comparisons link the EnergyPlus implementation to the VBA implementation which was verified against the Fluent

model, which ensures the quality of the EnergyPlus implementation. The model appears to slightly increase the computation time of EnergyPlus, but only on the order of 5% compared to the simple pipe model. Detail of the computation time study is offered in section 8.6.

Although this model operates properly, future work is already desired to improve the generality, accuracy, and computation time of the model. These are presented in the following section.

### 9.3 Future Work

- Validation: It would be desirable to provide experimental validation source for this model. Validation would provide much stronger assurance of model accuracy than verification. Validation data could come from either a new facility, or from previously recorded data for a buried pipe.
- Enhanced Configurations (Multiple Pipe Layouts): The general buried pipe model should be able to handle multiple pipes in a single buried trench, including the effects of insulation on each pipe, and fluid flowing through the pipe in different directions.
- Moisture Transfer: Although in many cases where the temperatures in the model do not change significantly, the moisture interactions are not required, it would be desirable to have a general purpose model which could account for moisture migration.
- Response Factor Development: The buried pipe model increased computation time by 5% over the simple pipe model and 10% over the interior zone pipe model. This computation is not significant when there are a minimal number of buried pipes. As more buried pipes are added, this computation time will be

more significant, and response factors may be required to improve computation time.

- Transient Pipe Insulation Calculation: The pipe currently contains insulation, but it is steady state for simplicity. For better simulation, a new update equation should be developed for this region in order to account for heat storage in the pipe insulation.
- Expansion to full 3D simulation: Laying pipe in foundation trenches is becoming more popular. The addition of the foundation in the vicinity of the pipe will require a more robust model, especially when modeling the corners where the pipe bends. This will require a full 3D model capable of handling this complex geometry.

## BIBLIOGRAPHY

- Abu-Hamdeh, N. H. & Reeder, R. C. (2000), 'Soil thermal conductivity: Effects of density, moisture, salt concentration, and organic matter'.
- Al-Ajmi, F., Loveday, D. L. & Hanby, V. I. (2006), 'The cooling potential of earth-air heat exchangers for domestic buildings in a desert climate', *Building and Environment* **41**(3), 235–244.
- Allen, E. M. (1983), Heatplan: A microcomputer program for geothermal district heating assessment, *in* 'Geothermal Resources 1983 Annual Meeting: Energy on Tap!', Vol. 7, Geothermal Resources Council, Davis, CA, USA, Portland, OR, USA, pp. 563–565.
- Arimilli, R. V. & Parang, M. (1983), 'Numerical analysis of heat transfer in buried horizontal heat-exchanger tubes', *AIChE Symposium Series* **225**, 121–129.
- Baxter, D. (1992), 'Energy exchanges and related temperatures of an earth-tube heat exchanger in the heating mode', *Transactions of the ASAE* **35**(1), 275–285.
- Baxter, D. (1994), 'Energy exchanges and related temperatures of an earth-tube heat exchanger in the cooling mode', *Transactions of the ASAE* **37**(1), 257–267.
- Bierbaum, A. (1986), 'Recommended installation practices for water source heat pumps'.
- Bohm, B. (2000), 'On transient heat losses from buried district heating pipes', *International Journal of Energy Research* **24**(15), 1311–1334.

- Bohm, B. & Kristjansson, H. (2005), ‘Single, twin and triple buried heating pipes: on potential savings in heat losses and costs’.
- Bojic, M., Papadakis, G. & Kyritsis, S. (1999), ‘Energy from a two-pipe, earth-to-air heat exchanger’, *Energy* **24**(6), 519–523.
- Bose, J. E. & Smith, M. D. (1992), ‘Performance of new ground heat exchanger configurations for heat pumps’.
- Chiasson, A. & Spitler, J. D. (2000), Modeling approach to design of a ground-source heat pump bridge deck heating system, *in* ‘Proceedings of the 5th International Symposium on Snow Removal and Ice Control Technology’, Roanoke, VA, USA.
- Chuanshan, D. (1997), ‘Thermal analysis of indirect geothermal district heating systems’, *Geothermics* **26**(3), 351–364.
- De Paepe, M. (2002), ‘3d unstructured finite volume technique for modelling earth air heat exchangers’, *Computational Studies* **4**, 471–480.
- De Paepe, M. & Janssens, A. (2003), ‘Thermo-hydraulic design of earth-air heat exchangers’, *Energy and Buildings* **35**(4), 389–397.
- Dos Santos, G. H. & Mendes, N. (2006), ‘Simultaneous heat and moisture transfer in soils combined with building simulation’, *Energy and Buildings* **38**(4), 303–314.
- EnergyPlus (2007a), *EnergyPlus Engineering Reference*, U. S. Department of Energy.
- EnergyPlus (2007b), *EnergyPlus Input/Output Reference*, U. S. Department of Energy.
- EnergyPlus (2007c), *EnergyPlus Module Developer’s Guide*, U. S. Department of Energy.

- Eriksson, D. & Sunden, B. (1998), ‘Heat and mass transfer in polyurethane insulated district cooling and heating pipes’, *Journal of Thermal Envelope and Building Science* **22**(July), 49–71.
- Eskilson, P. (1987), *Thermal Analysis of Heat Extraction Boreholes*, 1 edn, Department of Mathematical Physics, University of Lund, Sweden.
- Fischer, R. D. (1983), Models of simultaneous heat and moisture transfer in soils, Technical report, Battelle Columbus Laboratories.
- Fisher, D. E., Rees, S. J., Padhmanabhan, S. & Murugappan, A. (2006), ‘Implementation and validation of ground-source heat pump system models in an integrated building and system simulation environment’, *HVAC&R Research* **12**(3a), 693–710.
- Froling, M. (2002), ‘Environmental and thermal performance of district heating pipes’, *Doktorsavhandlingar vid Chalmers Tekniska Hogskola* **1865**, 1–59.
- Gabrielaitiene, I., Bohm, B. & Sunden, B. (2007), ‘Modelling temperature dynamics of a district heating system in naestved, denmark—a case study’, *Energy Conversion and Management* **48**(1), 78–86.
- Hanby, V., Loveday, D. & Al-Ajmi, F. (2005), ‘The optimal design for a ground cooling tube in a hot, arid climate’, *Building Services Engineering Research and Technology* **26**(1), 1–10.
- Hanby, V., Wright, J., Fletcher, D. & Jones, D. (2002), ‘Modeling the dynamic response of conduits’, *HVAC and R Research* **8**(1), 1–12.
- Hellstrom, G. (1991), *Ground Heat Storage: Thermal Analyses of Duct Storage Systems, Part I*, 1 edn, Department of Mathematical Physics, University of Lund, Sweden.

- Hittle, D. C. (1979), Calculating building heating and cooling loads using the frequency response of multilayered slabs, PhD thesis, University of Illinois at Urbana-Champaign.
- Holman, J. P. (1981), *Heat Transfer*, 5 edn, McGraw Hill, New York.
- Hu, Q. & Feng, S. (2003), ‘A daily soil temperature dataset and soil temperature climatology of the contiguous united states’, *Journal of Applied Meteorology* **42**(8), 1139–1156.
- Hwang, C.-C. & Jiang, Y.-H. (2003), ‘Extensions to the finite element method for thermal analysis of underground cable systems’, *Electric Power Systems Research* **64**(2), 159–164.
- Inalli, M. & Esen, H. (2004), ‘Experimental thermal performance evaluation of a horizontal ground-source heat pump system’, *Applied Thermal Engineering* **24**(14–15), 2219–2232.
- Incorporated, F. (2006), ‘Fluent user’s guide’, Lebanon, N.H.
- Incropera, F. P. & DeWitt, D. P. (2002), *Introduction to Heat Transfer*, 4 edn, John Wiley and Sons, Hoboken, NJ.
- Ingersoll, L. R. & Plass, H. J. (1948), ‘Theory of the ground pipe source for the heat pump’, *ASHVE Transactions* **54**, 339–348.
- Jacovides, C. P. & Mihalakakou, G. (1995), ‘An underground pipe system as an energy source for cooling/heating purposes’, *Renewable Energy* **6**(8), 893–900.
- Kilkis, I. B. (1996), ‘Low enthalpy geothermal district heating system in nevsehir, turkey’, *Proceedings of the Intersociety Energy Conversion Engineering Conference* **3**, 1642–1646.



- Klimkowski, H., Braud, H. J. & Baker, F. E. (1985), ‘Performance of a horizontal earth heat exchanger with a water-source heat pump’, *Paper - American Society of Agricultural Engineers* p. 12.
- Kristjansson, H. & Bohm, B. (2006), ‘Optimum design of distribution and service pipes’, *Euroheat and Power* **3**(4), 1–20.
- Kumar, G. S. & Kaushik, S. C. (1995), ‘Theoretical earth temperature profiles for different soils and soil conditions’, *International Journal of Solar Energy* **17**(4), 199–209.
- Kusuda, T. & Achenbach, P. (1965), ‘Earth temperature and thermal diffusivity at selected stations in the united states’, *ASHRAE Transactions* **71**(1), 61–75.
- Lamarche, L. & Beauchamp, B. (2007), ‘New solutions for the short-time analysis of geothermal vertical boreholes’, *International Journal of Heat and Mass Transfer* **50**(7-8), 1408–1419.
- Lee, K. H. & Strand, R. K. (2006), Implementation of an earth tube system into energypplus program, *in* ‘SimBuild 2006’, MIT, Cambridge, Mass.
- Lei, T. K. (1993), ‘Development of a computational model for a ground-coupled heat exchanger’, *ASHRAE Transactions* **99**(1), 149–159.
- Li, X., Zhao, J. & Zhou, Q. (2004), ‘Theoretical model of underground heat exchanger and numerical simulation on underground temperature field’, *Taiyangneng Xuebao/Acta Energiæ Solaris Sinica* **25**(4), 492–496.
- Liu, X., Rees, S. J. & Spitler, J. D. (2007*a*), ‘Modeling snow melting on heated pavement surfaces. part 1: Model development’, *Applied Thermal Engineering* **27**(5-6), 1115–1124.

- Liu, X., Rees, S. J. & Spitler, J. D. (2007*b*), ‘Modeling snow melting on heated pavement surfaces. part 2: Experimental validation’, *Applied Thermal Engineering* **27**(5-6), 1125–1131.
- Marsili-Libelli, S. (1997), ‘Simple model of a transport/diffusion system’, *IEEE Proceedings: Control Theory and Applications* **144**(5), 459–465.
- Mei, V. C. (1986*a*), Horizontal ground-coil heat exchanger theoretical and experimental analysis, Technical report, Oak Ridge National Laboratory.
- Mei, V. C. (1986*b*), ‘Theoretical heat pump ground coil analysis with variable ground farfield boundary conditions’, *AIChE* **32**(7), 1211–1215.
- Mei, V. C. (1988), ‘Heat pump ground coil analysis with thermal interference’, *Journal of Solar Energy Engineering, Transactions of the ASME* **110**(2), 67–73.
- Mihalakakou, G. (2002), ‘On estimating soil surface temperature profiles’, *Energy and Buildings* **34**(3), 251–259.
- Mihalakakou, G., Santamouris, M. & Asimakopoulos, D. (1994), ‘Modelling the thermal performance of earth-to-air heat exchangers’, *Solar Energy* **53**(3), 301–305.
- Ozgener, L., Hepbasli, A. & Dincer, I. (2005), ‘Energy and exergy analysis of geothermal district heating systems: an application’, *Building and Environment* **40**(10), 1309–1322.
- Persson, C. & Claesson, J. (2005), Multipole method to compute heat losses from district heating pipes, in ‘Seventh Nordic Symposium on Building Physics’, Reykjavik Grand Hotel, Iceland.
- Phetteplace, G. (1995*a*), Efficiency of steam and hot water heat distribution systems, Technical report, Cold Regions Research and Engineering Lab, Hanover, NH.

- Phetteplace, G. (1995*b*), Optimal design of piping systems for district heating, Report review, US Army Cold Regions Research and Engineering Laboratory.
- Piechowski, M. (1996), A Ground Coupled Heat Pump System with Energy Storage, PhD thesis, University of Melbourne.
- Piechowski, M. (1998), 'Heat and mass transfer model of a ground heat exchanger: Validation and sensitivity analysis', *Energy research* **22**(11), 965–979.
- Piechowski, M. (1999), 'Heat and mass transfer model of a ground heat exchanger: Theoretical development', *Energy research* **23**(7), 571–588.
- Puri, V. M. (1985), 'Earth tube heat exchanger performance correlation using boundary element method', *Transactions of the American Society of Agricultural Engineers* **30**(2), 514–520.
- Puri, V. M. (1986), 'Feasibility and performance curves for intermittent earth tube heat exchangers', *Transactions of the ASAE* **29**(2), 526–532.
- Rafferty, K. (1996), 'Selected cost considerations for geothermal district heating in existing single-family residential areas'.
- Rees, S. J., Spitler, J. D., Deng, Z., Orio, C. D. & Johnson, C. N. (2004), 'A study of geothermal heat pump and standing column well performance', *ASHRAE Transactions* **110**(1), 3–13.
- Rees, S. J., Spitler, J. D. & Xiao, X. (2002), 'Transient analysis of snow-melting system performance', *ASHRAE Transactions* **108**(2), 406–423.
- Saastamoinen, J. J. (2007), 'Unsteady state temperature fields in a slab induced by line sources', *International Journal of Heat and Mass Transfer* **50**(3-4), 756–765.
- Saman, N. & Mahdi, H. (1996), 'Analysis of the delay hot/cold water problem', *Energy* **21**(5), 395–400.

- Seem, J. E. (1987), Modeling of heat transfer in buildings, PhD thesis, University of Wisconsin-Madison.
- Skoglund, T., Arzen, K.-E. & Dejmek, P. (2006), ‘Dynamic object-oriented heat exchanger models for simulation of fluid property transitions’, *International Journal of Heat and Mass Transfer* **49**(13-14), 2291–2303.
- Skoglund, T. & Dejmek, P. (2007), ‘A dynamic object-oriented model for efficient simulation of fluid dispersion in turbulent flow with varying fluid properties’, *Chemical Engineering Science* **62**(8), 2168–2178.
- Song, Y., Yao, Y. & Na, W. (2007), ‘Impact of soil thermal conductivity on temperature field of soil around horizontal buried pipe in ground-source heat pump’, *Journal of Harbin Institute of Technology* **14**, 381–384.
- Spitler, J. D., Fisher, D. E. & Zietlow, D. C. (1989), ‘A primer on the use of influence coefficients in building simulation’, *Building Simulation '89 Transactions* pp. 299–304.
- Strand, R. (1995), Heat Source Transfer Functions and Their Application to Low Temperature Radiant Heating Systems, PhD thesis, University of Illinois at Urbana-Champaign, Department of Mechanical and Industrial Engineering.
- Tarnawski, V. & Leong, W. (1993), ‘Computer analysis, design and simulation of horizontal ground heat exchangers’, *International Journal of Energy Research* **17**(6), 467–477.
- Thomas, H. R., Rees, S. W. & Sloper, N. J. (1998), ‘Three-dimensional heat, moisture and air transfer in unsaturated soils’, *International Journal for Numerical and Analytical Methods in Geomechanics* **22**(2), 75–95.

- Tzaferis, A., Liparakis, D., Santamouris, M. & Argiriou, A. (1992), ‘Analysis of the accuracy and sensitivity of eight models to predict the performance of earth-to-air heat exchangers’, *Energy and Buildings* **18**(1), 35–43.
- Wilhelm, W. V., Jones, J. T., Beard, R. J. & Ribando, B. K. (1996), ‘Thermal performance of horizontal closed-loop ground-coupled heat pump systems using flowable-fill’, *Proceedings of the Intersociety Energy Conversion Engineering Conference* **2**, 748–754.
- Yavuzturk, C. & Chiasson, A. D. (2002), ‘Performance analysis of u-tube, concentric tube, and standing column well ground heat exchangers using a system simulation approach’, *ASHRAE Transactions* **108**(1), 925–938.
- Yavuzturk, C. & Spitler, J. D. (1999), ‘A short time step response factor model for vertical ground loop heat exchangers’, *ASHRAE Transactions* **105**(2), 475–485.
- Yavuzturk, C. & Spitler, J. D. (2001), ‘Field validation of a short time step model for vertical ground-loop heat exchangers’, *ASHRAE Transactions* **107**(1), 617–625.
- Yavuzturk, C., Spitler, J. D. & Rees, S. J. (1999), ‘A transient two-dimensional finite volume model for the simulation of vertical u-tube ground heat exchangers’, *ASHRAE Transactions* **105**(2), 465–474.
- Zhao, J., Zhang, C., Li, X., Yu, L. & Song, D. (2006), ‘Three dimensional heat transfer model and experimental analysis of u-pipe heat exchanger’, *Taiyangneng Xuebao/Acta Energiæ Solaris Sinica* **27**(1), 63–66.

## APPENDIX A

### Earth Tube Model Code

```
Sub Earthtube()

Dim T_air_lookup(8760) As Single

'Read in temperature data from spreadsheet
For i = 1 To 8760
    T_air_lookup(i) = Cells(i + 3, 4).Value
Next i

'Input Pipe information
Pi = 3.14159265358 'Pi [-]
z = Cells(3, 4).Value 'Pipe burial depth [m]
L = Cells(4, 4).Value 'Pipe length [m]
Radius_pipe = Cells(5, 4).Value 'Pipe radius [m]
Thick_pipe = Cells(6, 4).Value 'Pipe thickness [m]
k_p = Cells(7, 4).Value 'Pipe thermal conductivity
Diam = Radius_pipe * 2 'Pipe Radius [m]
A_c = (Pi / 4) * Diam ^ 2 'Pipe cross sect. area [m2]

'Input Soil Information
```

```

alpha = Cells(10, 4).Value 'Avg gnd thermal diff [m2/day]
k_s = Cells(15, 4).Value    'Soil thermal conductivity

'Input Fluid Properties
V_dot_f = Cells(18, 4).Value 'Mass flow rate [kg/s]
Rho_f = Cells(19, 4).Value    'Density of fluid [kg/m3]
m_dot_f = V_dot_f * Rho_f
Cp_f = Cells(20, 4).Value     'Spec Heat [J/kg-K]
Nu = Cells(21, 4).Value       'Kinematic Viscosity
Pr = Cells(22, 4).Value       'Fluid Prandtl Number
k_f = Cells(23, 4).Value      'Fluid thermal conductivity

'Input Constants and Definitions
'Day of min surf temp (phase shift) [days]
T_shift = Cells(26, 4).Value

'Annual average soil surf temp [C]
T_surf = Cells(27, 4).Value

'Annual amplitude of soil surf temp [C]
T_amp = Cells(28, 4).Value

'Number of simulation days
NumDays = Cells(29, 4).Value

A_s = T_amp

```

```

'Pre-calculations

r_1 = Radius_pipe
r_2 = Thick_pipe
r_3 = 2 * Radius_pipe

'**Now the time stepping equations and loop structure
TS = 1 / 24    'Days (hourly)

TS_Integer = 0

For TimeStepper = 0 To NumDays Step TS

'--TS_Integer is integer time step
' TS=1 at time=0, TS=2 at time=1 hour, ...
    TS_Integer = TS_Integer + 1

    T_air = T_air_lookup(TS_Integer)

'Find temperature at pipe depth
T_g_zpipe=T_surf-A_s*Exp(-z*((Pi/(365*alpha))^(0.5))) *
    Cos((2*Pi/365)*(TimeStepper-T_shift-(z/2) *
    ((365/(Pi*alpha))^(0.5))))

'Pipe Flow Information
V = m_dot_f / (A_c * Rho_f)          'Pipe fluid velocity
Re = Diam * V / Nu
If (Re <= 2300) Then                  'Correlations from E+

```



```

Nuss = 3.66
ElseIf (Re <= 4000) Then
    fr = (1.58 * Log(Re) - 3.28) ^ (-2)
    Process1=(fr/2)*(Re-1000) *
        Pr/(1+12.7*((fr/2)^(0.5))*(Pr^(2/3)-1))
    Nuss=(Process1-3.66)/(1700)*Re +
        (4000*3.66-2300*Process1)/1700
Else
    fr = (1.58 * Log(Re) - 3.28) ^ (-2)
    Nuss=(fr/2)*(Re-1000) *
        Pr/(1+12.7*((fr/2)^(0.5))*(Pr^(2/3)-1))
End If

h_c = Nuss * k_f / (2 * Radius_pipe)

'Resistance calculations-Removed Length(Error in Paper)
R_c = (2 * Pi * r_1 * h_c) ^ -1
R_p = (1 / (2 * Pi * k_p)) * Log((r_1 + r_2) / r_1)
R_s=(1/(2 * Pi * k_s))*Log((r_1 + r_2 + r_3)/(r_1+r_2))
R_t = R_c + R_p + R_s
U_t = 1 / R_t

'Almost-done calculations--Eq (33) in paper
A=(m_dot_f*Cp_f*Log(Abs(T_air-T_g_zpipe))-U_t*L) /
    (m_dot_f*Cp_f)

'Calculate output temperature

```

```

T_inlet = T_air

If T_inlet > T_g_zpipe Then
    T_exit = T_g_zpipe + Exp(A)

ElseIf T_inlet = T_g_zpipe Then
    T_exit = T_inlet

ElseIf T_inlet < T_g_zpipe Then
    T_exit = T_g_zpipe - Exp(A)

End If

Cells(TS_Integer + 1, 2) = TimeStepper + 1
Cells(TS_Integer + 1, 3) = T_inlet
Cells(TS_Integer + 1, 4) = T_exit
Cells(TS_Integer + 1, 5) = m_dot_f*Cp_f*(T_inlet-T_exit)
Cells(TS_Integer + 1, 6) = T_g_zpipe

Next TimeStepper

End Sub

```

## APPENDIX B

### Gambit Journal File

```
/ Create the base 2D vertices
vertex create "v.1" coordinates 0 0 0
vertex create "v.2" coordinates 5 0 0
vertex create "v.3" coordinates 5 5 0
vertex create "v.4" coordinates 0 5 0
vertex create "v.5" coordinates 0 2.75 0
vertex create "v.6" coordinates 0.25 2.5 0
vertex create "v.7" coordinates 0 2.25 0

/ Generate edges from the vertices, still 2D
edge create "e.1" straight "v.1" "v.2"
edge create "e.2" straight "v.2" "v.3"
edge create "e.3" straight "v.3" "v.4"
edge create "e.4" straight "v.4" "v.5"
edge create "e.5" threepoints "v.5" "v.6" "v.7" arc
edge create "e.6" straight "v.7" "v.1"
edge create "e.7" straight "v.5" "v.7"

/ Generate faces for pipe and soil, still 2D
face create "f.1" wireframe "e.1" "e.2" "e.3" "e.4" "e.5" "e.6" real
face create "f.2" wireframe "e.5" "e.7" real

/ Extrude both faces 25m in z direction
volume create "vol.1" translate "f.1" vector 0 0 25
```

```

volume create "vol.2" translate "f.2" vector 0 0 25
/ Mesh both volumes
volume mesh "vol.2" cooper source "face.12" "f.2" size 0.25
volume mesh "vol.1" cooper source "face.9" "f.1" size 0.5
/ Apply continuum conditions
physics create "Soil" ctype "SOLID" volume "vol.1"
physics create "Pipe" ctype "FLUID" volume "vol.2"
/ Apply boundary conditions
physics create "SoilBack" btype "SYMMETRY" face "f.1"
physics create "PipeExit" btype "OUTFLOW" face "f.2"
physics create "DeepGround" btype "WALL" face "face.3"
physics create "LeftSoilSym" btype "SYMMETRY" face "face.4" "face.7"
physics create "RightSoilSym" btype "SYMMETRY" face "face.6"
physics create "PipeWall" btype "WALL" face "face.5"
physics create "GroundSurface" btype "WALL" face "face.8"
physics create "SoilFront" btype "SYMMETRY" face "face.9"
physics create "PipeCL" btype "SYMMETRY" face "face.10"
physics create "PipeInlet" btype "VELOCITY_INLET" face "face.12"
/ Export mesh file in Fluent format
export fluent5 "3DFluentEarthTube.msh"

```

## APPENDIX C

### Entering Water Temperature Summary

Day	EWT	Day	EWT	Day	EWT	Day	EWT
1	14.383	21	12.882	41	14.629	61	15.853
2	12.912	22	14.498	42	12.718	62	15.214
3	13.038	23	12.586	43	12.267	63	15.319
4	13.763	24	12.855	44	14.037	64	13.296
5	14.799	25	13.819	45	16.506	65	14.195
6	14.884	26	14.619	46	14.017	66	14.616
7	12.605	27	14.697	47	14.65	67	13.753
8	13.161	28	15.196	48	14.672	68	14.742
9	12.521	29	14.86	49	14.081	69	14.816
10	11.503	30	12.78	50	14.579	70	15.151
11	12.077	31	12.504	51	16.605	71	14.342
12	14.506	32	12.289	52	18.497	72	13.789
13	14.011	33	14.456	53	13.562	73	15.615
14	11.987	34	14.436	54	14.729	74	15.115
15	14.106	35	12.525	55	14.753	75	14.871
16	12.345	36	13.013	56	14.351	76	14.857
17	11.884	37	11.721	57	14.206	77	19.197
18	12.961	38	12.266	58	16.888	78	22.95
19	14.539	39	14.391	59	21.157	79	20.975
20	14.687	40	14.597	60	23.268	80	18.793

Day	EWT	Day	EWT	Day	EWT	Day	EWT
81	19.556	101	24.606	121	24.508	141	26.957
82	15.695	102	25.187	122	25.956	142	21.83
83	15.29	103	16.659	123	26.622	143	21.236
84	21.013	104	15.919	124	17.344	144	24.536
85	22.984	105	22.17	125	16.566	145	17.561
86	21.695	106	24.527	126	24.791	146	16.952
87	16.695	107	20.983	127	25.362	147	26.292
88	21.643	108	20.027	128	18.866	148	27.154
89	16.045	109	24.707	129	23.868	149	27.473
90	15.496	110	16.705	130	24.81	150	27.66
91	16.597	111	16.055	131	17.323	151	27.777
92	17.438	112	23.882	132	16.657	152	18.276
93	21.836	113	19.077	133	25.946	153	17.428
94	15.945	114	23.37	134	26.779	154	17.84
95	15.383	115	24.282	135	25.835	155	21.325
96	15.431	116	24.867	136	26.338	156	25.323
97	15.369	117	17.019	137	21.758	157	27.342
98	15.336	118	16.329	138	17.281	158	27.664
99	21.412	119	16.786	139	16.786	159	18.254
100	22.351	120	20.282	140	26.1	160	17.456

Day	EWT	Day	EWT	Day	EWT	Day	EWT
161	26.746	181	18.305	201	19.878	221	30.11
162	27.572	182	27.623	202	19.016	222	20.509
163	27.856	183	28.442	203	28.351	223	19.639
164	28.045	184	28.729	204	29.156	224	28.985
165	28.188	185	28.89	205	29.417	225	29.779
166	18.668	186	28.977	206	29.561	226	30.047
167	17.833	187	19.39	207	29.665	227	30.194
168	27.103	188	18.514	208	20.061	228	30.304
169	27.898	189	27.793	209	19.176	229	20.663
170	28.155	190	28.571	210	28.499	230	19.806
171	28.301	191	28.835	211	29.316	231	29.199
172	28.408	192	28.98	212	29.585	232	30.037
173	18.874	193	29.087	213	29.736	233	30.327
174	18.004	194	19.508	214	29.86	234	30.521
175	27.279	195	18.647	215	20.262	235	30.667
176	28.102	196	27.993	216	19.413	236	21.001
177	28.381	197	28.831	217	28.785	237	20.121
178	28.541	198	29.124	218	29.606	238	29.501
179	28.675	199	29.321	219	29.892	239	30.298
180	19.145	200	29.471	220	30.055	240	30.55

Day	EWT	Day	EWT	Day	EWT	Day	EWT
241	30.691	261	29.034	281	23.451	301	23.692
242	30.575	262	29.413	282	27.007	302	26.399
243	21.112	263	27.3	283	23.449	303	20.18
244	20.231	264	21.101	284	22.107	304	20.183
245	29.612	265	20.444	285	20.687	305	27.021
246	30.439	266	29.958	286	20.475	306	21.185
247	26.261	267	30.43	287	28.259	307	20.668
248	27.775	268	26.432	288	24.373	308	19.641
249	29.782	269	26.922	289	23.79	309	21.999
250	21.09	270	26.518	290	26.986	310	20.636
251	20.337	271	21.152	291	25.666	311	20.012
252	29.797	272	20.6	292	21.088	312	21.795
253	30.643	273	24.26	293	20.621	313	20.458
254	30.94	274	29.52	294	26.202	314	20.324
255	31.107	275	30.304	295	28.68	315	21.087
256	25.23	276	31.178	296	28.861	316	21.385
257	20.951	277	31.366	297	27.718	317	21.244
258	20.415	278	21.707	298	26.417	318	20.021
259	26.739	279	20.834	299	21.313	319	19.873
260	28.066	280	24.922	300	20.772	320	20.21



Day	EWT	Day	EWT	Day	EWT
321	20.209	341	20.001	361	17.811
322	19.782	342	20.05	362	19.608
323	23.991	343	18.217	363	19.723
324	22.934	344	19.231	364	18.67
325	25.872	345	17.862	365	20.313
326	27.697	346	17.544		
327	21.171	347	19.226		
328	20.563	348	19.77		
329	20.944	349	19.838		
330	21.802	350	20.931		
331	21.514	351	22.705		
332	21.061	352	20.411		
333	17.748	353	20.121		
334	20.009	354	19.595		
335	20.134	355	19.888		
336	19.825	356	19.901		
337	20.359	357	17.989		
338	20.25	358	17.81		
339	19.656	359	19.614		
340	18.983	360	19.558		

## APPENDIX D

### Modified Piechowski Model Code

```
Sub Main()  
  
  'Define Variables  
  Call VarDefs  
  
  'Retrieve pipe film coefficient (only needed once for const flow)  
  Call FILMCOEF(H, f, Re, Nu, Dp, Mw, V, RHOf, VISCf, Pr, Kf)  
  
  'Input all hourly water inlet temperatures  
  Call InputHourlyData  
  
  'Initialize Data  
  Call InitializeData(Ldim, Ts, NR, Mdim, Np, dS, Mp)  
  
  'Initialize soil coefficients  
  Call COEF_SOIL(A1, A2, CB1, CB2, CB3, S1, S2, NR)  
  
  'New TimeStepping Routine  
  For TimeCounter = 1 To NumTimeSteps  
    SimTime = (TimeCounter - 1) * dTIME  
    nDAYS = Int(SimTime / 86400) + 1
```

```

'Update Boundary conditions
Call UpdateBoundaries(Ldim, Mdim, dS, nDAYS, K, Tbsurf, Tbbot)

'Read in Loop On/Off Status
LOOPStatus = "-EMPTY-"
LoopStatusNum = Worksheets("Input").Cells(TimeCounter + 5, 12)
If LoopStatusNum = 1 Then LOOPStatus = "ON"
If LoopStatusNum = 0 Then LOOPStatus = "OFF"

'Read in entering water temperature
Twin = EWTFunc(SimTime)
TAMB = HourlyDB(SimTime)

'Call Main Loop Simulation Routine
Call GLOOP(Ldim, Mdim, Mp, Np, Twin, TAMB, LOOPStatus, NR)

'Write water temperatures
Call WriteData(SimTime, Twin, TW(2, Ldim), Tbsurf, _
    Tbbot, TimeCounter)

Next TimeCounter

End Sub

*****

Sub VarDefs()

```

```

'-----Required simulation data

NumTimeSteps = Worksheets("Input").Cells(6, 7).Value

Pi = Worksheets("Input").Cells(8, 7).Value

dTIME = Worksheets("Input").Cells(7, 7).Value 'Timestep [s]

RadialErrorFlag = False


'-----Fluid information

VISCF = Worksheets("Input").Cells(6, 3).Value

Pr = Worksheets("Input").Cells(7, 3).Value

Kf = Worksheets("Input").Cells(8, 3).Value

Kp = Worksheets("Input").Cells(9, 3).Value

HAMB = Worksheets("Input").Cells(10, 3).Value

RHOf = Worksheets("Input").Cells(11, 3).Value

Cf = Worksheets("Input").Cells(12, 3).Value


'-----Soil Information

RHOS = Worksheets("Input").Cells(16, 3).Value

Cs = Worksheets("Input").Cells(17, 3).Value

KSOILConstant = Worksheets("Input").Cells(22, 3).Value

AlphaS = KSOILConstant / (RHOS * Cs) ' [m2/s]

AlphaS2 = AlphaS * 3600 * 24 ' [m2/day]

AvgTsurf = Worksheets("Input").Cells(23, 3).Value

AvgTsurfAmp = Worksheets("Input").Cells(24, 3).Value


'-----Specifying node which contains the pipe and Pipe Radii

Mp = Worksheets("Input").Cells(25, 7).Value

Np = Worksheets("Input").Cells(26, 7).Value

```

```

Rpi = Worksheets("Input").Cells(12, 7).Value
Rpo = Worksheets("Input").Cells(13, 7).Value

'-----Specifying numbers of nodes and Nodal Spacing
Ldim = Worksheets("Input").Cells(21, 7).Value
Mdim = Worksheets("Input").Cells(22, 7).Value
NR = Worksheets("Input").Cells(23, 7).Value
dX = Worksheets("Input").Cells(18, 7).Value
dS = Worksheets("Input").Cells(19, 7).Value

'-----SOME CALCS

'Pipe Diameter
Dp = 2 * Rpi

'Cuts a full grid in half in anticipation of setting up pipe node
Rr = dS / 2

'Radial Spacing: edge of pipe to the end of half node,
'divided by # of radial nodes
dR = (Rr - Rpo) / (NR - 1)

'-----Fluid Flow
Vol = Worksheets("Input").Cells(13, 3).Value
Mw = (0.001 / 60) * Vol * RHOf
V = (0.001 / 60) * Vol / (Pi * Rpi ^ 2)

End Sub

*****

Sub FILMCOEF(H, f, Re, Nu, Dp, Mw, V, RHOf, VISCf, Pr, Kf)

```

```

V = 4 * Mw / (3.14 * Dp * Dp * RHOf)
Re = V * Dp * RHOf / VISCF

If Re >= 2300 Then
    H = 0.023 * (Re ^ 0.8) * (Pr ^ 0.4) * Kf / Dp
Else
    H = 48 * Kf / (11 * Dp)
End If

Nu = 0.0155 * (Re ^ 0.83) * (Pr ^ 0.5)
f = -0.046 * (Re ^ (-0.2))

End Sub

*****

Sub InputHourlyData()

For ColNum = 1 To 2
    For RowNum = 1 To 8760
        a(RowNum, ColNum) = Cells(RowNum + 5, ColNum + 9)
        adb(RowNum, ColNum) = Cells(RowNum + 5, ColNum + 13)
    Next RowNum
Next ColNum

End Sub

```

```

*****

Sub InitializeData(Ldim, Ts, NR, Mdim, Np, dS, Mp)

Ks = KSOILConstant

'Initially set ambient temp for time = 0
TAMB = HourlyDB(0)

DEPTH = (Mp - 1) * dS
Ts = TBND(DEPTH, 0) 'Time step zero

'Loop through time steps 1 and 2, initializing data
For K = 1 To 2
    'Loop through all lengths of pipe
    For L = 1 To Ldim
        'Initialize Water Temperatures
        TW(K, L) = Ts
        'Loop through all radial nodes near pipe
        For I = 1 To NR
            'Initialize soil temperature
            TR(K, L, I) = Ts
        Next I
        'Loop through all depth
        For m = 1 To Mdim
            'Loop through all width
            For n = 1 To Np
                DEPTH = (m - 1) * dS

```

```

        'Initialize soil temperature
        T(K, L, m, n) = -3# + TBND(DEPTH, 0)

    Next n

Next m

Next L

Next K

End Sub

*****

Sub COEF_SOIL(A1, A2, CB1, CB2, CB3, S1, S2, NR)

Dim R(15) As Single

'AlphaS = Ks / (RH0s * Cs)
Fo = AlphaS * dTIME / (dS * dS) 'Eq. D4
A1 = Fo / (1 + 4 * Fo) 'Eq. D2
A2 = 1 / (1 + 4 * Fo) 'Eq. D3

R(1) = RPo
For I = 2 To NR
    R(I) = R(I - 1) + dR
Next I

CBa = 2 * 3.14 * Ks * dTIME / Log(R(NR) / R(NR - 1))
CBb = 2 * Ks * dTIME
CBc = (dS^2-3.14*(R(NR-1)+dR/2)*(R(NR-1)+dR/2))*RH0s*Cs

```



CB = CBa + 4 \* CBb + CBc

CB1 = CBa / CB

CB2 = CBb / CB

CB3 = CBc / CB

'S1 = 1 / (2 \* (HAMB \* dX / Ks + 2))

S1 = 1 / (2 \* (HAMB \* dS / Ks + 2)) 'Eq. D8

'S2 = HAMB \* dX / (HAMB \* dX + 2 \* Ks)

S2 = HAMB \* dS / (HAMB \* dS + 2 \* Ks) 'Eq. D9

End Sub

\*\*\*\*\*

Sub UpdateBoundaries(Ldim, Mdim, dS, nDAYS, K, Tbsurf, Tbbot)

'Update Boundary conditions

For K = 1 to 2

For L = 2 To Ldim

For I = 1 To Mdim

DEPTH = (I - 1) \* dS

T(K, L, I, 1) = TBND(DEPTH, nDAYS) 'Farfield Bndry

Next I

DEPTH = 0#

Tbsurf = TBND(DEPTH, nDAYS) 'Soil Surface Temperature

DEPTH = (Mdim - 1) \* dS

Tbbot = TBND(DEPTH, nDAYS) 'Lower soil boundary

For I = 1 To Np

```

        T(K, L, 1, I) = Tbsurf 'Top side of boundary
        T(K, L, Mdim, I) = Tbbot 'Bottom side of boundary
    Next I
Next L
Next K

End Sub

```

```

*****

```

```

Function EWTFunc(time)
'Interpolates within a 2D array, "a", of time-water temp pairs
Dim i1 As Single, i2 As Single, I As Single
Dim irange As Single, fract As Single

If time <= a(1, 1) Then
    EWTFunc = a(1, 2)
ElseIf time >= a(8760, 1) Then
    EWTFunc = a(8760, 2)
Else
    i1 = 1
    i2 = 8760
    Do While ((i2 - i1) > 1)
        irange = i2 - i1
        I = i1 + irange / 2
        If (time < a(I, 1)) Then
            i2 = I
        Else

```

```

        i1 = I
    End If

    Loop

        I = i2

        fract = (time - a(I - 1, 1)) / (a(I, 1) - a(I - 1, 1))

        EWTFunc = a(I - 1, 2) + fract * (a(I, 2) - a(I - 1, 2))

    End If

End Function

*****

Function HourlyDB(time)
'Interpolates within 2D array, "adb", of time-outdoor DB pairs
Dim i1 As Single, i2 As Single, I As Single
Dim irange As Single, fract As Single

    If time <= adb(1, 1) Then
        HourlyDB = adb(1, 2)
    ElseIf time >= adb(8760, 1) Then
        HourlyDB = adb(8760, 2)
    Else
        i1 = 1
        i2 = 8760

        Do While ((i2 - i1) > 1)
            irange = i2 - i1
            I = i1 + irange / 2

            If (time < adb(I, 1)) Then

```

```

            i2 = I
        Else
            i1 = I
        End If
    Loop
        I = i2
        fract=(time-adb(I-1,1))/(adb(I,1)-adb(I-1,1))
        HourlyDB=adb(I-1,2)+fract*(adb(I,2)-adb(I-1,2))
    End If

End Function

*****

Sub GLOOP(Ldim, Mdim, Mp, Np, Twin, TAMB, LOOPStatus, NR)

'Variables dimensioned for only this subroutine
Dim T_0(50, 30, 30) As Single

K = 2
TW(K, 1) = Twin
EPS_A = 0.01

ITER = 1
1: If ITER > 10 Then
    MsgBox "Too many iterations in GLOOP"
    Exit Sub
End If

```

```

'Store computed values in T_0 array
For L = 2 To Ldim
    For m = 1 To Mdim - 1
        For n = 2 To Np
            T_0(L, m, n) = T(K, L, m, n)
        Next n
    Next m
Next L

'Loop along entire length of pipe, analyzing cross sects
For L = 2 To Ldim
    For m = 1 To Mdim - 1
        For n = 2 To Np
            If m = 1 Then 'Soil Surface Boundary
                If n = Np Then 'Symmetric centerline boundary
                    T(K, L, m, n) = _
                        2*S1*(T(K,L,m+1,n)+T(K,L,m,n-1))+S2*TAMB
                Else 'Soil surface, but not on centerline
                    T(K, L, m, n) =
                        S1*(2*T(K,L,m+1,n)+T(K,L,m,n-1)+ _
                            T(K,L,m,n+1))+S2*TAMB 'Eq. D7
                End If
            ElseIf n = Np Then 'On Symmetric centerline boundary
                If m = Mp Then 'Pipe node
                    Call RADIAL(LOOPStatus,L,Mp,Np,CB1,CB2,CB3,NR)
                ElseIf m <> 1 Then 'Not surface node

```

```

        T(K,L,m,n)=A1*(T(K,L,m+1,n)+T(K,L,m-1,n)+ _
        2*T(K,L,m,n-1))+A2*T(K-1,L,m,n)

    End If

    Else    'All Interior Nodes

        T(K,L,m,n)=A1*(T(K,L,m+1,n)+T(K,L,m-1,n)+ _
        T(K,L,m,n+1)+T(K,L,m,n-1))+A2*T(K-1,L,m,n)  'Eq. D1

    End If

Next n

Next m

Next L

'Check for convergence

For L = 2 To Ldim
    For m = 1 To Mdim - 1
        For n = 2 To Np
            If Abs(T_0(L, m, n) - T(K, L, m, n)) > EPS_A Then GoTo 1
        Next n
    Next m
Next L

'Now store 'new temperatures' into 'old temperature'
'array in preparation for next time step

For L = 2 To Ldim
    'Water temperatures

    If LOOPStatus = "OFF" Then
        TW(1, L) = TR(K, L, 1)
    Else

```

```

        TW(1, L) = TW(K, L)
    End If

    'Radial temperatures and moisture values
    For I = 2 To NR
        TR(1, L, I) = TR(K, L, I)
    Next I

    'Soil temperatures
    For m = 1 To Mdim
        For n = 2 To Np
            T(1, L, m, n) = T(K, L, m, n)
        Next n
    Next m
Next L

K = 2

End Sub

*****

Sub RADIAL(LOOPStatus, LX, Mp, Np, CB1, CB2, CB3, NR)

    'Variable Arrays for just this subroutine
    Dim TRX(15) As Single, TOR(15) As Single

    'Originally this header included a loop through all

```

```

'nodes and assigned TRX = TR
K = 2
EPS_A = 0.01
ITER = 1

1: If ITER > 25 Then
    If RadialErrorFlag = False Then
        MsgBox "Too many errors in Radial"
        RadialErrorFlag = True
    End If
    Exit Sub
End If

ITER = ITER + 1

For I = 2 To NR
    TOR(I) = TRX(I)
Next I

'Loop through radial nodes
For I = 2 To NR
    If I <> NR Then
        Call COEF_RAD(I, LX, NR, AT, BT, CT, DT, _
            FT, GT, BH, CH, DH, FH, GH)
        TR(K,LX,I)=AT*(TR(K,LX,I+1)-TR(K,LX,I-1))+ _
            BT*(TR(K,LX,I+1)-TR(K,LX,I-1))+ _
            CT*(TR(K,LX,I-1)+TR(K,LX,I+1))+DT*TR(K-1,LX,I)
    End If
Next I

```



```

        TRX(I) = TR(K, LX, I)
    Else
        TR(K,LX,I)=CB1*TR(K,LX,NR-1)+CB2*(T(K,LX,Mp+1,Np)+ _
            T(K,LX,Mp-1,Np)+2*T(K,LX,Mp,Np-1))+CB3*TR(K-1,LX,I)
        TRX(I) = TR(K, LX, I)
        T(K, LX, Mp, Np) = TR(K, LX, I)
    End If
Next I

'Apply boundary conditions
If LOOPStatus = "ON" Then
    Call BOUNDARY(LX)
Else
    TR(K, LX, 1) = TR(K, LX, 2)
    TW(K, LX) = TR(K, LX, 1)
End If

'Check convergence
For I = 1 To NR
    If Abs(TOR(I) - TRX(I)) > EPS_A Then GoTo 1
Next I

End Sub

*****

Sub BOUNDARY(LX)

```

'Calculates the boundary temperatures at the pipe interface  
'for both the fluid node and the first radial node

K = 2

U = 1 / (1 / H + RPi / Kp \* Log(RPo / RPi))

B1 = -V \* dTIME / dX

B2 = 2 \* U \* dTIME / (RHOf \* Cf \* RPi)

c = 1 - B1 + B2 'Denominator in Eqs. C22-C24

C1 = -B1 / c 'Eq. C22

C2 = B2 / c 'Eq. C23

C3 = 1 / c 'Eq. C24

KSO = KSOILConstant

b = (dR / KSO) \* (RPi / RPo) \* U

CPa = 1 / ((1 + b) \* (1 - BC) - b \* C2)

CP1 = b \* CPa

CP2 = (1 - BC \* (1 + b)) \* CPa

TR(K,LX,1)=CP1\*(C1\*TW(K,LX-1)+C3\*TW(K-1,LX))+CP2\*TR(K,LX,2)

TW(K,LX)=C1\*TW(K,LX-1)+C2\*TR(K,LX,1)+C3\*TW(K-1,LX) 'Eq. C21

End Sub

```

*****

Function TBND(z, TimeDays)

'Replaced with Kusuda and Achenbach, T_shift placed as 'zero'
' in equation, assuming sim. starts on date of min surf temp

TBND=AvgTsurf-AvgTsurfAmp*Exp(-z*((Pi/(365*AlphaS2))^(0.5)))* _
Cos((2*Pi/365)*(TimeDays-0-(z/2)*((365/(Pi*AlphaS2))^(0.5))))

End Function

*****

Sub WriteData(SimTime, Twin, TWout, Tbsurf, Tbbot, TimeCounter)

Cells(1, 1).Value = "Simulation Time [s]"
Cells(TimeCounter + 1, 1).Value = SimTime
Cells(1, 2).Value = "Entering Water Temp [C]"
Cells(TimeCounter + 1, 2).Value = Twin
Cells(1, 3).Value = "Exiting Water Temp [C]"
Cells(TimeCounter + 1, 3).Value = TWout 'TW(2, Ldim)
Cells(1, 4).Value = "Surface Temperature"
Cells(TimeCounter + 1, 4).Value = Tbsurf
Cells(1, 5).Value = "Deep Ground Temp"
Cells(TimeCounter + 1, 5).Value = Tbbot

'Shortened for brevity

End Sub

```

## APPENDIX E

### Modified Mei Model Code

```
'*****
```

```
Sub Main()
```

```
'Initially Define Variables
```

```
Call DefineVariables
```

```
'Bring in hourly EWT and outdoor DB
```

```
Call InputHourlyData
```

```
'Initialize Data and Spreadsheet
```

```
Call ClearOutput
```

```
Call InitializeDomain
```

```
'Output Initial Data
```

```
Call InitialOutput
```

```
FirstOutput = True
```

```
'Convert Units to minutes and inches
```

```
Call ConvertUnits
```

```
'Set Constants
```

```

Call SetConstants

'Output Initial Temperature Distribution
CurTimeDays = 0

'Begin Transient Calculations
For TimeStepIndex = 0 To NumTimeSteps
'New Time Step for which we are calculating values
    NewTimeStep = TimeStepIndex + 1
    DTIMEHours = DTIME / 60      'TimeStep in Hours
    CurTimeHours = NewTimeStep * DTIMEHours
    CurTimeSecs = CurTimeHours * 3600
    CurTimeDays = CurTimeHours / 24

    TH20 = EWTFunc(CurTimeSecs)

'Simulate Buried Pipe Loop
    Call SimLoop

'Write out current time step data
    Call WriteOutput(FirstOutput)
    FirstOutput = False

Next TimeStepIndex

End Sub

```

```
'*****
```

```
Sub DefineVariables()
```

```
'*****Input Data from Spreadsheet
```

```
'Required Parameters
```

```
Pi = Cells(6, 6).Value
```

```
H1 = Cells(7, 6).Value 'Fluid-Pipe Conv Coeff. 'Btu/hr/ft2/F
```

```
VINNER = Cells(8, 6).Value 'ft/s
```

```
AvgTsurf = Cells(9, 6).Value 'Annual Average Surface Temp [F]
```

```
AvgTsurfAmp = Cells(10, 6).Value 'Avg Surf Temp Variation [F]
```

```
DPTH = Cells(11, 6).Value
```

```
'Fluid Properties
```

```
RKF = Cells(14, 4).Value 'Thermal Conductivity 'Btu/hr/ft/F
```

```
RHOF = Cells(15, 4).Value 'Density 'lb/ft3
```

```
CPF = Cells(16, 4).Value 'Specific Heat 'Btu/lb/F
```

```
ALPHAF = RKF / (RHOF * CPF) 'Thermal Diffus. 'ft2/hr
```

```
'Pipe Wall Properties
```

```
RK1 = Cells(14, 5).Value 'Thermal Conductivity 'Btu/hr/ft/F
```

```
RH01 = Cells(15, 5).Value 'Density 'lb/ft3
```

```
CP1 = Cells(16, 5).Value 'Specific Heat 'Btu/lb/F
```

```
ALPHA1 = RK1 / (RH01 * CP1) 'Thermal Diffus. 'ft2/hr
```

```
'Backfill Properties
```

```
RK2 = Cells(14, 6).Value 'Thermal Conductivity 'Btu/hr/ft/F
```

```
RH02 = Cells(15, 6).Value 'Density 'lb/ft3
```

```

CP2 = Cells(16, 6).Value      'Specific Heat      'Btu/lb/F
ALPHA2 = RK2 / (RH02 * CP2)    'Thermal Diffus.    'ft2/hr

'Soil Properties

RK3 = Cells(14, 7).Value      'Thermal Conductivity 'Btu/hr/ft/F
RH03 = Cells(15, 7).Value      'Density              'lb/ft3
CP3 = Cells(16, 7).Value      'Specific Heat        'Btu/lb/F
ALPHA3 = RK3 / (RH03 * CP3)    'Thermal Diffus.      'ft2/hr
ALPHA3PERDAY = ALPHA3 * 24     'Convert to ft2/day for Kusuda

R1 = Cells(18, 4).Value        'Coil Inside Radius   'inches
R2 = Cells(19, 4).Value        'Coil Outside Radius  'inches
R3 = Cells(20, 4).Value        'Backfill-Soil Boundary Rad. 'in
R4 = Cells(21, 4).Value        'Farfield Radius       'inches
ZMAX = Cells(22, 4).Value      'Length of pipe       'ft

NZ = Cells(18, 8).Value        'Nodal points in axial direction
NPIPE = Cells(19, 8).Value     'Nodal points in coil wall
NFREEZ = Cells(20, 8).Value    'Nodal points in backfill
NSOIL = Cells(21, 8).Value     'Nodal points in soil region
NRAD = Cells(22, 8).Value      'Nodal points in theta direction

DTIME = Cells(24, 4).Value     'Time step for fluid, soil 'min
PDTIME = Cells(25, 4).Value    'Time step for coil wall   'min
NumTimeSteps = Cells(26, 4).Value 'Number of Time steps

For I = 1 To NSOIL - 1

```

```

        DRSOIL(I) = Cells(I + 27, 4).Value
Next I

'*****Preliminary Calculations
STOPPER = False
RFAR = DPTH
EPS = 0.05

Ac = Pi * R1 ^ 2           'Pipe Cross Sectional Area 'in2
V1 = VINNER
VolDot = V1 * Ac * 60 / 144 'Pipe Volume Flow Rate      'ft3/min=CFM
GPM = VolDot * 7.480519    'Pipe Volume Flow Rate      'GalPerMin
Vel1 = VINNER
VINNER = VINNER * 12 * 60  'Convert from ft/s to inch/min

'Some Calcs, to change # of grid points to # of internal elements
NSOIL1 = NSOIL - 1
NPM1 = NPIPE - 1
NFZM1 = NFREEZ - 1
NZM1 = NZ - 1
NRAD1 = NRAD - 1

End Sub

'*****
Sub InputHourlyData()

```



```

For ColNum = 1 To 2
    For RowNum = 1 To 8760
        a(RowNum, ColNum) = Cells(RowNum + 5, ColNum + 9).Value
    Next RowNum
Next ColNum

```

```

For RowNum = 1 To 8760
    OnOff(RowNum) = Cells(RowNum + 5, 13).Value
Next RowNum

```

```

End Sub

```

```

'*****

```

```

Sub ClearOutput()

    Worksheets("Output Data").Select
    Cells.Select
    Selection.ClearContents
    Cells(1, 1).Select

```

```

End Sub

```

```

'*****

```

```

Sub InitializeDomain()

```

```

'Initial State: Time = 0

```

```

CurTimeDays = 0

```

```

PipeFlow = True

'Set a few variables
DZ = ZMAX / NZ           'Axial grid spacing, feet
DANGLE = Pi / (NRAD - 1) 'Angular Grid Spacing, rad.
DRPIPE = (R2 - R1) / NPM1 'Pipe Wall Grid Spacing
MaxTimeHours = NumTimeSteps * DTIME 'Ending time, hours
MaxTimeSecs = MaxTimeHours * 3600   'Ending time, seconds
R3R2 = R3 - R2                     'Backfill width, inches

'Use Kusuda and Achenbach to fill temperature arrays
For K = 1 To 2                 'Loop through timesteps 1 and 2
    For J = 1 To NZ            'Loop along length of pipe
        For I = 1 To NSOIL     'Loop along radial soil nodes

            If I = 1 Then       'For the first I
                R = R3          'Radius = Backfill-soil boundary rad.
            Else                 'All other I
                R = R + DRSOIL(I - 1) 'Calculate the radius
            End If

            '***Loop along all theta points, calculate a depth,
            '***calculate an S, assign SOILT(theta) to the
            '***current outermost node at length = 1

        For M = 1 To NRAD
            Z = (DPTH - R * Sin(Pi / 2 - (M - 1) * DANGLE)) / 12
            S(I,J,M,K)=AvgTsurf- _

```

```

    AvgTsurfAmp*Exp(-Z*((Pi/(365*ALPHA3PERDAY))^(0.5))) _
    *Cos((2*Pi/365)*(CurTimeDays-Tshift-(Z/2)*((365/(Pi*_
ALPHA3PERDAY))^(0.5))))

    SOILT(M) = S(NSOIL, 1, M, K)

Next M

Next I

For I = 1 To NPIPE      'Loop along radial points in pipe
    T(I, J, K) = S(1, J, (NRAD + 1) / 2, K)

Next I

For M = 1 To NRAD      'Loop along all theta
    For I = 1 To NFZM1  'Loop along in backfill
        F(1, J, M, K) = T(NPIPE, J, K)
        F(I + 1, J, M, K) = S(1, J, M, K)
    Next I
Next M

U(J, K) = T(1, J, K)

Next J

Next K

DZ = 12 * ZMAX / NZ      'Convert to inches
DRFZ = R3R2 / NFZM1      'Backfill Grid Spacing

For IZ = 1 To NZ
    DEPTH(IZ) = IZ * DZ / 12
Next IZ

End Sub

```

```

'*****

Sub ConvertUnits()

ZMAX = 12 * ZMAX      'Axial pipe length [ft] to [inch]

RK1 = RK1 / (60 * 12)  ' [Btu/hr/ft/F] to [Btu/minute/inch/F]
RK2 = RK2 / (60 * 12)  ' [Btu/hr/ft/F] to [Btu/minute/inch/F]
RK3 = RK3 / (60 * 12)  ' [Btu/hr/ft/F] to [Btu/minute/inch/F]

H1 = H1 / (60 * 144)   ' [Btu/hr/ft2/F] to [Btu/min/in2/F]

RHOF = RHOF / 1728      ' [lb/ft3] to [lb/in3]
RH01 = RH01 / 1728      ' [lb/ft3] to [lb/in3]
RH02 = RH02 / 1728      ' [lb/ft3] to [lb/in3]
RH03 = RH03 / 1728      ' [lb/ft3] to [lb/in3]

ALPHA1 = RK1 / (RH01 * CP1) 'Pipe Diffusivity, now in [in2/min]
ALPHA2 = RK2 / (RH02 * CP2) 'Backfill Diff., now in [in2/min]
ALPHA3 = RK3 / (RH03 * CP3) 'Soil Diffusivity, now in [in2/min]

End Sub

'*****

Sub SetConstants()

```

DTDZ = PDTIME / DZ 'min / inches > [min/inch]

'Beta Coefficients used to update water temperature nodes

BETA2 = VINNER \* DTDZ 'in/min \* min/inch > [-]

BETA3 = 2 \* H1 \* PDTIME / (RHOF \* CPF \* R1) 'Dim'less [-]

BETA1 = 1 - BETA2 - BETA3 'Dim'less [-]

'A1\*DT/DR Coefficients used here and to calculate Mu Coeffs

A1DTDR = ALPHA1 \* PDTIME / DRPIPE 'in<sup>2</sup>/min \* min/inch [inches]

A2DTDR = ALPHA2 \* DTIME / DRFZ '[inches]

A3DTDR = ALPHA3 \* DTIME / DRSOIL(1) '[inches]

'Gamma Coefficients used to update pipe-water boundary nodes

GAMMA2 = A1DTDR \* (2 / DRPIPE + 1 / R1) 'in\*(1/in)=Dim'less [-]

GAMMA3 = 2 \* A1DTDR \* H1 / RK1 'Dim'less [-]

GAMMA1 = 1 - GAMMA2 - GAMMA3 'Dim'less [-]

'Sand Coefficients used to update backfill-soil boundary nodes

SAND1 = RK3 / RK2 \* 2 \* A2DTDR / DRSOIL(1) 'Dim'less [-]

SAND2 = 2 \* A2DTDR \* (1 / DRFZ - 1 / 2 / R3) 'Dim'less [-]

SAND3 = DRFZ \* A2DTDR / ((R3 \* DANGLE) ^ 2) 'Dim'less [-]

SAND4 = 1 - SAND1 - SAND2 - 2 \* SAND3 'Dim'less [-]

'C\_R Coefficients used to update internal pipe nodes

For I = 1 To NPIPE

R = R1 + (I - 1) \* DRPIPE '[inches]

C2R(I) = A1DTDR \* (1 / DRPIPE + 1 / R) 'in\*(1/in) = [-]

```

        C3R(I) = A1DTDR / DRPIPE          'inches/inches = Dim'less [-]
        C1R(I) = 1 - C2R(I) - C3R(I)      'Dim'less [-]
Next I

End Sub

'*****
Function EWTFunc(time)
'Interpolates within a 2D array, "a", of time-water temp pairs
Dim i1 As Single, i2 As Single, I As Single
Dim irange As Single, fract As Single

If time <= a(1, 1) Then
    EWTFunc = a(1, 2)
ElseIf time >= a(8760, 1) Then
    EWTFunc = a(8760, 2)
Else
    i1 = 1
    i2 = 8760
    Do While ((i2 - i1) > 1)
        irange = i2 - i1
        I = i1 + irange / 2
        If (time < a(I, 1)) Then
            i2 = I
        Else
            i1 = I
        End If
    End While
End Function

```

```

    Loop
        I = i2
        fract = (time - a(I - 1, 1)) / (a(I, 1) - a(I - 1, 1))
        EWTFunc = a(I - 1, 2) + fract * (a(I, 2) - a(I - 1, 2))
    End If

End Function

'*****
Sub SimLoop()

For J = 1 To NZ      'Loop along all nodes along length of pipe
    'Mu Coefficients are used to update outermost pipe node
    MU2 = 2 * RK2 / RK1 * A1DTDR / DRFZ
    MU3 = A1DTDR * (2 / DRPIPE - 1 / R2)
    MU1 = 1 - MU2 - MU3
    If NFZM1 >= 2 Then
        For I = 2 To NFZM1
            R = R2 + (I - 1) * DRFZ
            D2R(I) = A2DTDR * (1 / DRFZ + 1 / R)
            D3R(I) = A2DTDR / DRFZ
            D1R(I) = 1 - D2R(I) - D3R(I)
        Next I
    End If
    R = R3
    For I = 2 To NSOIL1
        R = R + DRSOIL(I - 1)
    End For
End Sub

```

```

    DRAVG = (DRSOIL(I) + DRSOIL(I - 1)) * 0.5
    E2R(I) = 2 * ALPHA3 * DTIME / DRSOIL(I) / DRSOIL(I - 1)
    E3R(I)=ALPHA3*DTIME/DRSOIL(I-1)*(2/DRSOIL(I-1)-1/R)
    E4R(I) = ALPHA3 * DTIME / ((R * DANGLE) ^ 2)
    E1R(I) = 1 - E2R(I) - E3R(I) - 2 * E4R(I)
Next I
'Calculate Fluid Temperature
KK = DTIME / PDTIME + 0.1
SUM(J) = 0
For M = 2 To NRAD1
    SUM(J) = SUM(J) + S(2, J, M, 1)
Next M
SUM(J) = SUM(J) + (S(2, J, 1, 1) + S(2, J, NRAD, 1)) * 0.5
SUM(J) = SUM(J) / NRAD1
SUM(J) = 0
For M = 2 To NRAD1
    SUM(J) = SUM(J) + F(2, J, M, 1)
Next M
SUM(J) = SUM(J) + (F(2, J, 1, 1) + F(2, J, NRAD, 1)) * 0.5
SUM(J) = SUM(J) / NRAD1
For K = 1 To KK
    If OnOff(TimeStepIndex) > 0.5 Then
        If J = 1 Then
            U(1,2)=BETA1*U(1,1)+BETA2*TH20+BETA3*T(1,1,1)
        Else:
            U(J,2)=BETA1*U(J,1)+BETA2*U(J-1,1)+BETA3*T(1,J,1)
        End If
    End If

```



```

    T(1,J,2)=GAMMA1*T(1,J,1)+GAMMA2*T(2,J,1)+GAMMA3*U(J,1)
Else:
    U(J,2)=2*RK1*(T(2,J,1)- _
        T(1,J,1))*PDTIME/(RHOF*CPF*R1^2)/Log(1+DRPIPE/R1)+U(J,1)
    T(1, J, 2) = U(J, 2)
End If
If NPM1 >= 2 Then
    For I = 2 To NPM1
        T(I,J,2)=C1R(I)*T(I,J,1)+C2R(I)*T(I+1,J,1)+ _
            C3R(I)*T(I-1,J,1)
    Next I
End If
T(NPIPE,J,2)=MU1*T(NPIPE,J,1)+MU2*SUM(J)+MU3*T(NPM1,J,1)
'Store new values in old value array
U(J, 1) = U(J, 2)
For I = 1 To NPIPE
    T(I, J, 1) = T(I, J, 2)
Next I
Next K
For M = 1 To NRAD
    F(1, J, M, 2) = T(NPIPE, J, 2)
Next M
If NFZM1 >= 2 Then
    For M = 1 To NRAD
        For I = 2 To NFZM1
            F(I,J,M,2)=D1R(I)*F(I,J,M,1)+D2R(I)*F(I+1,J,M,1)+ _
                D3R(I)*F(I-1,J,M,1)

```

```

        Next I

    Next M

End If

For M = 1 To NRAD

    If M = 1 Then

        BF = 2 * F(NFREEZ, J, M + 1, 1)

    ElseIf M = NRAD Then

        BF = 2 * F(NFREEZ, J, M - 1, 1)

    Else:

        BF = F(NFREEZ, J, M + 1, 1) + F(NFREEZ, J, M - 1, 1)

    End If

    F(NFREEZ, J, M, 2) = SAND1 * S(2, J, M, 1) + SAND2 * F(NFZM1, J, M, 1) + _
        SAND3 * BF + SAND4 * F(NFREEZ, J, M, 1)

Next M

'Update Farfield Boundary
Call UpdateFarfield

For M = 1 To NRAD

    S(NSOIL, J, M, 2) = SOILT(M)

    If R3R2 > EPS Then

        S(1, J, M, 2) = F(NFREEZ, J, M, 2)

        S(1, J, M, 1) = F(NFREEZ, J, M, 1)

    Else

        S(1, J, M, 2) = T(NPIPE, J, 2)

        S(1, J, M, 1) = T(NPIPE, J, 1)

    End If

    For I = 2 To NSOIL1

        Intermediate = E1R(I) * S(I, J, M, 1) + E2R(I) * S(I + 1, J, M, 1) + _

```

```

        E3R(I)*S(I-1,J,M,1)
    If M = 1 Then
        S(I, J, M, 2)=Intermediate+E4R(I)*2*S(I, J, M + 1, 1)
    ElseIf M = NRAD Then
        S(I, J, M, 2)=Intermediate+E4R(I)*S(I, J, M - 1, 1)*2
    Else: 'M <> 1 and M <> NRAD
        S(I,J,M,2)=Intermediate+E4R(I)*(S(I,J,M+1,1)+S(I,J,M-1,1))
    End If

    ESum = E1R(I) + E2R(I) + E3R(I) + 2 * E4R(I)

Next I

Next M

Next J

'Store new values of S and F in old array
For J = 1 To NZ
    For M = 1 To NRAD
        For I = 1 To NFREEZ
            F(I, J, M, 1) = F(I, J, M, 2)
        Next I
        For I = 1 To NSOIL
            S(I, J, M, 1) = S(I, J, M, 2)
        Next I
    Next M
Next J

End Sub

```

```

'*****

```

```

Sub UpdateFarfield()

    R = RFAR

    For M = 1 To NRAD

        ZZ = (DPTH - R * Sin(Pi / 2 - (M - 1) * DANGLE)) / 12

        SOILT(M)=AvgTsurf- _
        AvgTsurfAmp*Exp(-ZZ*((Pi/(365*ALPHA3PERDAY))^(0.5)))* _
        Cos((2*Pi/365)*(CurTimeDays-Tshift-(ZZ/2)*((365/(Pi* _
        ALPHA3PERDAY))^(0.5))))

        If M = Int(NRAD / 2) Then SoilTempAtPipeDepth =SOILT(M)

        If M = 1 Then SoilTempAtGroundSurf = SOILT(M)

        If M = NRAD Then SoilTempAtDeepGround = SOILT(M)

    Next M

End Sub

```

## APPENDIX F

### Analytic Constant Wall Temperature Code

```
Sub PiecewiseAnalytic()  
  
Rad = Cells(6, 11).Value  
mdot = Cells(10, 11).Value  
Cp = Cells(11, 11).Value  
T1 = Cells(12, 11).Value  
h = Cells(13, 11).Value  
  
For I = 1 To 5  
    Tenter = T1  
    L = Cells(15 + I, 10).Value  
    Ts = Cells(15 + I, 11).Value  
    dL = L / 25  
  
    For J = 1 To 25  
  
        Num1 = mdot * Cp * Tenter  
        Num2 = h*3.141592*2*Rad*dL*(Ts-(Tenter/2))  
        Num = Num1 + Num2  
        Denom = mdot * Cp + (h * 3.1415926535 * Rad * dL)
```

```
Texit = Num / Denom
```

```
Tenter = Texit
```

```
Next J
```

```
Cells(15 + I, 12).Value = Texit
```

```
Next I
```

```
End Sub
```

## APPENDIX G

### EnergyPlus IDD Object

Example of the input object definition in the EnergyPlus input dictionary file. EnergyPlus references this object at the beginning of a simulation so that when it comes across a similar object in the input data file, the appropriate measures can be taken for proper data input.

```
PIPE:UNDERGROUND,  
    \memo Buried Pipe model using finite  
    \memo    difference techniques  
A1, \field name of pipe  
    \required-field  
A2, \field Construction name  
    \required-field  
    \type object-list  
    \object-list ConstructionNames  
A3, \field Fluid inlet node  
    \type alpha  
    \required-field  
A4, \field Fluid outlet node  
    \type alpha  
    \required-field  
A5, \field Fluid name  
    \note (water, ethylene glycol, etc.)
```

```

\type object-list
\object-list GlycolConcentrations
\required-field
\default water
N1, \field Outdoor Ground Convection Coefficient
\type real
\units W m-2 K-1
\minimum> 0
N2, \field Pipe inside diameter
\memo (thickness is defined in the construction data)
\type real
\units m
\minimum> 0
\ip-units in
N3; \field Pipe length
\type real
\units m
\minimum> 0.0

```



## APPENDIX H

### EnergyPlus IDF Object

Example of the input object required in the EnergyPlus input data file for simulation of a buried pipe. Note that this object references a construction object which must contain at least soil and pipe wall material definitions. Grout or pipe insulation are optional. The Pipe:Underground object also references a required set of ground surface temperatures. An example of this input is given here as well.

```
PIPE:UNDERGROUND,
    Pipe Heat Transfer Towers,      !- Name
    Insulated Buried Pipe,         !- Construction name
    Condenser Tower Outlet Node,    !- Comp1 Inlet Node Name
    HTPipe Outlet Node,            !- Comp1 Outlet Node Nam
    Water,                         !- Fluid name
    75,                            !- Ground Surface Conv. Coeff.
    0.05,                          !- Pipe Inside Diameter
    100.0;                         !- pipe length

GROUNDTEMPERATURES:Surface,
    4,                             !- January Avg Ground Temp
    4,                             !- February Avg Ground Temp
    6,                             !- March Avg Ground Temp
    6,                             !- April Avg Ground Temp
    10,                           !- May Avg Ground Temp
```

10,	!- June Avg Ground Temp
15,	!- July Avg Ground Temp
15,	!- August Avg Ground Temp
14,	!- September Avg Ground Temp
14,	!- October Avg Ground Temp
8,	!- November Avg Ground Temp
8;	!- December Avg Ground Temp

## APPENDIX I

### EnergyPlus Input Output Reference Contribution

#### Pipe: Underground

This object specifies inputs which are used to simulate the heat transfer from a plant loop pipe buried underground. This model is currently only implemented on plant condenser loops, although a future revision should expand the model to any location where a normal pipe object could be used. The data definition for Pipe:Underground object from the Energy+.idd is given in appendix G. The object requires five alpha inputs, and three numerical inputs. Each of these inputs are described here.

- Pipe Name: This alpha field is used as an identifying field for the pipe.
- Construction Name: This alpha field references a 'wall' construction object that gives a layer-by-layer description of the pipe wall and soil. The construction object follows standard conventions, describing material properties for each layer beginning with the outermost layer, the soil, and ending with the pipe wall layer. The construction object may have either two or three layers. If only two, then the materials must be the soil and the pipe wall. If three, then an intermediate layer (either insulation or grout) is utilized. Note that when defining the soil layer, the thickness should be the thickness of soil between the pipe wall and the ground surface.
- Fluid Inlet Node: This alpha field contains the name of the pipe fluid inlet node.
- Fluid Outlet Node: This alpha field contains the name of the pipe fluid outlet

node.

- Fluid Name: This alpha field contains the fluid name. This name will be validated against a set of fluid names in the input file. Water and glycol mixtures are typically used for these cases.
- Outdoor Convection Coefficient: This numeric field contains the ground to outdoor air convection coefficient. The finite difference model contains the interaction at the surface, so the convection coefficient is entered directly. An average value throughout the year should be used. The units are  $\frac{W}{m^2K}$ .
- Pipe Inside Diameter: This field is used to enter the inside diameter of the pipe in units of m. Pipe inside diameter must be a positive quantity.
- Pipe Length: This field is used to enter the length of the pipe in units of m. Pipe length must be a positive quantity.

In addition to the basic Pipe:Underground object, there must be a construction object for the pipe/soil layers, and also a GroundTemperatures:Surface object. This object inputs average monthly surface temperatures. These temperatures are then used to develop average ground surface data. This ground surface data can then be used as part of the model boundary condition set. Without a set of surface ground temperatures, the model will provide a fatal error describing the problem to the user. An example of the input data object in an IDF is given in appendix H.

The outputs for the program are listed here.

- HVAC, Average, Pipe Heat Transfer Fluid Heat Transfer Rate [W]
- HVAC, SUM, Pipe Heat Transfer Fluid Heat Transfer Energy [J]
- HVAC, Average, Pipe Heat Transfer Mass Flow Rate [kg/s]
- HVAC, Average, Pipe Heat Transfer Inlet Temperature [C]

- HVAC, Average, Pipe Heat Transfer Outlet Temperature [C]
- HVAC, Average, Pipe Heat Transfer Pipe Velocity [m/s]
- HVAC, Average, Pipe Heat Transfer Fluid Density [kg/m3]
- HVAC, Average, Pipe Heat Transfer Fluid Specific Heat [kg/m3]
- HVAC, Average, Pipe Heat Transfer Predicted Ground Surface Temp [C]
- HVAC, Average, Pipe Heat Transfer Predicted Pipe Depth Temp [C]
- HVAC, Average, Pipe Heat Transfer Predicted Deep Ground Temp [C]

Each of these outputs are described here.

- Pipe Heat Transfer Fluid Heat Transfer rate [W]: The output provides the total amount of heat loss/gain in the fluid from pipe inlet to outlet.
- Pipe Heat Transfer Fluid Heat Transfer Energy [J]: Total energy fluid has lost/gained between pipe inlet and outlet. It is metered on EnergyTransfer with an end use of Pipes.
- Pipe Heat Transfer Mass Flow Rate [kg/s]: Mass flow rate of the fluid in the pipe
- Pipe Heat Transfer Inlet Temperature [C]: Temperature of fluid entering pipe
- Pipe Heat Transfer Outlet Temperature [C]: Temperature of fluid exiting pipe
- Pipe Heat Transfer Pipe Velocity [m/s]: Velocity of fluid in pipe
- Pipe Heat Transfer Fluid Density [kg/m3]: Average density of fluid in pipe
- Pipe Heat Transfer Fluid Specific Heat [kg/m3]: Average specific heat of fluid in pipe

- Pipe Heat Transfer Predicted Ground Surface Temp [C]: Predicted ground surface temperature for current time step. This is calculated from a correlation using the annual ground surface temperature data and the current time of year.
- Pipe Heat Transfer Predicted Pipe Depth Temp [C]: Predicted ground temperature at pipe depth at current time step. This is calculated from a correlation using the annual ground surface temperature data, pipe depth, and the current time of year.
- Pipe Heat Transfer Predicted Deep Ground Temp [C]: Predicted ground temperature at domain depth at current time step. This is calculated from a correlation using the annual ground surface temperature data, domain depth, and the current time of year.

Note that when the fluid properties are given data which corresponds to frozen conditions, the fluid properties may be returned as zero. One can output the density and specific heat to monitor this behavior in buried pipes.

## APPENDIX J

### EnergyPlus Engineering Reference Contribution

The engineering reference document contains the information necessary for a user to understand the model operation, assumptions, capabilities, and limitations. The current documentation contains information for the non-buried pipes, so the buried pipe model will be added to this section. This current section will therefore also act as a brief summary of chapter 6 in this current work. One note about the model is that in its current status, the buried pipe may be only implemented in condenser loops, although a future revision will allow the buried pipe model to be used anywhere the normal pipe model is allowed. In the final documentation, figures and equations may be included which are only needed in such an independent document, and not needed within this current work.

The buried pipe model in EnergyPlus is significantly different from the pipe models for zone or outdoor environments. In these models, the outer boundary condition on the pipe was easily specified based on either current outdoor air, current zone air, or a scheduled air temperature. For a buried pipe, the boundary is the ground surface, and the ground between the pipe and the surface must be modeled. For a shallow buried pipe, the HeatExchanger:Surface object may be used, which uses modified conduction transfer functions to model the ground. However, beyond a certain thickness, the transfer function method fails, and EnergyPlus will call for a fatal error due to convergence problems. Therefore, when a pipe is buried deeper than about one meter, this new buried pipe model should be used.

The buried pipe model develops a grid around the pipe, extending from the ground

surface down to a calculated distance below the pipe. The domain extends from the center of the pipe to accommodate symmetry; this domain then extends horizontally to a calculated distance from the pipe. The grid also stretches along the full length of the pipe. At each cross section, 2D cartesian finite difference techniques are used, updating each node except the node centered on the pipe. Therefore, axial heat transfer is not modeled in the soil. When the model encounters the pipe node, a separate routine is called, which develops a radial mesh in the near pipe region. In this region, 1D heat transfer is modeled, assuming axisymmetric behavior. In this region, soil is modeled, as well as the pipe wall and any insulation or grout that is specified. Note that currently heat transfer in the pipe wall and insulation is modeled as steady state. A heat balance at the water-pipe interface is then utilized to update the water temperature. The pipe model calculates heat transfer whether the pipe flow is on or off. If the flow is off, the water node is set to radially adiabatic, and the temperature will float accordingly, though it is only updated in the EnergyPlus output reports when the pump is turned back on.

Within EnergyPlus, the buried pipe model is handled in the exact manner as the other pipe heat transfer models. First, EnergyPlus calls to get input and initialize the pipe model. These initializations include temperature array initializations, and generating the finite difference mesh. At the beginning of each time step, the boundary condition is updated, and the loop status (flow on or off) is determined from the current mass flow rate. The time step is also adjusted according to the current system time step. The main calculation routine is then called. This routine begins by storing previous time step temperatures, and then starts stepping through the nodes at the current cross section. Each node is updated with a specific equation according to adiabatic, convection, or known temperature boundary position. When this routine reaches the node containing the pipe, a second routine is called. This routine similarly starts by storing previous temperatures. Then the routine sweeps through



all the radial domain in the near pipe region, updating each temperature with the appropriate location. When this routine reaches the water boundary, a third routine is called. This routine updates the water temperature based on two separate choices: if the flow on or off, and if there pipe insulation/grout surrounding the pipe. With the water temperature updated, the routine exits, and the radial routine then checks for convergence. The radial routine repeats until convergence. Once converged, control passes back to the cartesian, outer routine, which also checks for convergence. Once converged, the model is complete.

Although it appears from the description that the model may be computationally intensive, it is in fact quite efficient. The model does run through many iterations at the beginning while the domain is initializing, but once the overall temperature distribution in the domain is set, the model does not require a large number of iterations at each time step. If there is a minimal change in entering water temperature from the previous time step, the system can converge with just one iteration.

## VITA

Edwin Lee

Candidate for the Degree of  
Master of Science

Thesis: DEVELOPMENT, VERIFICATION, AND IMPLEMENTATION  
OF A HORIZONTAL BURIED PIPE GROUND HEAT  
TRANSFER MODEL IN ENERGYPLUS

Major Field: Mechanical Engineering

Biographical:

Personal Data: Born in Tulsa, Oklahoma, United States of America on October 29, 1982.

Education:

Received the B.S. degree from Oklahoma State University, Stillwater, Oklahoma, 2006, in Mechanical Engineering

Completed the requirements for the degree of Master of Science with a major in Mechanical Engineering at Oklahoma State University in May, 2008.

Experience:

Worked as an engineering intern with Specific Systems, LTD. in Tulsa, OK. Involved with light development work for custom HVAC equipment, and unit testing in research and development department. Worked during graduate school as a consultant for Oak Ridge National Laboratory performing EnergyPlus simulations of different building envelope materials, including solid wood, solid concrete, 2x4 framing, 2x6 framing, and phase change materials on a low rise residential building.

Professional Memberships:

ASHRAE student member throughout Masters degree coursework  
President of ASHRAE student branch January 2007-Current

Name: Edwin Lee

Date of Degree: May, 2008

Institution: Oklahoma State University

Location: Stillwater, Oklahoma

Title of Study: DEVELOPMENT, VERIFICATION, AND IMPLEMENTATION  
OF A HORIZONTAL BURIED PIPE GROUND HEAT  
TRANSFER MODEL IN ENERGYPLUS

Pages in Study: 197

Candidate for the Degree of Master of Science

Major Field: Mechanical Engineering

A buried pipe heat transfer model was developed and implemented within the EnergyPlus simulation program. A literature review revealed different solutions attempted for this problem, including analytic methods, finite difference solutions, and transfer function methods. Three separate models: a modified earth tube model, a fully radial finite difference model, and a mixed-coordinate finite difference model were tested against a robust verification model developed in Fluent. Fluent was used due to its ease of setting boundary conditions and developing a sufficient mesh. The earth tube model is currently implemented in EnergyPlus, and was tested both as an earth tube and a pipe. The model's extreme simplicity led to poor tests upon verification. The radial model encountered significant stability problems due to the explicit formulation of the model. The mixed-coordinate model proved the most stable and accurate of the finite difference models. Although transfer function methods were investigated, they were not selected due to convergence problems in thick soil. In addition to verification against the Fluent model, the models were tested under high flow rate testing which removes axial heat transfer, and constant pipe wall testing. After implementation and testing in VBA, the mixed-coordinate system model was selected for implementation in EnergyPlus. This model utilizes a radial coordinate system in the near pipe region, with a coarse Cartesian system throughout the rest of the domain. The finite difference update equations are implicitly derived. At each cross section, 2D heat transfer is modeled, neglecting axial heat transfer. The far-field boundary is a function of time of year and ground depth based on known surface temperature data. The initial implementation in VBA agreed to the verification model with an annual RMS error of  $1.72^{\circ}\text{C}$  on the exiting fluid temperature. The final implementation in EnergyPlus agreed to the VBA implementation to within  $0.12^{\circ}\text{C}$ . This small deviation is related to the time step management difference between the two implementations. This model is currently implemented in the plant manager of EnergyPlus, and is available to better predict heat gains and losses in the ground for all buried pipes.

ADVISOR'S APPROVAL: \_\_\_\_\_ Dr. Daniel Fisher \_\_\_\_\_